

Article Title: Hyperconjugation

Article type: Advanced review

Authors:

Igor V Alabugin*

0000-0001-9289-3819, Florida State University, alabugin@chem.fsu.edu, this author declares no conflicts of interest

Gabriel dos Passos Gomes

0000-0002-8235-5969, Florida State University, ggomes@chem.fsu.edu, this author declares no conflicts of interest

Miguel A Abdo

0000-0002-2009-6340, Florida State University, maa13k@my.fsu.edu, this author declares no conflicts of interest

Keywords

Bond theory, Hyperconjugation, Stereoelectronic effects, Delocalization, Orbital

Graphical abstract

This review outlines the role of hyperconjugative interactions in the structure and reactivity of organic molecules. After defining the common hyperconjugative patterns, we discuss the main factors controlling the magnitude of hyperconjugative effects, including orbital symmetry, energy gap, electronegativity, and polarizability. The danger of underestimating the contribution of hyperconjugative interactions are illustrated by a number of spectroscopic, conformational, and structural effects. The stereoelectronic nature of hyperconjugation offers useful ways for control of molecular stability and reactivity. New manifestations of hyperconjugative effects continue to be uncovered by theory and experiments.

Hyperconjugation, conjugation and σ -conjugation:

The classic picture of covalent chemical bonding starts by creating the framework of two-center/two-electron bonds. These bonds are formed by sharing of electron pairs which is a quantum mechanical phenomenon based on the constructive interference of atomic wavefunctions. Although the introductory chemical courses describe the result by using the familiar lines and dots adding up the Lewis structure of a molecule, this simple picture is incomplete because the underlying quantum nature of molecules does not disappear once the “first-order” two-center bonding interactions are formed.¹

Because molecules are intrinsically delocalized quantum objects, their accurate description has to transcend a single Lewis structure where delocalization is limited to the formation of two-center chemical bonds. The concept of electronic delocalization provides a way to incorporate the quantum nature of matter as a “second order correction” to the Lewis structure description. Of course, such correction is only needed when one starts from a localized point. Delocalization is the natural part of Molecular Orbital (MO) description of chemical systems where the concept of localized Lewis structure loses its foundational value.

The delocalizing deviations from the localized Lewis-structure description are mediated by the “2nd order” interactions between the electronic orbitals. Such interactions can be generally classified as one of three ubiquitous effects: conjugation, hyperconjugation and σ -conjugation. This classification is based on the type of orbitals involved in the interactions. Although the word “conjugation” is sometimes used to describe all types of delocalization, it refers, more specifically, to interactions either between π -bonds or between π -bonds and p-orbitals. IUPAC defines interaction between σ - and π -orbitals as hyperconjugation. Interaction of σ -orbitals is sometimes referred to as sigma conjugation but, more often, it is also called hyperconjugation.

The diversity of delocalizing effects is summarized in Figure 1, which provides the nine patterns corresponding to the different types of participating orbitals, i.e., lone pairs, σ - and π -orbitals. Note that five of the nine patterns involve at least one σ -bond.

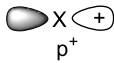
	non-bonding X:	π -bond =Y	σ -bond -Z	Donors
 =Y π^*				
				
				
Acceptors				

Figure 1. Types and examples of delocalizing interactions (hyperconjugative interactions are shown on the grey background).

Although these examples are based on two-electron interactions, many of such patterns can be readily extended to systems with a different number of electrons (radicals, radical-cations, and radical-anions).

Each of these effects describes the electronic consequences of delocalization and can be expressed as the difference between a perfectly localized, single Lewis structure, system and a real molecule. Delocalization decreases the electronic energy by allowing “parts” of the molecules (e.g., different functional groups or group orbitals) to interact. Although the interaction of π -orbitals, or conjugation, has been a prominent feature of theoretical organic chemistry for a long time, the importance of delocalizing interactions involving σ -bonds^{2,3} has not been equally recognized.

The separation of σ -conjugation, hyperconjugation, and conjugation into three different effects is based on an arbitrary decision to treat σ - and π -orbitals on a different basis. Because the separation is artificial, the lines between the three effects are often blurred. For example, the term conjugation is also extended to the analogous interaction involving a double bond and a non-bonding p-orbital. Note that the interactions of π -bonds with lone pairs starts to blur the line between hyperconjugation and conjugation because lone pairs are often hybridized and possess significant s-character.⁴ Analogously, in the process of an allylic sigma C-Cl bond stretching and breaking in allyl chloride, hyperconjugation with the sigma-bond is smoothly transformed into conjugation with the non-bonding orbital (the cationic or radical center). This absence of a well-defined border further indicates that distinction between hyperconjugation and conjugation is artificial (Figure 2) and separation of these two effects has mostly historic value. *Hyperconjugation and conjugation describe the same fundamental phenomenon and are different only within the σ,π -model.*

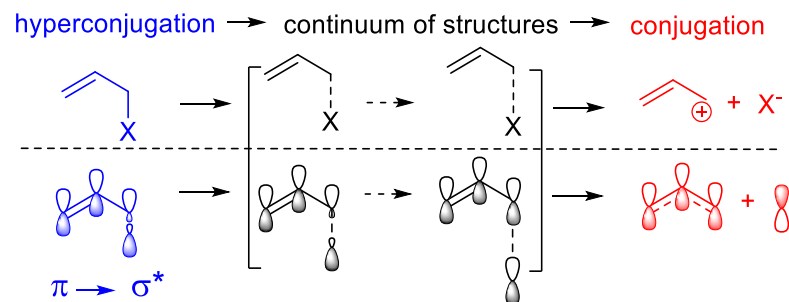


Figure 2. Transition from hyperconjugation to conjugation proceeds without a well-defined border.

Interestingly, R. Mulliken in his seminal 1941 paper titled “Hyperconjugation”⁵ emphasized that “differences in conjugating power” among saturated and unsaturated groups are “quantitative rather than qualitative”.^{5,6} He suggested to use terms “second order conjugation, or first order hyperconjugation” for the σ,π -interaction and “third-order conjugation, or second-order hyperconjugation” for the σ,σ -interaction. Mulliken’s analysis remains valid - the basic stereoelectronic guidelines, and orbital interaction patterns, are similar as those for the three types of delocalizing interactions. In fact, σ -conjugation is often referred to as hyperconjugation

in modern scientific literature. In this review, we will follow the spirit of Mulliken's treatment and combine both types of interactions including σ -bonds under one title "hyperconjugation".

Descriptions of hyperconjugation:

In VB theory, hyperconjugation arises from the presence of additional resonance structures (the double bond/no bond resonance in Figure 3a). In MO theory, hyperconjugation is commonly described as the interaction between electronic orbitals, one of which corresponds to a σ -bond. In order for the interaction to be stabilizing, the higher energy orbital has to be at least partially empty (0 or 1 electrons), and the lower energy orbital has to be at least partially filled. The most common scenario, illustrated in Figure 3, corresponds to a two-electron interaction where the lower energy orbital (a bond or a lone pair) is completely filled whereas the higher energy antibonding orbital is empty. Two-center/one-electron and two-center/three-electron hyperconjugation patterns are also possible and play important roles in odd-electron species such as radicals, radical-ions and excited states.^{7,8}

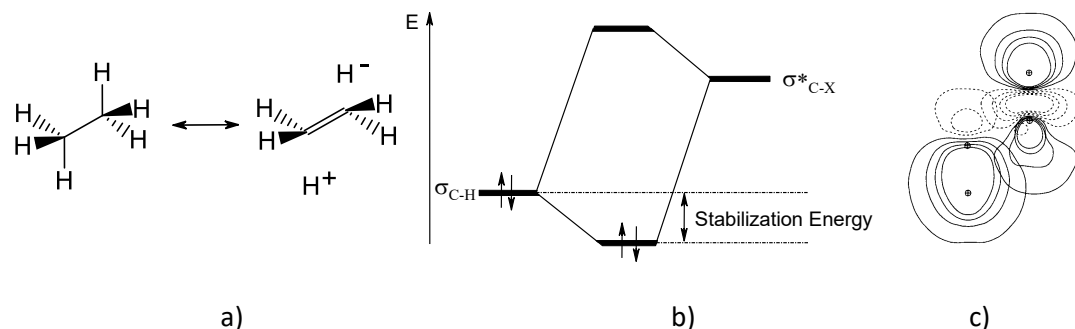


Figure 3. a) Description of the vicinal $\sigma_{\text{C-H}} \rightarrow \sigma^*_{\text{C-H}}$ interaction in ethane in terms of resonance theory ("double bond/no bond resonance"). b) Energy lowering due to hyperconjugative interaction between $\sigma_{\text{C-H}}$ and $\sigma^*_{\text{C-X}}$ orbitals. c) NBO plots illustrating overlap of vicinal $\sigma_{\text{C-H}}$ and $\sigma^*_{\text{C-H}}$ orbitals in ethane.

Theoretical approaches to analysis of hyperconjugation.

Conformational energy profiles.

An "ideal" reaction for the analysis of an electronic effect would involve no changes in hybridization and the types of bonds. None of these parameters change upon conformational changes as a result of rotation around a single bond, whereas many hyperconjugative effects are stereoelectronic (depend on orbital overlap in space) and can be "switched off and on" through conformational changes. Conformational analysis has played an important historical role in the development of theoretical organic chemistry and proved to be very useful for the understanding of hyperconjugative effects. However, such an analysis is complicated by the fact that conformational equilibrium often is controlled by a complex mixture of factors, of which hyperconjugation is only a single contributor. Furthermore, switching one effect off frequently activates a different effect.

Isodesmic reactions.

Very often delocalization is estimated through thermochemical data and application of hypothetic reactions (isogyric, isodesmic, hypohomodesmotic, homodesmotic, or hyperhomodesmotic)⁹ which are designed to isolated the desired effect. For example, the equation in Figure 4 can be used to evaluate the hyperconjugative stabilization of an alkene by a methyl group.¹⁰

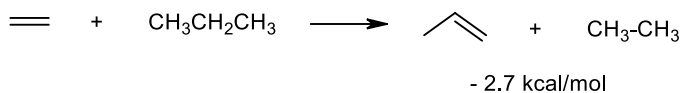


Figure 4. A possible way to estimate hyperconjugation in propene through a bond separation reaction.

The advantage of these equations is that, in many cases, the thermochemical data can be either obtained experimentally or calculated with a high degree of accuracy. The challenge is in isolating the key electronic effect without introducing additional structural and electronic perturbations. For example, the above equation suffers from an imbalance in the hybridization, such as a different number of $\text{sp}^3\text{-sp}^3$ and $\text{sp}^2\text{-sp}^3$ C-C bonds and vinyl C-H bonds in the reactant and product. It is important to note that, of course, the total energy of this equation is NOT the energy of hyperconjugation but rather a difference between hyperconjugation and sigma conjugation (i.e., the interaction of an alkyl substituent with a methyl group).

An “ideal” reaction for the analysis of a delocalizing electronic effect would involve no changes in hybridization and the bond types. In addition, it should also have negligible changes in steric and electrostatic factors. Although meeting all of these requirements is often a challenge, such equations can provide useful information.

For example, the calculated energy for the transformation of 1,4-dioxane into 1,3-dioxane ($\Delta G = -5.4$ kcal/mol, Figure 5) indicates the presence of a stabilizing effect, inherent to 1,3-dioxane, i.e., the generalized anomeric effect that will be discussed later in this review). The 2nd equation shows that ether and peroxide can stabilize each other as well, albeit to a smaller extent. Finally, the last equation provides an explanation to the paradoxical stability of bis-peroxides connected via a one-carbon link. It shows that the presence of two such peroxide moieties in a six-membered cycle leads to ~ 4 kcal/mol increase in stability relative to the mono-peroxide.¹¹ We will discuss later how this observation indicates the reemergence of anomeric effect in peroxides. Due to the presence of the two 1,3-dioxa fragments, bis-peroxides are stereoelectronically analogous to bis-acetals (vide infra).

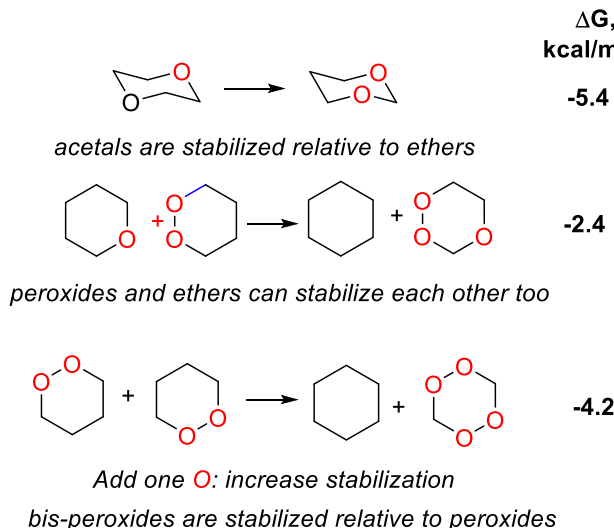


Figure 5. Increases stability of acetals and the resurgence of anomeric effect in bis-peroxides

Wavefunction analysis.

A different approach which has a conceptual advantage over such conventional delocalization energy assessments involves direct computational dissection of delocalized wavefunctions. In order to describe and quantify delocalizing interactions, one needs to evaluate the energy penalty which occurs when this interaction is absent. The difference in energy between this state (sometimes called diabatic state) and the full state (sometimes called adiabatic) can be taken as the interaction energy. The main challenge lies in defining the appropriate correct localized state to serve as a reference point. Three approaches have emerged for dissecting delocalizing interactions: Natural Bond Orbital (NBO) analysis, Energy Decomposition Analysis (EDA),¹² and Block-Localized Wavefunction method (BLW).¹³

All of these methods share a conceptual similarity in comparing the full wavefunction with a hypothetical localized construct. However, an important difference between these methods lies in the starting basis set of orbitals used to describe delocalization. Whereas NBO utilizes orthogonal orbitals to describe the localized reference, the other methods start with non-orthogonal orbitals.¹⁴ This difference leads to significant variations in the magnitude of delocalizing interactions obtained and exaggerates the role of steric effects in those methods based on non-orthogonal orbitals.

From the conceptual perspective, the non-orthogonal initial orbitals cannot be the eigenfunctions of any imaginable physical (Hermitian) Hamiltonian that can serve as the "unperturbed system" for such an analysis. Although the overlap contamination effects do not change energies evaluated on the basis of the *overall* molecular wave functions (whether orbitals of a determinantal wavefunction are orthogonal or not does not affect the overall expectation value), orbitals (and charge density) attributed to one group have overlap with (and thus could equally well be attributed to) orbitals of the other group. If the "bond" of one group overlaps with the antibond of the other group, such overlap will automatically be labeled "exchange repulsion" in a scheme based on non-orthogonal orbitals.¹⁵

The observed differences between alternative computational dissections are due to the ambiguity about which non-orthogonal subunits receives credit for unaccounted density in the overlap region. The associated overlap density can be assigned to the filled orbital (and counted toward steric effects) or to the unfilled orbital (and counted toward hyperconjugative charge-transfer). All methods that harbor such overlap ambiguities are expected to differ sharply from NBO-based assessments of intramolecular or intermolecular interactions.

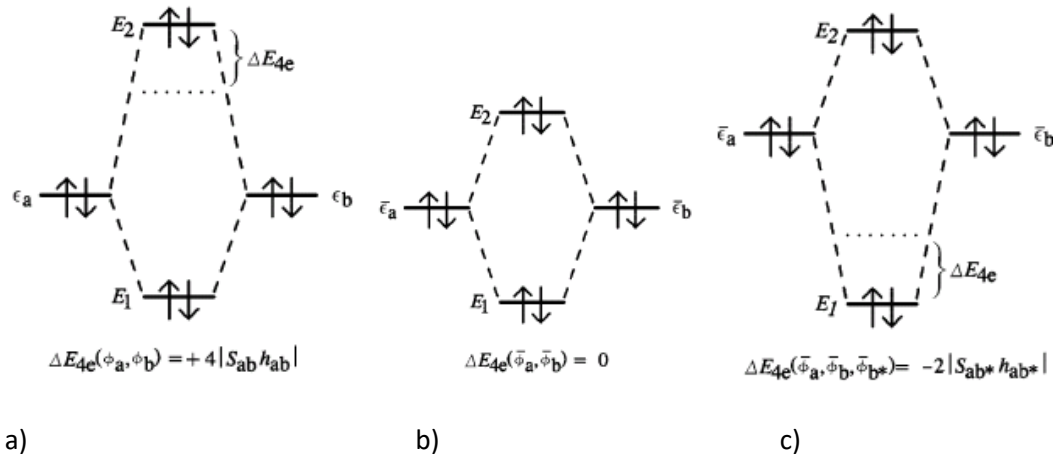


Figure 6. a) Four-electron destabilizing interaction expressed in terms of nonorthogonal “unperturbed” orbitals (for which there is no imaginable Hermitian perturbation theory). b) Four-electron nonstabilizing interaction expressed in terms of orthogonalized unperturbed orbitals (for which there exists a valid Hermitian). c) Four-electron stabilizing interaction for a proper three-term description of orbital energies in terms of Löwdin-orthogonalized basis orbitals [Reprinted with permission from ref.16].

Figure 6a illustrates the origin of “four-electron destabilization” between two non-orthogonal filled orbitals often taken as the physical origin of the steric destabilization. However, it is simply a mathematical artifact of non-orthogonality and does not, in fact, correspond to a physical interpretation of any imaginable physical process. Once orbitals are orthogonalized, the “four-electron destabilization” disappears (Figure 6b). When at least one unoccupied orbital is added to the system, the overall interaction becomes stabilizing (Figure 6c).¹⁶

The general concept outlined above has been implemented in several popular approaches discussed below.

Natural Bond Orbital (NBO) analysis:

The NBO analysis transforms the canonical delocalized Hartree-Fock (HF) MOs and non-orthogonal atomic orbitals (AOs) into the sets of localized “natural” atomic orbitals (NAOs), hybrid orbitals (NHOs) and bond orbital (NBOs). Importantly, each of these localized basis sets is complete and orthonormal and describes the wavefunction with the minimal number of filled orbitals in the most rapidly convergent fashion. Filled NBOs describe the hypothetical, strictly localized Lewis structure. NPA charge assignments based on NBO analysis correlate well with empirical charge measures.¹⁷

The interactions between filled and antibonding (or Rydberg) orbitals represent the deviation of the molecule from the Lewis structure and can be used as a measure of delocalizations. Since the occupancies of filled NBOs are highly condensed, the delocalizing interactions can be treated by a standard second order perturbation approach (Eq. 1) or by deletion of the corresponding off-diagonal elements of the Fock matrix in the NBO basis and recalculating the energy (referred to as E_{del} energies)^{18,19} where $\langle \sigma/F/\sigma^* \rangle$, or F_{ij} is the Fock matrix element between the orbitals (NBOs) i and j , ϵ_σ and ϵ_{σ^*} are the energies of the σ and σ^* NBO's, and n_σ is the population of the donor σ orbital.³ Usually, there is a good linear correlation between the deletion (E_{del}) and perturbation ($E(2)$) energies.²⁰ One can also delete some or all of the virtual localized natural bond orbitals, thus eliminating all interactions involving these orbitals.

$$E(2) = -n_\sigma \frac{\langle \sigma/F/\sigma^* \rangle^2}{\epsilon_{\sigma^*} - \epsilon_\sigma} = -n_\sigma \frac{F_{i,j}^2}{\Delta E} \quad \text{Eq. (1)}$$

It is important to mention a few caveats in using NBO method for quantifying delocalization. First, the accuracy of the perturbative estimation decreases strongly as the interactions grow stronger. Furthermore, the results of the global NBO deletions which deactivate all antibonding orbitals in a large molecule or in a significant part of the orbital space should be also used with caution. Such energies can be very large and only useful for general evaluations. These problems can be exacerbated for calculations with large basis sets which add a larger number of Rydberg orbitals to the NBO expansions.²¹

Natural Steric Analysis²² in the NBO procedure is based on the model of Weiskopff where orbital orthogonalization leads to the “kinetic energy pressure” that opposes interpenetration of matter.²³ As the orbitals begin to overlap, the physically required orthogonalization leads to additional oscillatory and nodal features in the orbital waveform, which correspond to increased wavefunction curvature and kinetic energy, the essential “destabilization” that opposes interpenetration. The overlap-type analysis of Pauli interactions can be introduced to the NBO framework through interactions of not orthogonalized pre-NBOs.

Energy Decomposition Analysis:²⁴

This analysis starts with “a zeroth-order” wavefunction from the overlapping orbitals of the isolated molecular fragments. In EDA, the interactions between these fragments are divided into three steps. In the first step the fragments, which are calculated with the frozen geometry of the entire molecule, are superimposed without electronic relaxation; this yields the quasiclassical electrostatic attraction ΔE_{elstat} . In the second step the product wave function becomes antisymmetrized and renormalized, which gives the repulsive term ΔE_{Pauli} , termed Pauli repulsion. In the third step the molecular orbitals relax to their final form to yield the stabilizing orbital interaction ΔE_{orb} . The latter term can be divided into contributions of orbitals having different symmetry which is useful for separation of σ - and π -effects. The sum of the three terms $\Delta E_{\text{elstat}} + \Delta E_{\text{Pauli}} + \Delta E_{\text{orb}}$ gives the total interaction energy ΔE_{int} .

Block localized wavefunction (BLW) method:²⁵

Mo and coworkers suggested that the electron delocalization to the cationic carbon and neutral boron center can be accurately studied by removing the vacant π -orbitals from the expansion

space of molecular orbitals. Although this simple orbital deletion procedure (ODP) technique is limited to the analysis of positive hyperconjugation in carbocations and boranes, it has been generalized and extended to the block localized wavefunction (BLW) method.^{13,26,27}

The BLW method combines the MO and VB theories. In this method, the wavefunction for a localized (diabatic) state is defined by limiting the expansion of each MO (called block-localized MO) to a predefined subspace instead of allowing all MOs to be a combination of all atomic orbitals, as in MO theory. Block-localized MOs belonging to different subspaces are generally non-orthogonal. The BLWs for diabatic states are optimized self-consistently, and the adiabatic state is a combination of a few (usually two or three) diabatic state wavefunctions.

For example, for propene, the delocalized and localized (BLW) wave functions can be expressed as $\Psi(\text{del}) = \hat{A}(\sigma 1a''^2 2a''^2)$ and $\Psi(\text{loc}) = \hat{A}(\sigma \pi^2_{\text{C=C}} \pi^2_{\text{CH}_3})$, where $\pi_{\text{C=C}}$ and π_{CH_3} are group orbitals expanded in $\text{CH}_2=\text{CH}$ and CH_3 groups and are non-orthogonal. In contrast, canonical MOs $1a''$ and $2a''$ are delocalized for the whole system and orthogonal. In this example, the energy difference between these two wave functions, which are independently optimized self-consistently, is taken as the vicinal hyperconjugative interaction between the π double bond and the adjacent methyl group.

NBO stereoelectronic map for a common functional group

In order to illustrate the utility of such theoretical approaches, we apply NBO analysis of ethanal to show that even simple molecules may contain multiple “layers” of conjugative interactions. The computational methods can provide a quantitative insight into the interplay between different electronic effects.²⁸ The carbonyl group provides a combination of five orbitals that can readily interact with the adjacent C-C and C-H bonds (Figure 7). From the stereoelectronic perspective, the carbonyl group is a “stereoelectronic chameleon”. Depending on the relative geometries, its interaction with the neighbors can be either controlled by two powerful acceptor orbitals (σ^*_{CO} and π^*_{CO}) or by a strong donor p-type lone pair on oxygen. Figure 7 illustrates how these interactions change for the eclipsed and bisected conformations of ethanal.

First, interactions of C-H bonds with $\pi_{\text{C=O}}$ increase when C-H bonds are anti to carbonyl (i.e., in the eclipsed conformation). The respective combined NBO energies for the donation to and from the carbonyl increase from 13.2 vs. 14.9 kcal/mol (Figure 7, top).

The “2nd level” of interactions includes the vicinal interactions between anti- and syn-periplanar σ -bonds. Each of these interactions changes dramatically between the conformers. For example, the 0.9 kcal/mol interaction between the synperiplanar the in-plane C-H bond with the $\sigma^*_{\text{C-O}}$ orbital increases to 4.8 kcal/mol for the anti-periplanar arrangement between these orbitals. However, the energy of $\sigma_{\text{C-H}} \rightarrow \sigma^*_{\text{C-H}}$ interactions between the two vicinal in-plane C-H bonds changes in the opposite direction and compensates for the difference in C-H/C-O interactions.

The 3rd level involves smaller interactions between the imperfectly aligned *syn*- and *anticlinal* vicinal σ -bonds. In particular, the $\sigma_{\text{C-H}} \rightarrow \sigma^*_{\text{C-H}}$ interactions favor the bisected conformation where these orbitals are anticlinal. However, this effect is smaller than the “Level 1” π -effects that favor the eclipsed conformation.

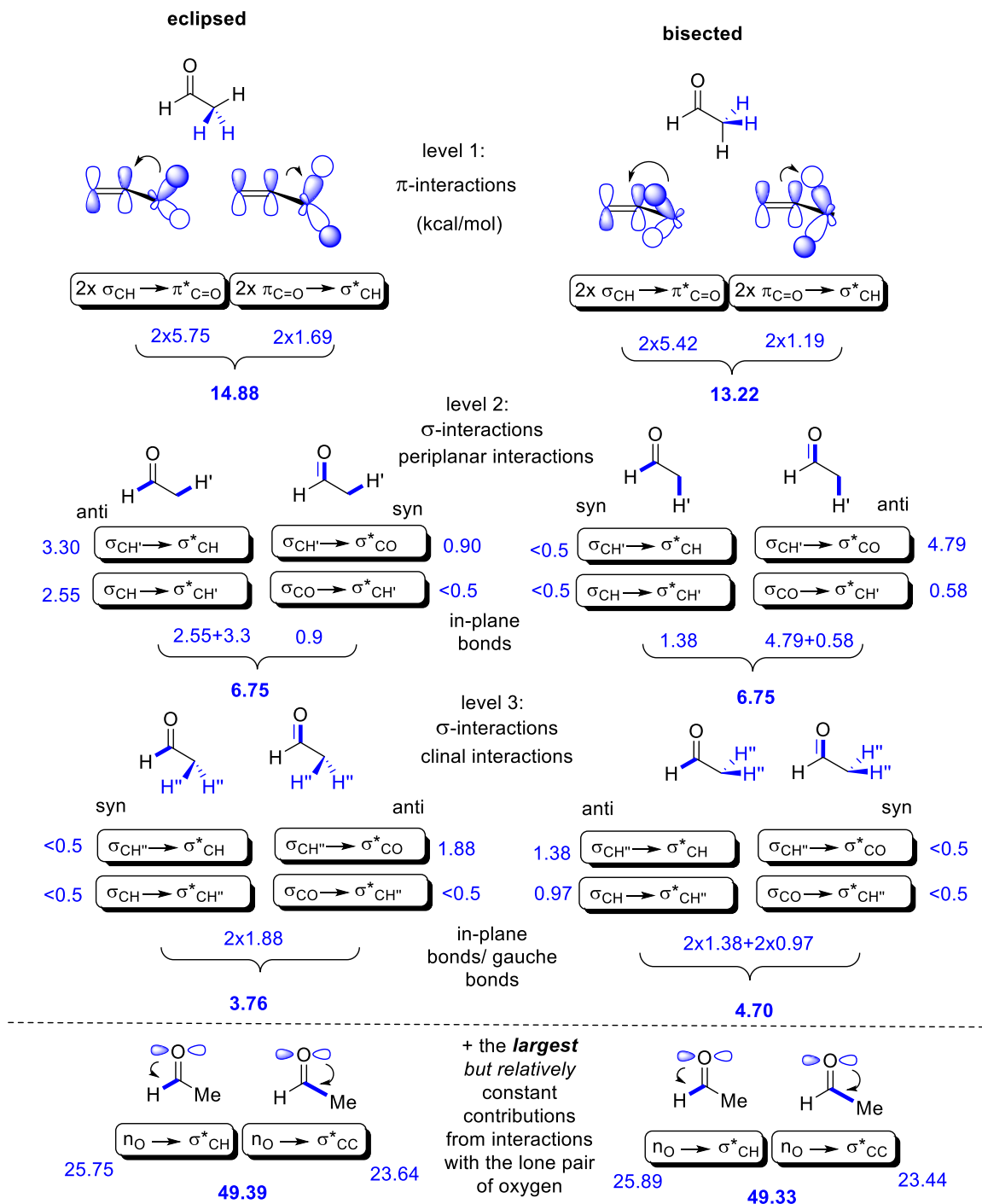


Figure 7. NBO analysis of hyperconjugative interactions involved in the conformational profile of ethanal. The combined energies are approximate because interaction with energies below the default NBO threshold of 0.5 kcal/mol were not used in determining the overall balance (reprinted with permission from ref. 1)

Finally, the strongest hyperconjugative effect in this system, the $n_{\text{O}} \rightarrow \sigma^*_{\text{C-H}}$ delocalization (23-26 kcal/mol) changes only slightly upon the conformational switch. Although this “bystander” interaction appears to have no influence on the conformational tug-of-war, it plays important

role in the overall stability and specific reactivity features of carbonyl compounds. For example, these, “invisible” for conformational equilibria, interactions evolve into a 2c,3e-bond of the acyl radical in the process of C-H bond scission. This hyperconjugative effect is the source of dramatic lowering of the aldehyde C-H bond dissociation energy (~88 kcal/mol) relative to the BDE for C-H bond in ethene (~111 kcal/mol).²⁹ Remarkably, the “sp² hybridized” C(O)-H bond in aldehydes is even weaker than a typical C-H bond in *alkanes*. The C-H weakening effect is also manifested in the spectroscopic properties of aldehydes - the sp² C-H IR stretching frequency for ethanal is >200 cm⁻¹ lower than the C-H IR stretching frequency of ethene.

NBO analysis shows how each of the multiple layers of conjugative interactions can relate to a different aspect of molecular stability and reactivity. It also shows that choosing a single stereoelectronic effect from this complex mixture of interrelated orbital interactions is always an approximation that needs to be reevaluated carefully for each new functionality.

Types of Hyperconjugation:

Isovalent vs. sacrificial hyperconjugation.

The characteristic resonance description of hyperconjugation involves the so called “double bond/no-bond resonance” contributing structure. Depending on the relative number of two-electron bonds in the two contributing structures, hyperconjugation is classified as either “heterovalent” (commonly referred to as “sacrificial”), or “isovalent” hyperconjugation. This classification dates back to Mulliken³⁰ who referred to heterovalent hyperconjugation in neutral systems as “ordinary” or “sacrificial”, and to hyperconjugation in cations as “strong” or “isovalent”.

In sacrificial hyperconjugation, the contributing structure contains one two-electron bond less than the main Lewis formula. In contrast, contributing structures describing the so-called “isovalent” hyperconjugation between σ -bonds and an unfilled or partially filled π - or p-orbital in carbenium ions, carbanions and radicals contain the same number of two-electron bonds as the main Lewis formula (Figure 8).

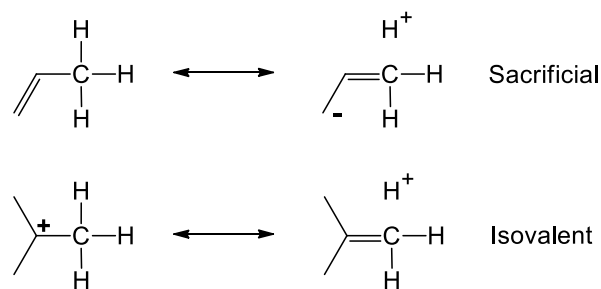


Figure 8. Comparison of contributing resonance structures in sacrificial and isovalent hyperconjugation

The two resonance patterns are not unique for hyperconjugation – the same distinction can be made for conjugation patterns. For example, resonance in butadiene can be taken as an example of sacrificial conjugation, whereas resonance in allyl systems (cation, anion and radical) can be considered as an example of isovalent conjugation.

Neutral, negative and positive hyperconjugation.

Another historically common classification of hyperconjugative interactions is based on their separation into neutral, negative, and positive hyperconjugation. The interactions between filled π - or p-orbitals and adjacent antibonding σ^* -orbitals are referred to as negative hyperconjugation. Donation of electron density from filled σ -orbitals into π^* -orbitals or p-type unfilled orbitals is called positive hyperconjugation. Both negative and positive hyperconjugation are two-electron stabilizing interactions which result in building π -character between nominally single-bonded atoms.

Classification of hyperconjugation as positive or negative is useful when either referring to an individual interaction or to an imbalanced situation, when a very strong donor or a strong acceptor orbital is present in the molecule and interaction of this unusual orbital with the rest of the molecule dominates over other delocalization effects. This imbalance often occurs when either a lone pair acts as a donor or when an empty p-orbital, or a strongly polarized π^* - or σ^* -orbital, acts as an acceptor.³¹ Use of these terms in other situations can be misleading.

In the absence of dominating unidirectional interactions, hyperconjugation is classified as neutral hyperconjugation. This is the most common hyperconjugative pattern which blends together the negative and positive hyperconjugation. For example, the delocalizing interaction between a π -bond and an adjacent σ_{C-X} bond in Figure 9 is displayed as a pair of donor-acceptor $\pi \rightarrow \sigma^*_{C-X}$ and $\sigma_{C-X} \rightarrow \pi^*$ interactions. In this case, the interaction is bidirectional and the same C-X moiety serves as both a σ -donor and a σ -acceptor.

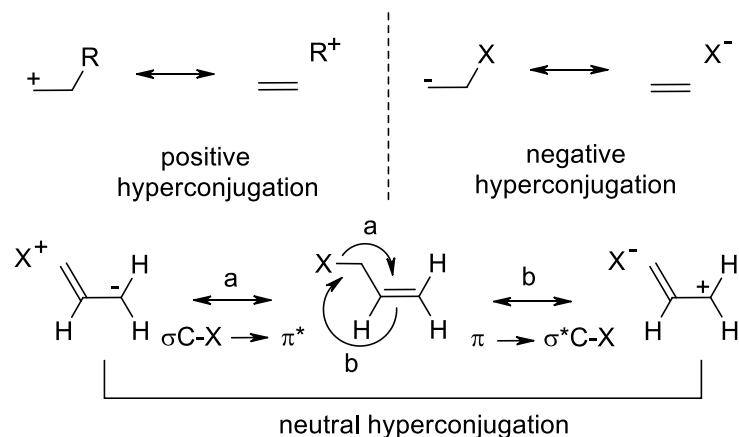


Figure 9. Contributing resonance structures for positive, negative and neutral hyperconjugation.

Negative hyperconjugation.

Donation of electron density from filled π -orbitals or lone pairs into σ^* -orbitals (negative hyperconjugation) is important not only in anions, but also in many neutral molecules. In particular, it is implicated in anomeric effect and its spectroscopic counterparts (i.e., the Bohlmann³² and the Perlin effects³³) Negative hyperconjugation which involves non-bonding orbitals is isovalent, negative hyperconjugation which involves π -orbitals is sacrificial (Figure 10). Negative hyperconjugation plays an important role in intermolecular interactions: For example, it serves as a provider of covalent character and directionality of H-bonding and a force that is accountable for the occurrence of S_N2 reactions.³⁴

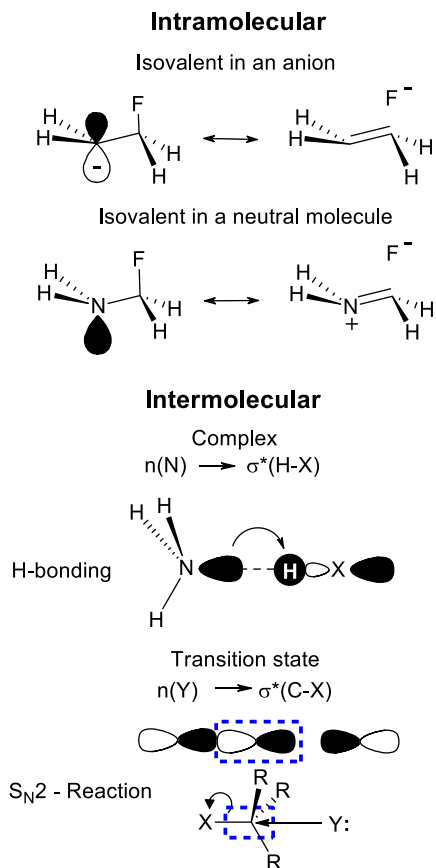


Figure 10. Selected patterns of intra- and intermolecular negative hyperconjugation

A more detailed description of chemical and spectroscopic manifestations of negative hyperconjugation will be given in the *last* section of this review.

Positive hyperconjugation.

This conjugation pattern dominates when a very strong p- or π -acceptor or a very strong σ -donor present in a molecule. In particular, positive hyperconjugation is very important in carbenium ions and boranes.³⁵ Structural and electronic effects of hyperconjugation lead to elongation and weakening of one of the C-H bonds and may assist in the evolution of carbenium ions into hypervalent non-classical structures (Figure 11).

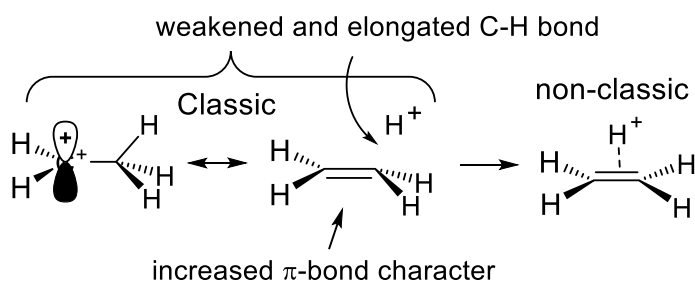


Figure 11. Positive hyperconjugation in a carbenium cation and its evolution in a non-classic structure

The effect of alkyl substituents on the stabilities of carbenium ions provides the electronic basis of the textbook Markovnikov's rule.³⁶ For a carbenium ion, the more alkyl groups that are connected to the cationic center, the more stable the carbocation is.³⁷ The stabilizing effect of hyperconjugation on the stability of carbenium ions is illustrated by the gas phase hydride ion affinities for the selected carbocations in Figure 12. In these gas phase data, the stabilizing potential of conjugation is expressed to its maximum degree because it is not attenuated by solvation effects. It is clear that the stabilizing effect of hyperconjugation is significant – under these conditions, a methyl group provides ca. 70% of stabilization by a double bond in the allyl cation. Although the stabilizing effects of second and third methyl groups are progressively smaller, positive hyperconjugation in secondary and tertiary cations provides much more stabilization to the cationic center than conjugation in the allyl cation and rivals stabilization provided by the lone pairs of oxygen in HOCH₂⁺, i.e., the stabilities increase in the order of methyl cation < primary < allyl < secondary < hydroxycarbenium < tertiary cation (Figure 12).

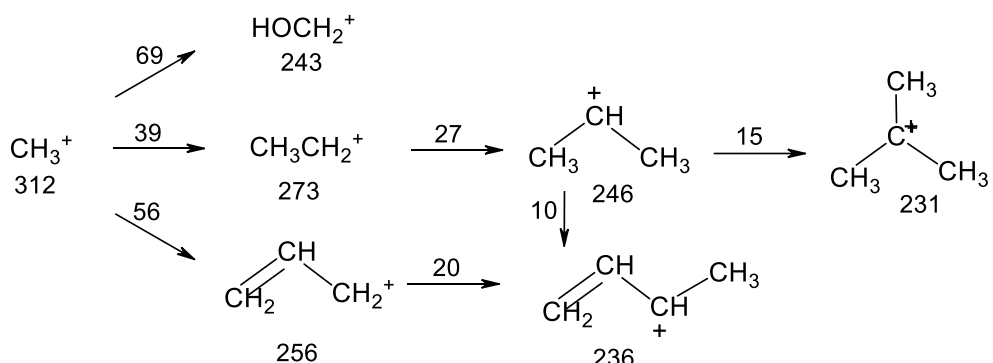


Figure 12. Absolute (data below the structures) and relative (data near the arrows) gas phase hydride ion affinities for selected carbocations. All energies are in kcal/mol and taken from ref. 38.

These trends agree well with the trends in relative stabilities of carbocations from gas phase heterolytic C-Br bond dissociation energies in alkyl bromides: CH_3^+ (0.0 kcal/mol) < CH_3CH_2^+ (36 kcal/mol) < $(\text{CH}_3)_2\text{CH}^+$ (55 kcal/mol) < $(\text{CH}_3)_3\text{C}^+$ (69 kcal/mol).³⁷ Hyperconjugation energies from ODP computations are noticeably smaller CH_3CH_2^+ - 13 kcal/mol, $(\text{CH}_3)_2\text{CH}^+$ - 21 kcal/mol and $(\text{CH}_3)_3\text{C}^+$ - 26 kcal/mol.²⁵ This discrepancy can be attributed to the structural relaxation, e.g., from pyramidal structure to planar structure.

The stabilizing effect of positive hyperconjugation increases for stronger σ -donors. For example, the stabilizing effect of a silyl substituent in β -silylethyl cation is calculated to be ca. 38 kcal/mol in the gas phase.³⁹ Effects of Ge, Sn and Hg are also substantial;⁴⁰ for example, hyperconjugative activation by a Sn-C bond can accelerate a reaction by a factor of >10.^{14,39,41}

Neutral hyperconjugation.

In this type of hyperconjugation, donor and acceptor interactions are balanced and often there is no dominating effect. As the result, although effects of hyperconjugation are documented for X-ray geometries of neutral molecules⁴² and although neutral hyperconjugation was suggested to define conformational profiles of ethane, methylcyclohexane, propene, toluene and other hydrocarbons, the importance of sacrificial hyperconjugation in neutral hydrocarbons has been controversial (vide infra).

Part of the challenge is that structural effects of neutral hyperconjugation are often small and indirect experimental approaches can be complicated.⁴³ However, neglect of neutral hyperconjugation can lead to serious fundamental misconceptions. For example, omission of hyperconjugative effects led to the apparent disappearance of conjugation between two triple bonds in butadiyne (see section “Neutral hyperconjugation in alkenes and alkynes”). We will further illustrate the importance of this ubiquitous phenomenon in the section “Examples/Stereoelectronic effects”.

Comparing the magnitude of negative, positive and neutral hyperconjugation.

To calibrate ourselves, it is instructive to compare the relative magnitudes for the three types of hyperconjugation using the same group (Me) as a reference point (Figure 13). In order to avoid the effects of charge, we will choose three neutral molecules: methyl amine, ethane and methyl borane.

The importance of positive hyperconjugative is the greatest (~14 kcal/mol) in agreement with the electron deficient nature of methyl borane. This molecule, isoelectronic to ethyl cation, cannot satisfy the octet rule and has to rely on the non-Lewis contributions as a supplementary source of stability. Negative hyperconjugation between the aligned C-H and the lone pair of nitrogen is smaller. However, this effect is still significant (~9 kcal/mol) because it provides a way to involve the non-bonding orbital into chemical bonding. The neutral C-H/C-H delocalization between the $\sigma_{\text{C-H}}$ bonds and the associated σ^* orbitals is the weakest from the three types. Even though it is manifested as a *pair* of symmetry-related interactions, their NBO total energy is only ~6 kcal/mol.

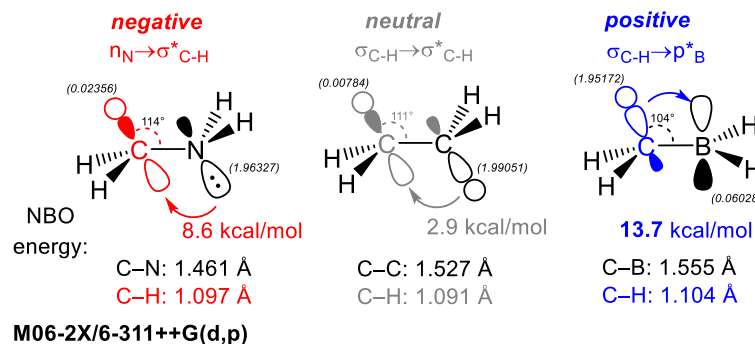


Figure 13. Neutral molecules with negative, neutral and positive hyperconjugation. Note that the NBO interaction energies for neutral hyperconjugation needs to be multiplied by two since it is bidirectional.

Patterns of hyperconjugation.

So far, we have classified delocalizing interactions by the type of orbitals and by directionality (or lack of thereof) of the overall electron density transfer. Topologically, it is often helpful to separate orbital interactions into three classes: vicinal, geminal and remote interactions. These three patterns correspond, respectively, to the interaction of orbitals at the same atom (geminal), adjacent atoms (vicinal) and atoms that are not directly bonded (remote) (Figure 14). Each of these patterns has its own unique features that we will discuss below.

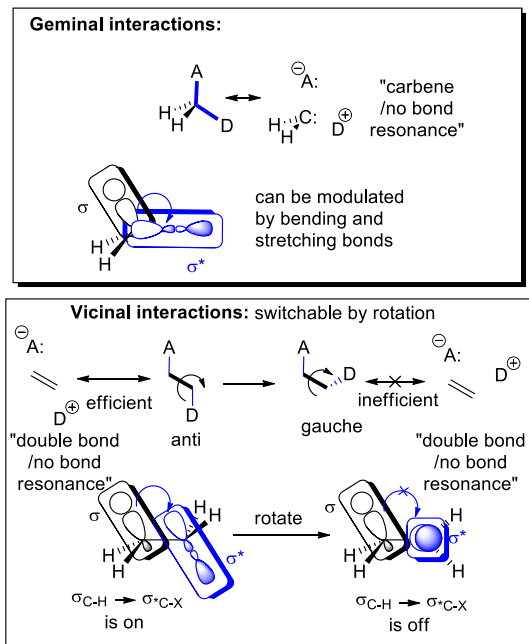


Figure 14. Geminal and vicinal hyperconjugative interactions

Geminal

Geminal interactions correspond to interactions of orbitals at the same atom (Figure 14). From the resonance point of view, geminal hyperconjugation is associated with the increased contribution of the carbenoid resonance structure. In general, its importance increases when the two substituents at the same carbon have drastically different electronegativity or when the carbene fragment is especially stabilized otherwise. Although such interactions are ubiquitous and provide important contribution to the overall molecular stability,^{44,45} they are not readily “switchable” by conformational changes and remain “invisible” in the conformational analysis. For the above reasons, the geminal effects are discussed relatively rarely. However, there is an accumulating evidence that this delocalization pattern plays an important, albeit often underappreciated, role in molecular stability.

In particular, geminal hyperconjugation was suggested to play an important role in the “alkane branching effect”, a fundamentally important fact that simple alkanes with branched carbon skeletons, for example, isobutane, are more stable than their linear isomers, for example, *n*-butane. In a similar way, the “kinks” (or “protobranches”) in the chains of linear alkanes were suggested to explain their greater stability relative to methane or ethane.⁴⁶ NBO analysis by Kemnitz and coworkers suggested that a significant part of this stabilization comes from the σ/σ* geminal interactions.⁴⁷

Vicinal

Vicinal interactions are very common because they correspond to the interactions of orbitals at two directly connected atoms. The stereoelectronic aspects of such interactions are immediately obvious when stability and reactivity change as a function of relative arrangement of the interacting bonds in space (i.e., via rotation around the bridging bond). Vicinal interactions are responsible for the majority of stereoelectronic effects. Because these interactions involve

orbitals at atoms that are already connected with a sigma bond, vicinal hyperconjugation is generally mediated by a π -type overlap of the donor and acceptor orbitals. We will provide numerous examples of vicinal hyperconjugations in this review.

Extended

Long range delocalization can follow a variety of patterns that are mediated by through bond (TB) and through space (TS) interactions. At the larger separations between the donor and the acceptor, remote interactions evolve into supramolecular contacts responsible for the presence of intermolecular interactions (e.g., H-bonding, *vide infra*). However, at the shorter separations, the delocalization patterns have distinct features. In this section, we will concentrate on such features for the donor/acceptor pairs separated by one or two atoms. When σ -orbitals are involved, these patterns are generally referred to as homohyperconjugation and double hyperconjugation.

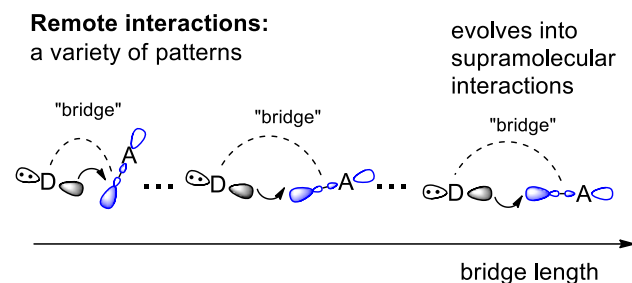


Figure 15. Remote hyperconjugative interactions

Homoconjugation and homohyperconjugation are observed when a saturated center intervenes between donor and acceptor orbitals. Homoconjugation is ubiquitous because π -bonds or lone pairs can serve as excellent donors. Interactions of donor and acceptor orbitals, that are not directly connected, serve as the electronic basis of such interesting phenomena as anchimeric assistance, neighboring group participation, transannular interactions etc. As the interactions grow stronger, they can transform into chemical bond formation in a cyclization reaction. Due to the immensity of the topic and the broad variations in geometries that allow such interactions, we will limit our discussion of such effects to several fundamentally important basic patterns.

The chemical community is accustomed to the idea that conjugation through π -arrays can provide long-range communication. For example, conjugated arrays are commonly used as bridges for electron/hole transport both in Nature's photosynthetic center and in artificial devices for light harvesting and conversion. Although it is less clear how far hyperconjugation extends, a number of extended hyperconjugation patterns have been investigated.⁴⁸ Some of these patterns are provided in Figure 16 which follows the lucid classification of Lambert and Ciro.⁴⁹

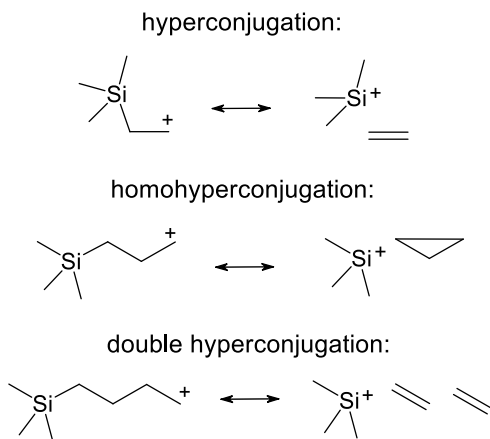


Figure 16. Comparison of normal and extended positive hyperconjugation.

Homohyperconjugation is observed when a saturated center intervenes between donor and acceptor orbitals. When the acceptor is a cationic p-orbital, the phenomenon is called the γ -effect or, sometimes, percaudal interaction. It has been particularly well studied for silicon and tin.⁵⁰ When the acceptor is a σ^* -orbital and donor is a lone pair, this effect is referred to as homoanomeric effect.⁵¹ Both the γ -effect and the homoanomeric effect are considered to result primarily from direct through-space interactions.

Double hyperconjugation extends the delocalization range even further by placing a σ -bridge between a donor and an acceptor. In chemistry of cations, this interaction has been called the δ -effect and found experimentally to be significant for silicon and tin.⁵² Expansion of these studies to a larger set of cations⁵³ found that, double hyperconjugation with a number of equatorial substituents can provide significant stabilization ($R = AlH_2, GaH_2, GeH_3, AsH_3, SiH_3, PH_2, BH_2, SeH$, or destabilization ($R = SH, Br, NH_2, Cl, O, F$) to the δ -cyclohexyl cation with the equatorially oriented empty p-orbital. These stabilization effects were used for the development of a new scale hyperconjugative donor ability of σ -bonds (see section “Hyperconjugation in acyclic and cyclic carbocations. Hyperconjomers” for additional details).

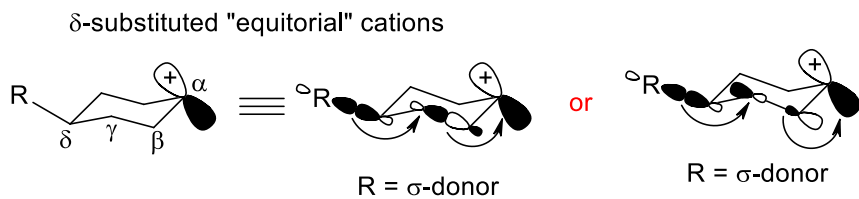


Figure 17. The significant stabilization of a δ -cyclohexyl cation by a series of equatorial substituents via double hyperconjugation.

The more extended versions of hyperconjugation where the donor and acceptor orbitals are separated by the larger number of bonds, the importance of intramolecular constraints decreases and the boundary between inter- and intramolecular interaction patterns starts to blur. For the larger separations, the favorable scenarios closely follow the general rules of supramolecular chemistry and, in the case of stronger interactions, evolve into the orbital preferences for the formation of new chemical bonds.⁵⁴

Factors controlling hyperconjugation:

Overlap/orbital symmetry.

Vicinal orbitals have to be coplanar to ensure the optimal interaction. Regarding the two possible coplanar geometries, the common stereoelectronic feature observed for the interaction of vicinal orbitals is the general preference of anti-periplanar arrangement over syn-periplanar geometry (Figure 18). This preference leads to a particularly simple, yet surprisingly powerful generalization, often referred to as the “main stereoelectronic rule”. The rule can be expressed as follows: “There is a stereoelectronic preference for conformations in which the best donor lone pair or bond is antiperiplanar to the best acceptor bond”.⁵⁵

Vicinal donor/acceptor interactions are increased when the donor and the acceptor orbitals are **antiperiplanar**

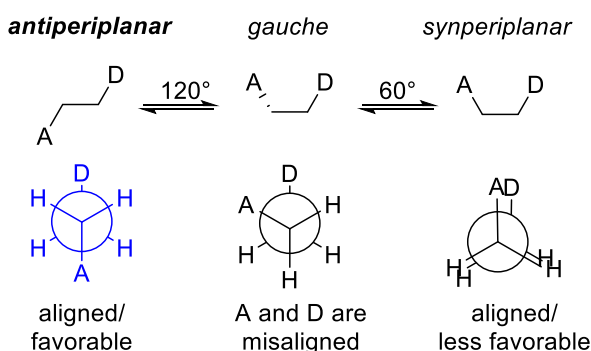


Figure 18. Newman projections showing the possible conformations in a donor/acceptor substituted ethane molecule. The “main stereoelectronic rule” favors the antiperiplanar conformation.

The general preference of the antiperiplanar arrangement over synperiplanar geometry is displayed in the higher stability of the staggered conformation of ethane, *s-trans* conformation of butadiene, eclipsed (an obvious misnomer, as we will show later!) conformation of propene (Figure 19), and a number of other stereoelectronic effects.

The origin of this preference, for the case of ethane, is illustrated in the bottom part of Figure 19, which clearly displays the unfavorable overlap between the $\sigma_{\text{C-H}}$ orbital and a node of the σ^* -orbital for the syn-periplanar arrangement in the eclipsed conformation.^{56,57}

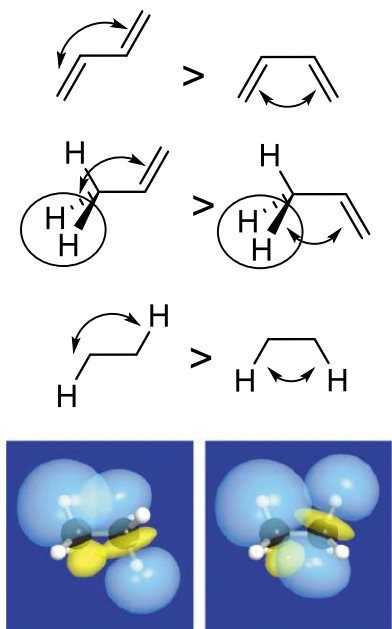


Figure 19. Top: The antiperiplanar stereoelectronic preference for vicinal conjugation and hyperconjugation. Bottom: Key hyperconjugative interactions between $\sigma_{\text{C-H}}$ and $\sigma^*_{\text{C-H}}$ orbitals. [Reprinted with permission from ref. 16]

Since vicinal hyperconjugation is increased in the antiperiplanar conformation, a number of hyperconjugative stereoelectronic effects are fully displayed in the most favorable geometry, where the best donor and the best acceptor are antiperiplanar to each other (see section “Examples/Stereoelectronic effects” for the illustrative examples).¹

A few caveats are worth keeping in mind. Of course, this preference cannot apply to systems where the notion of antiperiplanarity itself disappears, e.g., the case when the acceptor center is a pure p-orbital.¹ The antiperiplanar preference can be further masked by the effects of sterics and electrostatics. In addition, it is only applicable to intramolecular vicinal interactions. Intermolecular preferences are different.

For intermolecular interactions dominated by negative hyperconjugation, the best stereoelectronic arrangement involves a collinear arrangement where the donor orbital interacts with the back lobe of the σ^* -orbital. Such geometries are characteristic for $\text{S}_{\text{N}}2$ reactions and H-bonding, both of which involve electron density transfer from a lone pair to a back lobe of a polarized σ^* -orbital. Because such interactions lead to an increase in the population of an antibonding X-Y orbital, they elongate the X-Y bond,^{3,58} leading to the bond cleavage (for the $\text{S}_{\text{N}}2$ reaction) or the well-known red-shift in the IR-stretching frequency widely regarded as the “signature of H-bonding”.⁵⁹ The stereoelectronic covalent component of H-bonding is also responsible for the well-defined structural requirements such as the collinear Y...H-X arrangement which plays a key role in H-bonded supramolecular assemblies. H-bonding and $\text{S}_{\text{N}}2$ -type bond cleavage are merged together in the process of hyperconjugative Rg-H bond elongation in Rg-H...Y complexes, where Rg is a rare gas element.⁶⁰

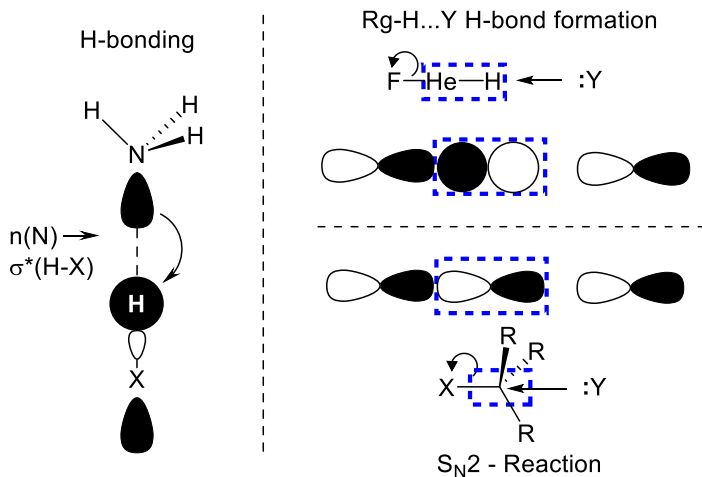


Figure 20. a) Hyperconjugative stabilization of H-bonded complexes. b) The analogy of $F^- \dots He \dots Y^+$ fragmentation of $FHeH \dots Y$ complexes with an S_N2 reaction.

For intermolecular positive hyperconjugation, the possible interaction geometry is not restricted to the back lobe of the σ -bond. Coordination of an electrophile can occur at the center of the donor bond, leading to a front-side attack in an S_E2 bond-cleavage event (Figure 21).⁶¹

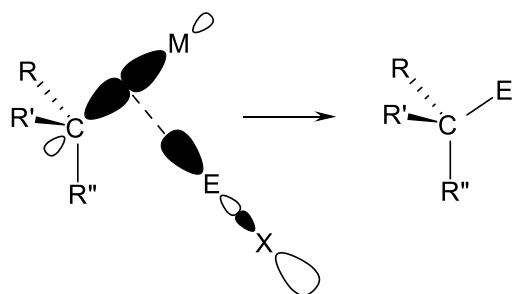


Figure 21. Intermolecular positive hyperconjugation in the TS for an S_E2 process with retention of configuration. M is an electrofuge, R is an alkyl group, and E is the electrophilic site in the reagent EX.

For remote hyperconjugative interactions, the above stereoelectronic requirements can blend into a complex picture. For example, homohyperconjugation has several favorable patterns different in the relative position of the donor and acceptor orbitals in space. Interaction of an equatorial lone pair with the back lobe of an equatorial σ^*_{C-Y} orbital (the W-effect) is important in azacyclohexanes^{51,62} but not in oxa- and thiacyclohexanes, where an alternative pattern (the Plough effect, Figure 22b) plays a more important role. The “mirror image” of the Plough effect, illustrated in Figure 22c, provides no hyperconjugative stabilization to the molecule (due to the same stereoelectronic reasons which disfavor a front lobe attack in an S_N2 process) but leads to a noticeable elongation of the axial bond. This observation seems to be the first documented hyperconjugative effect without a concomitant stabilization.⁶³ It shows that even when hyperconjugative interactions cannot lead to stabilization it may, when imposed by structural constraints, still change electronic distribution and geometries. Note the analogy between such effects and the known differences between the backside (favorable) and frontside (unfavorable) trajectories for an S_N2 attack.

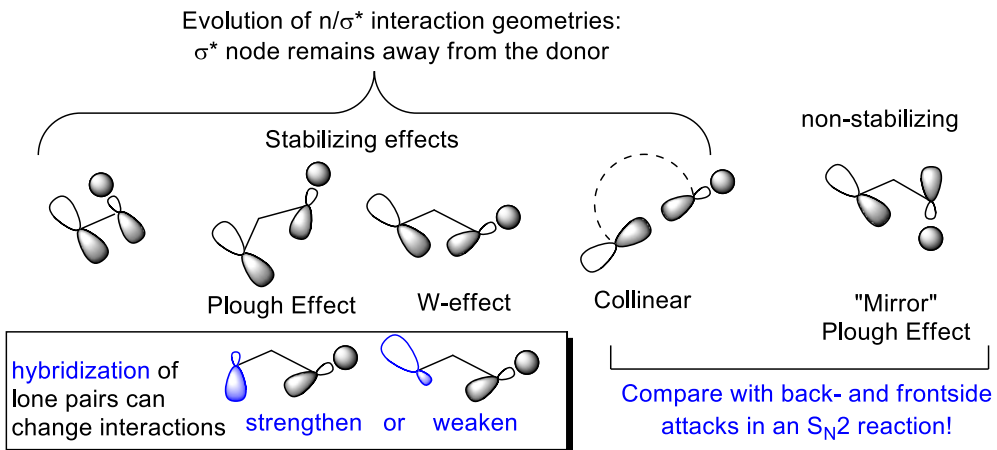


Figure 22. The comparison of possible homoanomeric interaction patterns in six-membered saturated heterocycles illustrates the connection between stabilizing to non-stabilizing hyperconjugative interactions. The bottom part of the figure shows how hybridization of the lone pair can change the efficiency of through-space interactions.

Acceptor ability of sigma bonds: the opposing roles of electronegativity and orbital energies.

A systematic study of the general trends in σ -acceptor properties of C-X bonds in monosubstituted ethanes, where X is a main group element from groups IVa - VIIa revealed that the acceptor ability of the C-X σ -bonds relative to the same donor (an antiperiplanar C-H bond) increases towards the end of a period and down a group (Figure 23).

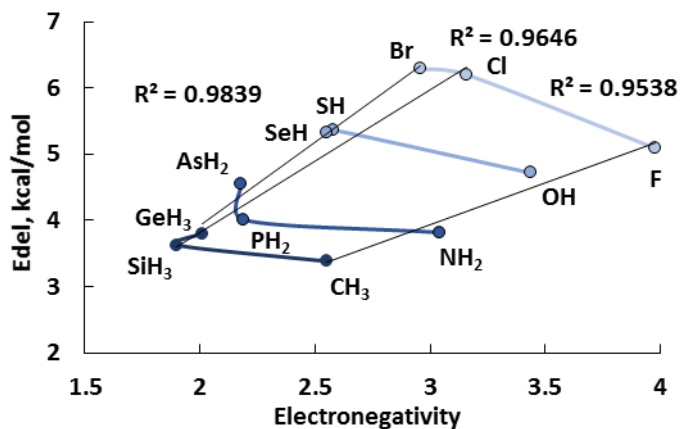


Figure 23. Correlation of energy of vicinal NBO $\sigma_{\text{C-H}} \rightarrow \sigma^*_{\text{C-X}}$ interaction, E_{del} with electronegativity of element X in substituted ethanes, $\text{CH}_3\text{CH}_2\text{X}$.

Enhancement of acceptor ability of C-X σ -bonds in periods parallels the increase in electronegativity of X as the result of favorable changes in the σ^* -polarization (Figure 24, Figure 25).^{20,64}

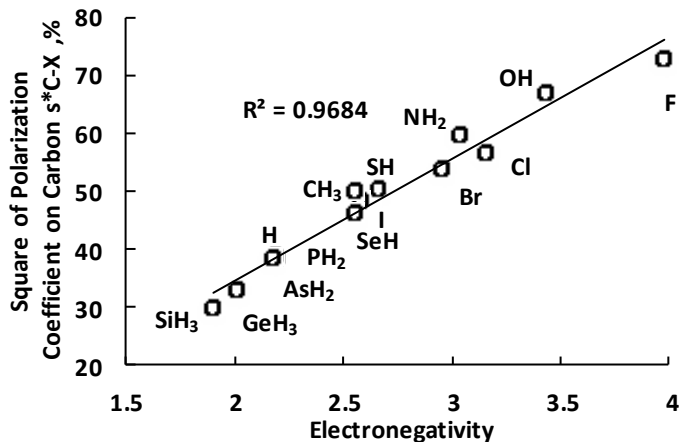


Figure 24. Correlation of polarization of σ^*_{CX} orbitals with electronegativity of element X in substituted ethanes, $\text{CH}_3\text{CH}_2\text{X}$. Adopted with permission from ref. 20.

On the other hand, augmentation of acceptor ability in these groups is opposite to the changes in electronegativity of X and in the C-X bond polarization, following instead the decrease in the energy of σ^*_{CX} orbitals when one moves from top to the bottom within a group (Figure 25). Even when polarity of C-X bonds decreases, the C-X bond can still function as a good acceptor as long as the σ^*_{CX} has low energy. These trends can be readily understood based on the Eq. 1 given in section “Wavefunction analysis”.

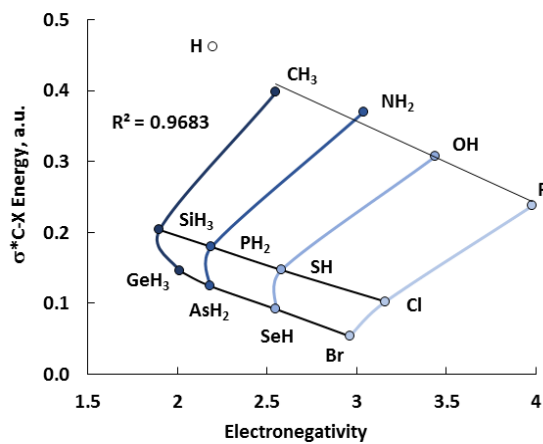


Figure 25. Correlation of energy of σ^*_{CX} orbitals with electronegativity of element X in substituted ethanes, $\text{CH}_3\text{CH}_2\text{X}$.

The NBO relative order of acceptor ability of σ^*_{CX} bonds towards an antiperiplanar C-H bond is in the following order (the energies of $\sigma_{C-H} \rightarrow \sigma^*_{CX}$ interactions are given in parentheses): X= Br (6.3)> Cl (6.2)> SH(1) (5.4)> F (5.1)> OH(1) (4.7) ≈ SH(2) (4.7) ≈ SeH (4.7) ≈ PH₂(1) (4.6) ≈ AsH₂ (4.5) ≈ NH₂(1) (4.5) > OH(2) (4.2) > PH₂ (2) (4.0) > NH₂(2) (3.8) ≈ GeH₃ (3.8) > SiH₃ (3.6) > CH₃ (3.4) > H (3.2). Two values for several substituents correspond to different conformers.

This simple picture of the acceptor ability of σ -bonds being controlled by electronegativity in periods and by σ^* -orbital energy in groups is changed in monosubstituted ethenes, where the role of electronegativity of the substituent X becomes more important due to increased overlap between σ -orbitals. As a result, the acceptor ability of the σ -bonds in monosubstituted ethenes changes in a more complex fashion. Overall the acceptor ability of σ -bonds can be significantly modified by substitution and is conformer-dependent.

Polarization of σ -bonds leads to the larger coefficient at the less electronegative of the two connected atoms. This trend accounts for anisotropy of intramolecular orbital interactions. For example, it explains why C-O bonds are stronger acceptors than O-C bonds. Interestingly, stereoelectronic effects displayed by C-X bonds with X from second and third periods are highly anisotropic (Figure 26). For example, C-chalcogen bonds are excellent σ -acceptors at the carbon end but poor σ -acceptors at the chalcogen end.²⁰ The later effect is mostly geometric and stems from the greater lengths of the C-S and C-Se bonds.

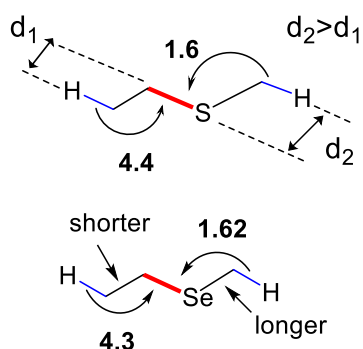
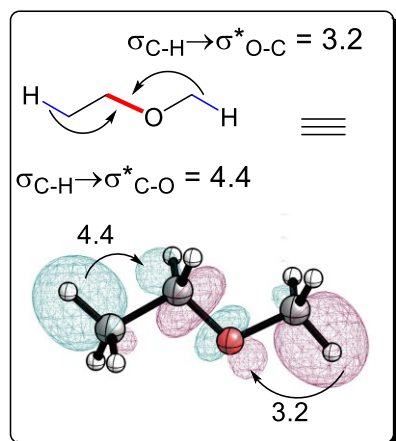


Figure 26. Comparison of acceptor ability (NBO E_{del} energies in kcal/mol) of C-X bonds in different directions.

Donor properties of lone pairs.

The relatively subtle differences in the hyperconjugative energies given in Figure 25 become more pronounced and chemically significant in hyperconjugative interactions with better donors, such as a lone pair at nitrogen. The NBO data of α -halogen amines indicates that both the high energy of the non-bonding orbital (decreasing the ΔE term) and its higher polarizability (increasing the F_{ij} term) account for the increased interaction energy.²⁰ Selected properties of

nonbonding electronic orbitals (lone pairs) of O, S, Se, and N are presented below and summarized in

Table 1 and Figure 27.⁵¹

Hybridization of lone pairs.

Differences in hybridization are particularly important for stereoelectronic hyperconjugative interactions due to several reasons. First, hybridization is directly related to molecular geometry and determines the valence angles and the direction in which non-bonding orbitals are projected in space for the overlap with acceptor orbitals. Second, hybridization controls the relative size of the two lobes of a lone pair. The front and back lobes are equivalent for purely p-lone pairs, whereas the back lobe decreases in size with decrease in the p-character in hybrid sp^n lone pairs. Third, hybridization of a donor orbital is related to its absolute energy (Figure 27). An increase in the p-character leads to an increase in orbital energy which decreases the energy gap between the donor lone pair and an acceptor σ^* - or π^* -orbital. In general, the donor ability parallels the amount of p-character of a lone pair - lone pairs with 100% p-character are intrinsically better donors than the respective sp^n hybrids.

Oxygen

In tetrahydropyran, the presence of a higher energy p-orbital (instead of a sp^3 hybrid) parallel to the vicinal axial acceptors maximizes the hyperconjugative anomeric $n \rightarrow \sigma^*_{C-Y}$ interaction. NBO analysis which determines “the best hybrids” describing a Lewis structure finds two lone pairs of different hybridization in tetrahydropyran: a purely p-orbital and a $sp^{1.3}$ hybrid. The deviation from sp hybridization predicted by the idealized model is readily explained by Bent’s rule.⁶⁵

Sulfur and Selenium

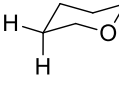
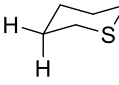
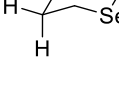
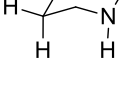
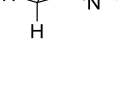
In contrast to oxygen, the sulfur atom in thiacyclohexane uses *more* p-character ($sp^{5.55}$) in its bond with carbon than one would expect from the idealized model. As a result, only a little p-character is left for the equatorial lone pair ($sp^{0.4}$). This makes this lone pair a relatively poor donor and explains the origin of the drastic differences between the equatorial lone pairs of sulfur and oxygen in respective saturated heterocycles.

Nitrogen

Nitrogen is more electronegative than carbon and hydrogen and, as expected from Bent’s rule, it uses hybrid orbitals with increased s-character for the formation of N-C and N-H bonds (

Table 1). This leaves more p-character for the lone pairs compared to what one would expect from the textbook sp^3 hybridization picture. This phenomenon leads to the well-known deviation of valence angles at nitrogen from the classic tetrahedral angle and contributes to the relatively high donor ability of nitrogen lone pairs. In general, an increase in the size of alkyl substituents at nitrogen leads to an increase in the p-character of the nitrogen lone pairs.⁵¹

Table 1. The NBO s-character, hybridization and energy of all lone pairs (X = N, O, S, Se) in selected saturated heterocycles at the B3LYP/6-31G** level, the NBO plots of the lone pairs and s-character in C-X bonds. The axial and equatorial lone pairs are drawn as dissected by H_{ax}-C3-X1 or H_{eq}-C3-X1 planes, respectively.

	s-character in n(X), % ^a	sp ^{n(X)}	E(X), a.u. ^a	n(X) _{ax} , e	n(X) _{eq} , e	s-character in C-X, % ^b
	0.03 (44.16)	p(sp ^{1.26})	-0.27(-0.54)			20.53 (C); 27.89 (O)
	0.03(69.89)	p(sp ^{0.43})	-0.22(-0.61)			20.54 (C); 15.18 (S)
	0.05 (76.66)	p(sp ^{0.30})	-0.21(-0.67)			18.51 (C); 11.74 (Se)
	17.99	sp ^{4.55}	-0.27	-		23.51 (C); 29.94 (N)
	17.86	sp ^{4.59}	-0.27		-	23.62 (C); 29.65 (N)

^aFor X=O, S, Se, the data for the equatorial lone pairs are given in parentheses. ^bs-Character in hybrid orbitals forming C-X (X = N, O, S, Se) bonds.

Energies of lone pairs

The orbital interaction energy is inversely proportional to the energy gap, ΔE in Eq. 1, which depends on the relative energies of lone pairs. Relative trends in the lone pair energies can be readily understood in terms of their hybridization (percentage of s-character) and the electronegativity of X. An increase in electronegativity and decrease in the p-character lowest the orbital energies of the lone pairs (Figure 22). Although oxygen is more electronegative than nitrogen, the purely p “axial” lone pair on oxygen has essentially the same energy as the ca. sp⁵ axial and equatorial nitrogen lone pairs. In this case, effects of hybridization and electronegativity compensate each other. In chalcogens, the energies (and donor ability) of the axial lone pairs increase when going from oxygen to selenium (O < S < Se), whereas the energies and donor ability of equatorial lone pairs fall in the opposite direction (O > S > Se). The first trend is explained by the difference in electronegativity and the period number, the second trend by the increase in the s-character for S and Se relative to that of O. As a result of these two effects, the energy gap between the axial and equatorial lone pairs of chalcogens increases with

their atomic number. In every case, the higher energy axial orbitals with 100% p-character are intrinsically better donors than the respective equatorial sp^n hybrids.

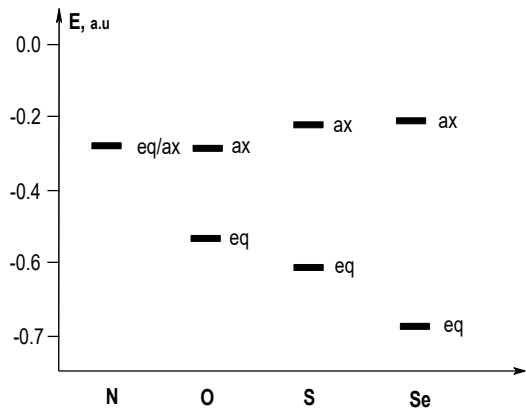


Figure 27. NBO energies (in a.u., 1 a.u. = 627.5 kcal/mol) of axial and equatorial lone pairs in oxa-, thia-, selena-, and azacyclohexane calculated at the B3LYP/6-31G** level.

Due to the above differences, stereoelectronic effects observed in O- and S-heterocycles cannot be automatically transferred to the N-heterocycles and vice versa. The analogy between different chalcogens (O, S, Se) is generally more reliable but the differences in the magnitudes of $n_{ax} \rightarrow \sigma^*_{ax}$ interactions call for caution as well.

The differences in hybridization of O and S lone pairs are also clearly manifested in the directionality of hydrogen bonds to carbonyls and thiocarbonyls (Figure 28). For sulfur, the sp^n -lone pair has so much s-character that it is hardly available for H-bonding and the preferred H...SC trajectories of H-bonding are much closer to 90 degrees.

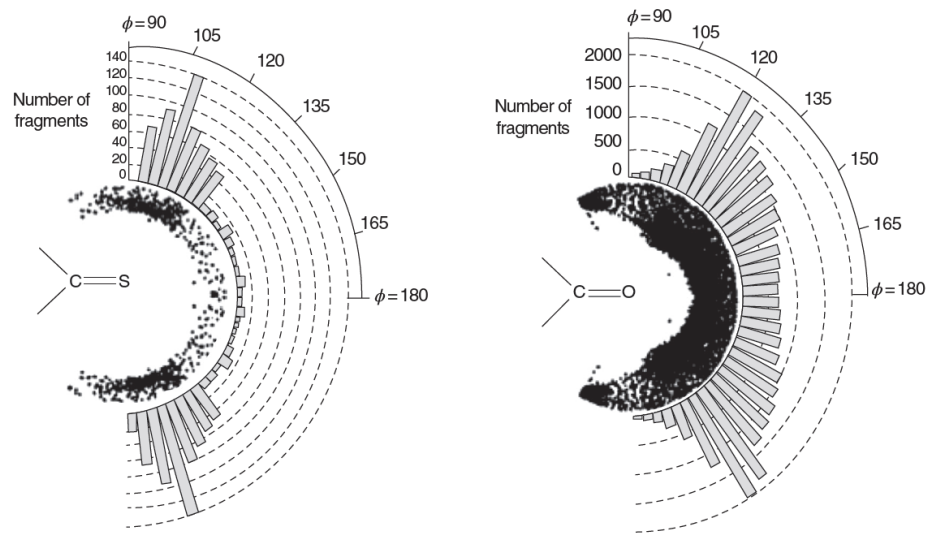


Figure 28. Acceptor directionality of C=S (left) and C=O (right) groups in N/O-H...O/S=C hydrogen bonds. Note that the directionality is much closer to the perpendicular approach (coordination

with the p-type lone pair) for C=S. (Reprinted with permission from ref. 66. Reproduced with permission of the International Union of Crystallography)

Contrasting effects of α -heteroatoms on the lone pair energies:

An important question at the heart of the so-called α -effect⁶⁷ is whether the lone pairs of two directly connected heteroatoms combine into a *more* powerful donor than each of the lone pairs taken *separately*. Simple MO arguments suggest that mixing of the two lone pairs should lead to formation of a higher energy antibonding MO (Figure 29A). However, the overall MO energy increase can be counterbalanced by the inductive and hybridization effects of the acceptor neighbor. According to Bent's rule, presence of electronegative group Y at atom X, increases the allocation of *p*-character of X in the X-Y orbital, thus making the lone pair of X have more *s*-character and be less donating.

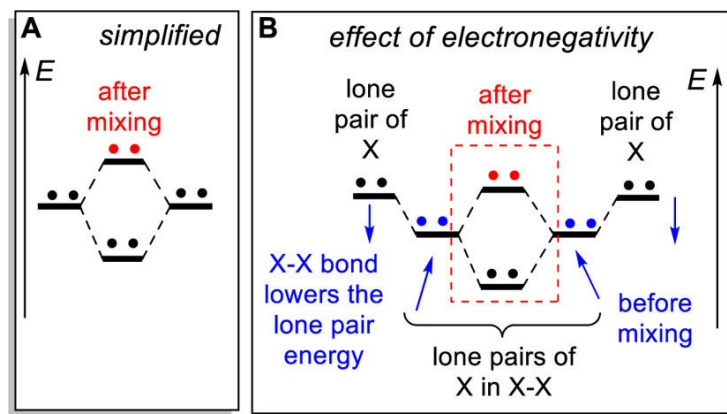


Figure 29. A. The simplified MO description of α -effect; B. Formation of X-X bond can lower the lone pair energy and compensate for the expected increase in the donor ability of stereoelectronically coupled lone pairs. Reprinted with permission from ref. 67.

The effect of α -heteroatoms on the lone pair energies can be understood by combining NBO analysis with the examination of highest occupied MOs (HOMOs) in ammonia, water and two conformers of hydrazine and hydrogen peroxide. Natural Bond Orbital (NBO) analysis provided energies and hybridizations for the individual lone pairs whereas the canonical MO analysis described the energetic consequences of the lone pairs' mixing with each other and/or other parts of the molecules. This analysis reveals differences between oxygen and nitrogen that originated from a shifting balance in the interplay between hybridization and electronegativity (Figure 30).

The addition of an α -heteroatom decreases the NBO lone pair energy in the most stable conformers of N_2H_4 and H_2O_2 relative to the lone pairs of NH_3 and H_2O , respectively. The observed energy lowering is greater for the introduction of oxygen, a more electronegative neighbor. When rotation around the N-N and O-O bond aligns the lone pairs at the two adjacent heteroatoms, an additional large effect on the lone pair energy in hydrazine is observed. The orbital alignment effect on the lone pair energies in H_2O_2 is much smaller. The much larger effect in the nitrogen case may indicate the greater importance of rehybridization⁴ where increase in pyramidalization and *s*-character in the lone pair are coupled to each other. For oxygen, rehybridization at the *s*-type lone pair and the associated energy decrease are much smaller.

The oxygen's *p*-type lone pair retains its original 100% *p*-character and shows a much smaller change in energy.

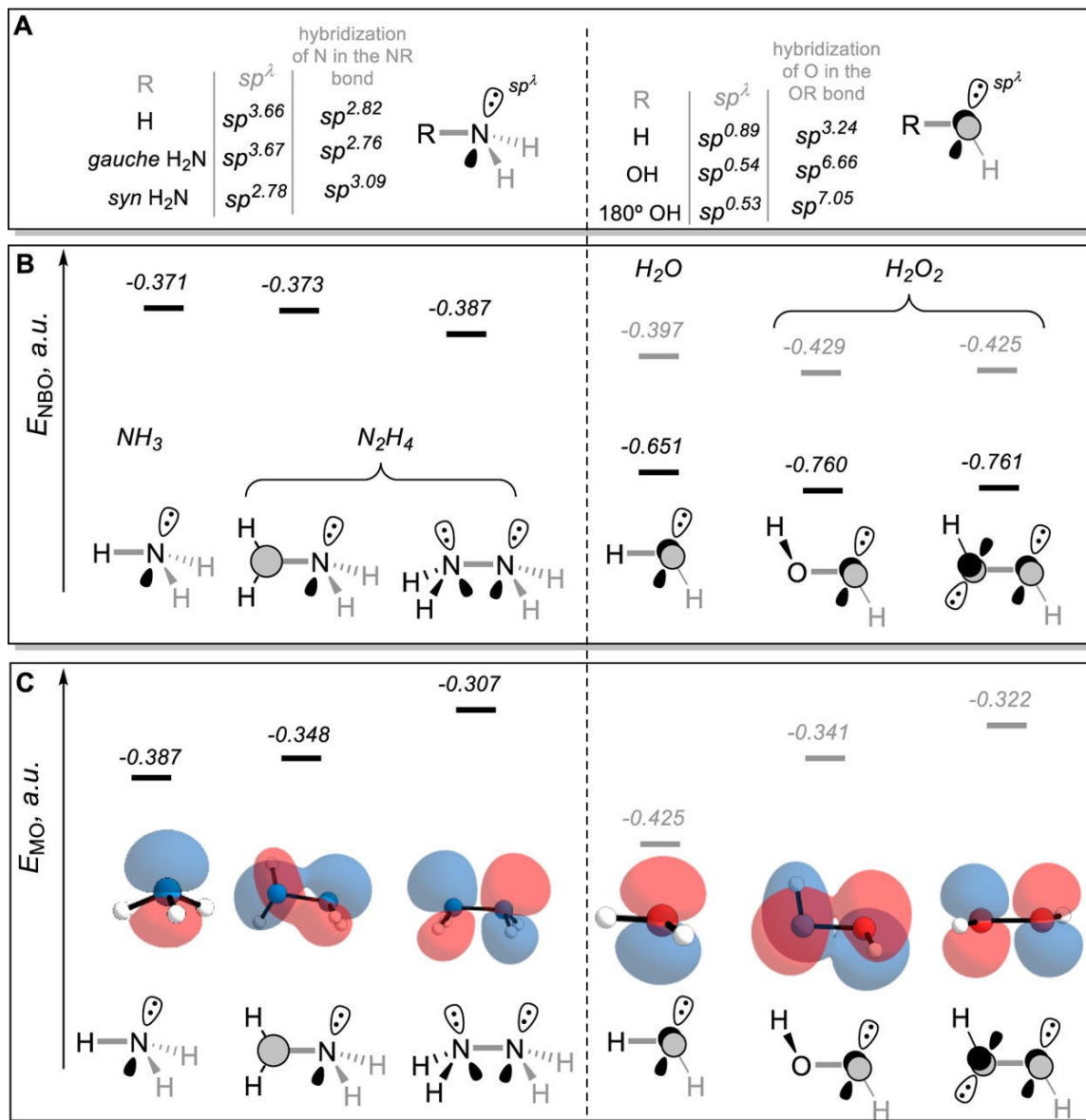


Figure 30. A: Hybridization for RNH_2 and ROH species. B: Energies of NBOs corresponding to individual lone pairs of O- and N-lone pairs. Grey values for the O-containing molecules correspond to the high energy *p*-lone pair, black values describe σ -type sp^n hybrid lone pair. C: The anti-symmetric lone-pair combination MOs in the representative conformations of hydrazine and hydrogen peroxide. Reprinted with permission from ref. 67

When the localized non-bonding orbitals at the heteroatoms mix to form the MOs of N_2H_4 and H_2O_2 , the resulting HOMOs are raised. For the most stable conformation of hydrazine, the HOMO is raised only moderately relative to that of NH_3 . In contrast, the HOMO of the most stable H_2O_2 conformation was much higher than the HOMO of H_2O . One can attribute these differences to hyperconjugative mixing with the σ_{NH}^* of the adjacent NH_2 moiety that can

stabilize the hydrazine HOMO. On the other hand, each of the oxygen atoms has two lone pairs and mixing of the non-bonding orbitals in the peroxide moiety is unavoidable. When the nitrogen lone pairs were aligned in the eclipsed conformations of hydrazine and H_2O_2 , the antisymmetric combination of the two lone pairs is significantly destabilized, as expected from the ground state destabilization model of the α -effect.

Donor ability of sigma bonds.

It is well established that such donors as C-Si, C-Ge and C-Sn bonds are capable of providing significant stabilization to a developing positive charge.^{39,68} For example, Lambert and coworkers reported that axial trimethylsilyl substitution can lead 10^{12} rate enhancements upon in the elimination of axial leaving groups (Figure 31).^{68b} The hyperconjugative interaction with the antiperiplanar TMS group was suggested to be responsible for $\sim 10^{10}$ acceleration, with the rest (10^2) originating from inductive interactions. The lower reactivity of the cis isomer stems from the less favorable (gauche) arrangement of the departing group relative to the C-Si donor.

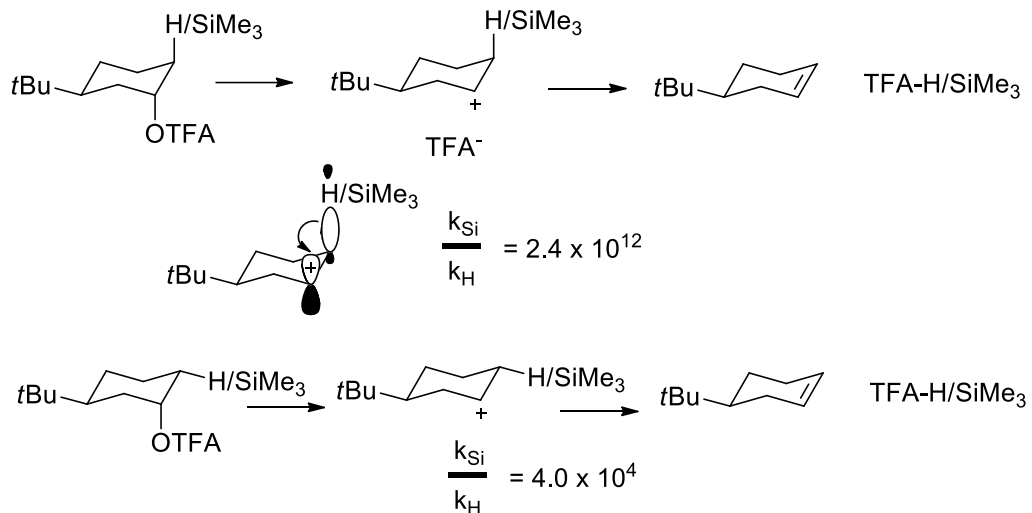


Figure 31. Conformational effects on the rate of cationic eliminations reflect stereoelectronics of the developing cation stabilization by C-Si σ -donors.

However, the relative ability of many common sigma donors, including the most ubiquitous case of C-H vs. C-C bonds, has been widely debated. The difference between these two bonds is small in ground state neutral molecules.⁶⁹ For example, a low temperature X-ray structural study by Spinello and White found that the differences in the donor abilities of C-C and C-H bonds towards $\sigma_{\text{C}-\text{O}}$ acceptors of variable electronic demand are comparable to the experimental uncertainty of measurements.⁷² Recent computational studies also found that these differences are small. Natural Bond Orbital (NBO) analysis indicates that C-H bonds are slightly better donors than sigma C-C bonds in cyclohexane and related molecules.⁷⁰ A similar conclusion was made by Rablen and coworkers in a theoretical study on the origin of gauche effect in substituted fluoroethanes.⁷¹ In contrast, EDA computations of Frenking and coworkers suggested a slight preference in the opposite direction.⁷²

Hyperconjugative effects are expected to be stronger in cations. Nathan and Baker reported that a Me group provides more stabilization to the developing positive charge at the p-benzylic

position than Et, i-Pr and t-Bu groups in the solvolysis of p-alkyl substituted benzyl bromides⁷³ and attributed this order of reactivity to the greater donating ability of C-H bonds compared to that of C-C bonds. Although these results are consistent with the trends in ¹³C NMR chemical shifts of the β -carbon in β -substituted styrenes in solvents of different polarity,⁷⁴ the opposite trend was found in the gas phase pyrolysis of 1-arylethyl acetates, which cast a shadow of doubt on the original interpretation of Nathan-Baker effect.⁷⁵

Local steric and electrostatic effects can be minimized and a more balanced description of relative donor ability of σ -bonds can be accomplished if the donor and acceptor sites are not *directly* connected. This approach has been tested computationally using two independent criteria: (a) relative total energies and geometries of two conformers (“hyperconjugomers”) of δ -substituted cyclohexyl cations (b) and Natural Bond Orbital (NBO) analysis of electronic structure and orbital interactions in these molecules.⁵³

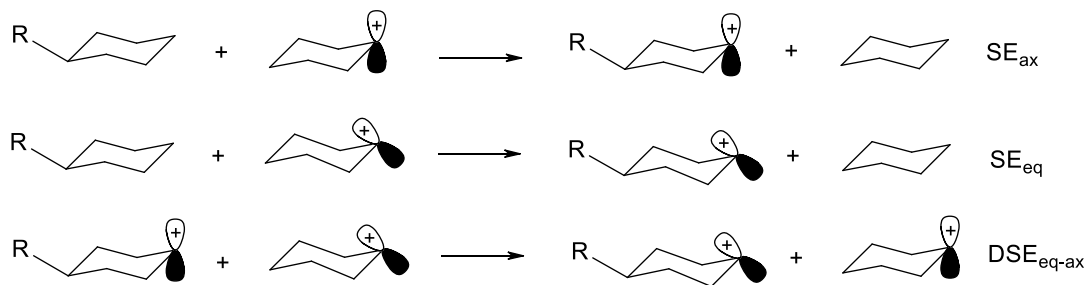


Figure 32. Three isodesmic equations used to calculate substituent stabilization energies (SE_{ax} (top), SE_{eq} (middle), ΔS_{eq-ax} (bottom)) in the equatorial and axial cyclohexyl cations.

These effects are estimated by the three isodesmic reactions given in Figure 32. The stabilization energies provided by these isodesmic reactions give different information. Effects of substituents in axial cations, which are described in the top part of Figure 32, include a complicated interplay of many factors such as hybridization, inductive and field effects, which are still present in these species even when double hyperconjugation is minimized. Interestingly, most of the δ -substituents are destabilizing when compared to the unsubstituted “axial” cation.

In sharp contrast with the situation in “axial” cations, many substituents have a stabilizing effect on the “equatorial” cations (Figure 32, middle). Such effects can be rather large indicating that δ_{C-X} bonds are capable of efficient interaction with the cation p-orbital as long as all orbitals participating in the double hyperconjugation interaction relay overlap efficiently. For the same reason, the destabilizing effects of sigma acceptors such as C-halogen bonds are also more pronounced in equatorial cations. Thus, the above “equatorial” stabilization energies (SE_{eq}) include stabilization or destabilization provided by σ_{C-X} donors through the double hyperconjugation mechanism. They also include other effects, such as those mentioned in the previous paragraph.

Subtraction of axial (SE_{ax}) from equatorial (SE_{eq}) stabilization energies provides the bottom equation of Figure 32 where the contributions of the above non-hyperconjugative (inductive, field etc) effects are partially compensated. Although this compensation is not perfect, the ΔS_{eq-ax} values give an improved estimate of the hyperconjugative stabilization of “equatorial” cations which has its source predominantly in double hyperconjugative stabilization.

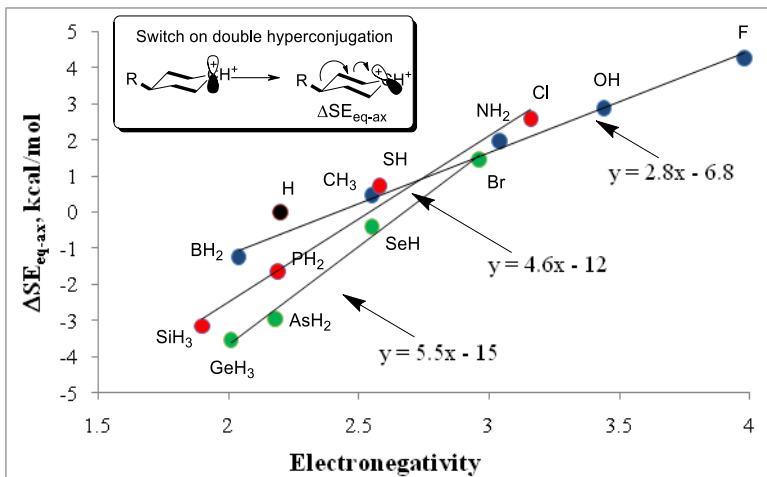


Figure 33. The correlations between the differences in stabilization energies of $\delta\text{-XH}_n$ substituents in the equatorial and axial cyclohexyl cations (Figure 17) and electronegativity of the X. Separate correlations are shown for each row. Calculations were performed at the B3LYP/6-31G** (B3LYP/6-311++G**) level (Reprinted with permission from ref. 53)

Although the ΔSE_{eq-ax} values from all periods are reasonably well described by a single correlation (Figure 33a), suggesting that the ΔSE_{eq-ax} values indeed provide a reasonable estimate of the relative trends in hyperconjugative donor ability of C-R bonds, the δ -substituents cluster into three groups. As shown in Figure 33a, the first group displays positive ΔSE_{eq-ax} values and consists of cation-destabilizing, strongly electronegative acceptors with Pauling electronegativity of ≥ 3 . The second group includes elements of intermediate electronegativity which form C-R bonds with donor abilities close to that of C-H bonds. The final group includes relatively electropositive substituents with negative ΔSE_{eq-ax} values. In this group, the ΔSE_{eq-ax} values are scattered, and electronegativity is not a good indicator of donor ability towards the δ -cationic center. The scattering is related to the differences in polarizabilities⁷⁶ of C-R bonds in the different periods, as shown in Figure 33b. The divergence of the curves for different periods is caused by the fact that the more polarizable C-R bonds with heavier elements are more sensitive to the introduction of a positive charge at the remote position even when the electronegativities of the respective elements are close (note H vs. B and B vs. Ge). The differences in polarizability between the elements of the first and second rows are especially pronounced.

Interestingly, the relative positions of carbon and hydrogen switch depending on the evaluation method. According to SE_{eq} values (“apparent donor ability” of substituent R) the CH_3 group is a stronger donor than the H substituent, a trend which is reversed according to ΔSE_{eq-ax} values (“apparent hyperconjugative donor ability” of σ_{C-R} bond). In addition, similar switches are observed for a number of other pairs including potentially important combinations of other orbitals of similar donor ability (Cl/O, Br/O, S/O, B/P, C/P, N/Se etc.).

The difference in the total energies of the axial and equatorial hyperconjugomers (ΔSE_{eq-ax}) gives an estimate of sigma donor ability that follow the order of (Al, Ga) \gg Ge $>$ As \geq Si $>$ P $>$ B $>$ S $>$ H $>$ C $>$ S $>$ Br $>$ N $>$ Cl $>$ O $>$ F (\geq means that difference is less than 0.5 kcal/mol, \gg stands for the difference more than 3 kcal/mol). Although this scale may not isolate hyperconjugation

completely from the other components, these stabilization energies are chemically meaningful and can be verified experimentally.

The hyperconjugative origin of these substituent effects has been confirmed with NBO dissection, which included analysis of the interaction energies and orbital populations. Interestingly, the C-C bond is not a spectator, but a dynamic gating factor capable of fine-tuning double hyperconjugation - shutting it off when a strong acceptor is present at the δ -position or turning it on when a strong donor at this position is available.

The above data illustrates that the somewhat larger intrinsic donor ability of the C-H bonds compared to that of C-C bonds can be overshadowed by cooperative double hyperconjugation with participation of remote substituents. As the result, the *apparent* donor ability of C-C bonds can vary in a wide range and the relative order of donor ability of C-H and C-C bonds can be easily inverted depending on the molecular connectivity and environment. Analogously, the order of donor ability of other sigma bonds in organic molecules is not set in stone but can be changed by communication with remote substituents via the σ -framework.

Decreasing the energy gap: Stretched bonds as donors and acceptors in hyperconjugative interactions.

The stretched bonds and distorted geometries are good partners in hyperconjugative interactions because such bonds create opportunities for amplification of stereoelectronic effects. In general, C-X bond deformation decreases the $\sigma_{C-X}/\sigma^*_{C-X}$ energy separation via simultaneous (albeit sometimes asynchronous) destabilization of σ_{C-X} and stabilization of σ^*_{C-X} orbitals as they are transformed into the non-bonding orbitals.

Stretched bonds are good donor and acceptor partners in hyperconjugative interactions because the bond stretching/weakening decreases the σ/σ^* or π/π^* energy separation via simultaneous destabilization of bonding orbitals and stabilization of antibonding orbitals (Figure 34).⁷⁷ As a consequence, the importance of hyperconjugation can increase significantly in the transition state geometries.

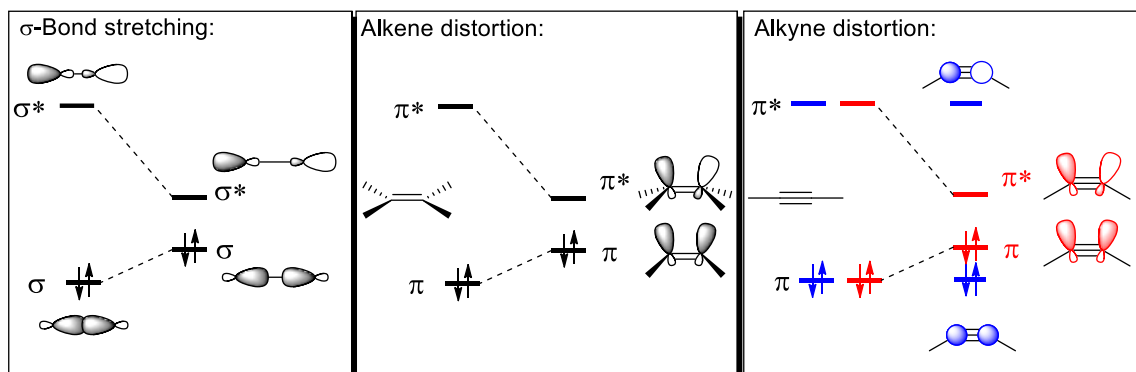


Figure 34. Changes in HOMO and LUMO energies can amplify stereoelectronic interactions associated with bond breaking in transition states.

Accentuation of homoanomeric interactions by stretching of acceptor bonds

In particular, the relatively small orbital interactions can be amplified dramatically when acceptor bonds are further stretched and polarized such as, for example, in the process of heterolytic bond cleavage as demonstrated in Figure 35.

Homoconjugative assistance by the lone pair of nitrogen plays a key role in the heterolytic C-Cl bond cleavage in β -chloropiperidine.⁵¹ As the C-Cl bond stretches, the energy of the $n_N \rightarrow \sigma^*_{C-Cl}$ interaction increases significantly even at β -C-N distances which are well above that for C-N covalent bond formation. Figure 35 also quantifies electron density transfer from the nitrogen lone pair to the acceptor σ^*_{C-Cl} orbital that results in a smooth transformation of this initially weak homohyperconjugative interaction into an intramolecular S_N2 reaction, as the line between hyperconjugation and chemical reaction fades.

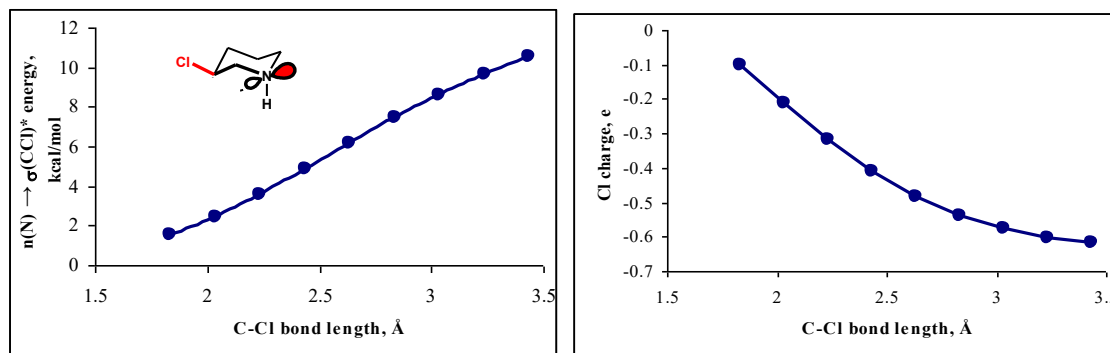


Figure 35. Correlation of C-Cl distance with the NBO energies of $n_N \rightarrow \sigma^*_{C-Cl}$ interaction and the NBO charge at Cl during the process of C-Cl bond stretching in 3-chloropiperidine.

Hyperconjugative assistance to alkyne bending

As the alkyne bends to attain the TS geometry, it becomes a better donor, making hyperconjugative interactions with the appropriately positioned substituents stronger. This strengthening is illustrated by the lower cost of bending of fluoro-2-butyne relative to 2-butyne (Figure 36), with a decreasing energy cost of bending in the following order: 2-butyne > 1-fluoro-2-butyne (gauche) > 1-fluoro-2-butyne (synperiplanar) > 1-fluoro-2-butyne (antiperiplanar).

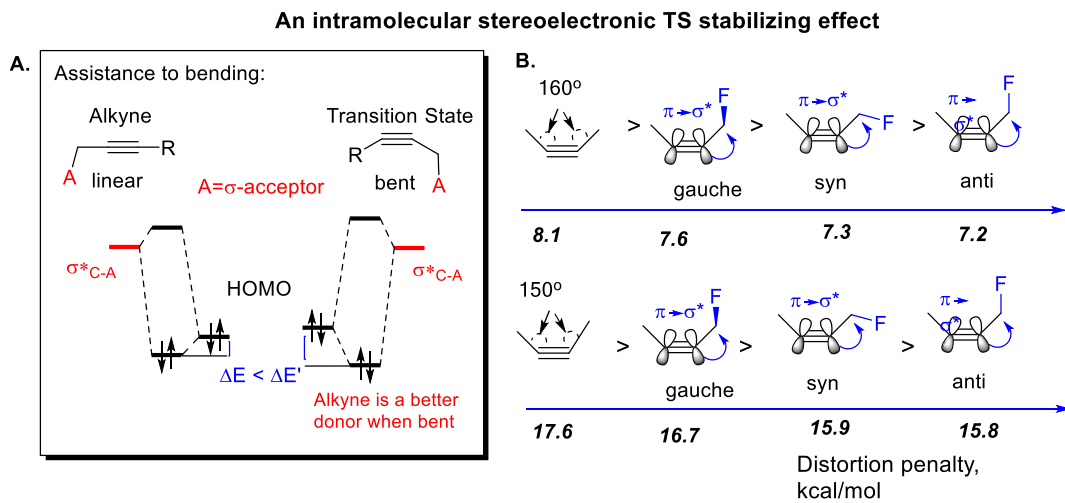


Figure 36. A: Stereoelectronic basis for assistance to alkyne bending utilized in TS stabilization in azide-alkyne cycloadditions. B: Symmetric bending scan of butyne and 2-fluorobutyne in the gauche, synperiplanar, and antiperiplanar conformations (reprinted with permission from ref. 1).

Cooperativity of hyperconjugative interactions:

Molecular symmetry can lead to an enhancement (or cancellation) of hyperconjugative hyperfine coupling in the EPR spectroscopy of cyclic π -conjugated organic radicals (Figure 37).⁷⁸ Davies suggested that this observation can be readily extended to hyperconjugation in spin-paired molecules as well.⁷⁹ For example, the cyclopentadienylmetal compound in Figure 37 has a symmetrical LUMO and should show symmetry-enhanced hyperconjugation. In contrast, triphenylstannylcycloheptatriene has an antisymmetric LUMO which renders the positive $\sigma_{C-Sn} \rightarrow \pi^*$ interaction less favorable.

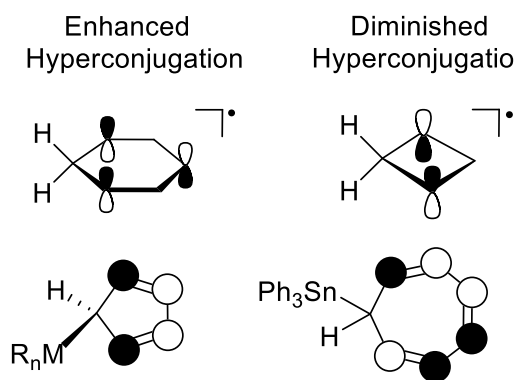


Figure 37. MO symmetry effects on hyperconjugation efficiency in cyclic systems

This effect has consequences for the relative isomer stabilities, bond lengths and angles, and one-bond NMR coupling constants. Systems in which the effect plays a significant role include the Wheland intermediates of electrophilic aromatic substitution, the loose complexes formed between metal cations and arenes, and η^1 -cyclopentadienylmetal compounds.⁷⁹

Even within the same overlap topology, one can change symmetry properties by populating additional molecular orbitals. Hyperconjugative patterns in saturated six-membered heterocycles illustrate how cooperativity depends on the number of electrons. In these systems, donation from a lone pair to two σ^*_{C-H} orbitals is cooperative (a 2-electron pattern) whereas donation from two lone pairs to the same σ^*_{C-H} orbital (a 4-electron pattern) is anticooperative (Figure 38).⁵¹ These effects are fully consistent with the different symmetry of the frontier MOs. Interestingly, when the strength of negative hyperconjugation increases 2.5-fold upon a change from σ^*_{C-H} to σ^*_{C-Cl} , the cooperativity effect increases four times. A further increase in acceptor ability of σ^* orbital transforms the $2 \sigma^* + n_x$ interaction into the classic σ -homoaromatic array.⁸⁰

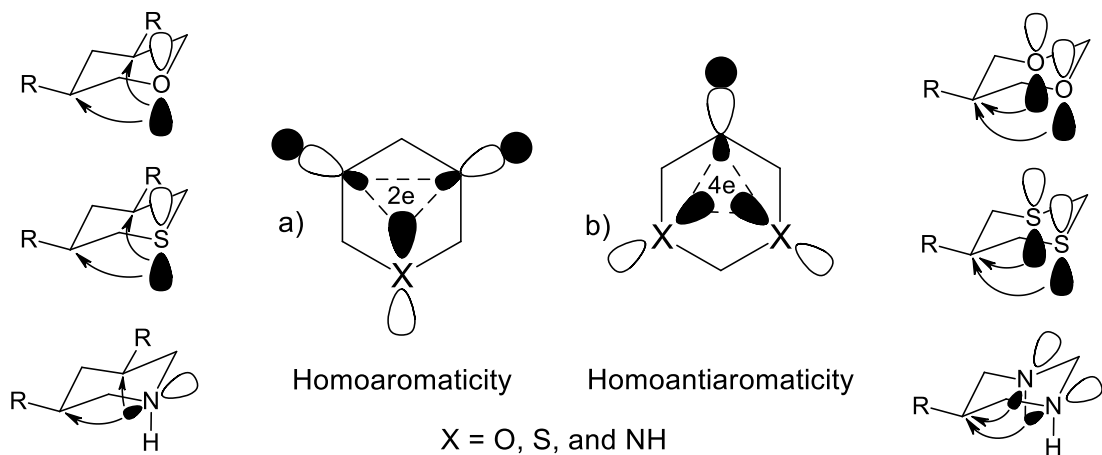


Figure 38. σ -Homoaromaticity (the two-electron system) and antiaromaticity (the four-electron system) in six-membered heterocycles.

Hyperconjugation with σ^* bridge orbitals can also provide an efficient coupling pathway (usually referred to as through bond (TB) coupling) for non-bonding electrons, which can compete with the direct through space interactions. The dominant role of TB interactions in coupling of the two radical centers in *p*-benzyne and related molecules is illustrated by observed energy lowering of the antisymmetric combination of the two radical centers with the σ^* orbitals of the bridge.⁸¹

Spectroscopic signatures of hyperconjugation

We continue with a brief discussion of IR and NMR methods that can provide additional insights into the structural effects of hyperconjugation.

IR analysis

When extracting structural information from IR spectra, one has to keep in mind that not all bands correspond to simple bond stretching or bending. The presence of overtones, combination bands, and Fermi resonances can shift the absorption from the expected positions. An elegant experimental technique for overcoming this problem and extracting structural information from IR spectra involves the deuterating all of the hydrogens except for the one under investigation. For example, the CHD_2 “isotopomer” can be used instead of a methyl group. McKean and coworkers, who used this technique in a number of comprehensive studies, referred to such frequencies as ‘isolated’ frequencies, $\nu_{\text{C-H}}^{\text{is}}$.⁸²

The consequences of $\sigma_{\text{C-H}} \rightarrow \sigma^*_{\text{C-H}}$ hyperconjugation are made apparent via the use of $\nu_{\text{C-H}}^{\text{is}}$ method.¹⁶⁰ For example, C-H frequencies in ethane are 42 cm^{-1} red-shifted in comparison to those in methane (Figure 39). The C-H bonds at the secondary carbon of propane (potentially antiperiplanar to two C-H bonds from the Me groups) display additional 30 cm^{-1} red shift whereas the tertiary C-H of isobutane (potentially antiperiplanar to three C-H bonds from the Me groups) is red-shifted by 30 cm^{-1} more.

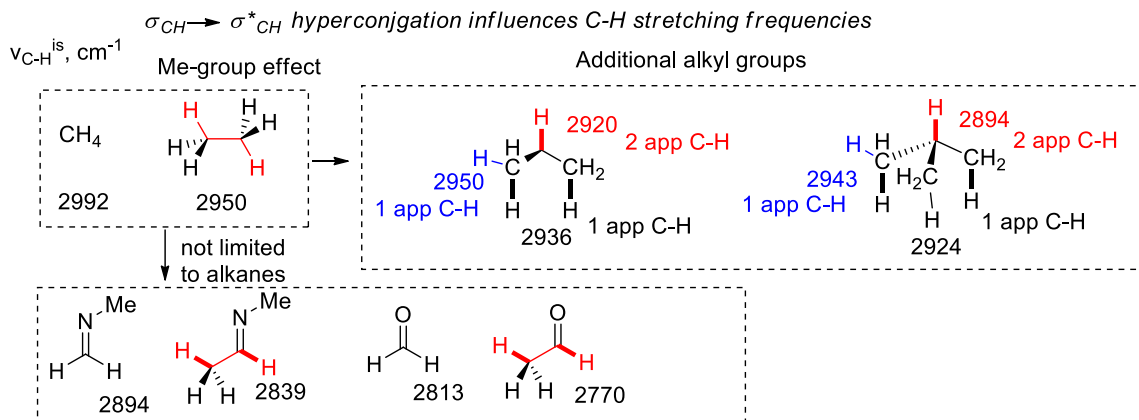


Figure 39. Selected effects of CH/CH hyperconjugation on C-H IR-stretching frequencies (app=antiperiplanar.)¹⁶⁰

In monosubstituted ethanes, β -substituents impose a larger effect on the antiperiplanar C-H bonds than on the gauche C-H bonds (Figure 40).¹⁶⁰ The observed F<Cl<Br<I trend is consistent with the relative acceptor abilities of the respective σ^*_{C-X} orbitals (F<Cl<Br<I).

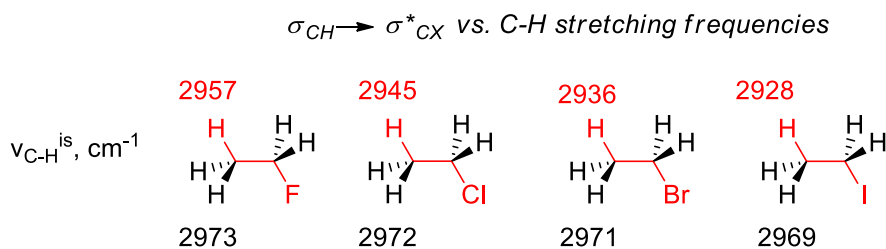
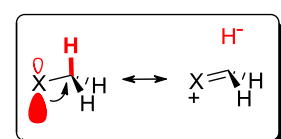


Figure 40. Selected effects of CH/CX hyperconjugation on C-H IR-stretching frequencies (app=antiperiplanar.)¹⁶⁰ Red-shifted H-bonds are shown in red.

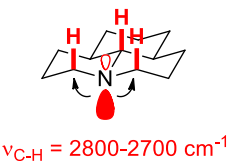
Bohlmann Effect

The connection between the bond length, bond strength and IR-stretching frequencies is the basis of the Bohlmann effect, a historically important manifestation of negative hyperconjugation.⁸³ In the 1957 work of Bohlmann^{32a} noted that characteristic red-shifted bands appeared in conformationally confined amines (~ 2800 – 2700 cm^{-1}). An analogous effect was observed in methylamine where the lower 2880 cm^{-1} stretching frequency is observed for the C-H bonds that is antiperiplanar to the lone pair of nitrogen and, thus, is lengthened and weakened by the $n_N \rightarrow \sigma^*_{CH}$ hyperconjugative interaction (Figure 41).¹⁶⁰ This spectroscopic feature can be observed for C-H bonds located near the oxygen atom of alcohols and ethers.

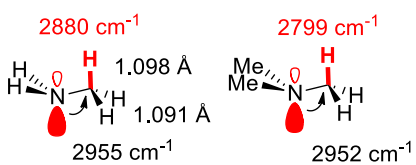
Bohlmann effect: lower IR-stretching frequency for the antiperiplanar C-H bond



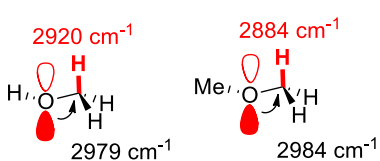
Bohlmann:



McKean: $\nu_{\text{C-H}}^{\text{is}}$



Amines:



Alcohols and Ethers:

Figure 41. Bohlmann effect reflects stereoelectronic effects in amines, alcohols, and ethers. C-H bonds with the red-shifted IR stretching frequencies are shown in red. Bond lengths calculated at the B3LYP/6-311G++(d,2p) level of theory. $\nu_{\text{C-H}}^{\text{is}}$ values from reference 160.

There is evidence of similar hyperconjugative interaction in F-substituted compounds. In particular, the $\nu_{\text{C-H}}^{\text{is}}$ for methyl fluoride is 16 cm^{-1} red-shifted relative to methane (2976 vs. 2992 cm^{-1}).¹⁶⁰ Because hybridization effects imposed by Bent's rule, should increase s-character in the C-H bonds and lead to the blue shift,¹⁶⁴ the experimentally observed red-shift confirms the importance of $n_{\text{F}} \rightarrow \sigma^*_{\text{C-H}}$ interactions.

The Bohlmann effect is also observed in C-H bonds antiperiplanar to lone pairs in systems where the lone pair containing heteroatom is doubly bound to the C-H carbon (i.e., aldehydes, imines, etc). The additional stereoelectronic feature of imines is the presence of geometric isomers that allow clear distinction between syn- and anti-periplanarity effects (Figure 42).⁸⁴ The stretching IR frequencies for the C-H bonds antiperiplanar to the nitrogen lone pair are noticeably red-shifted. Similar effects were observed for the N-H bonds in amides and hydrazides.⁸⁵

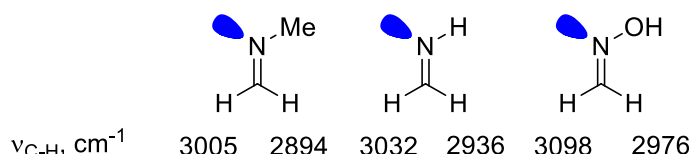


Figure 42. Bohlmann effect observed for the $\nu_{\text{C-H}}^{\text{is}}$ “isolated” frequencies in imines

The stretching frequencies for C-H bonds at the sp^2 carbons in aldehydes and formic acid derivatives are significantly red-shifted in comparison to the C-H bonds of ethylene. σ -Acceptors aligned with the in-plane p-type lone pair of the carbonyl oxygen weaken the Bohlmann effect by attenuating the $n_{\text{O}} \rightarrow \sigma^*_{\text{C-H}}$ interactions and lead to higher C-H stretching frequencies. This behavior is observed for acyl halides, esters, and amides. The order of C-H blue-shift parallels the σ -acceptor ability of X (F>O>N). An extreme version of this effect is observed upon Lewis acid coordination at the carbonyl. Such coordination shifts the C-H stretch back to higher frequencies, as the lone pair cannot participate in the $n_{\text{O}} \rightarrow \sigma^*$ interactions anymore.¹⁶⁰

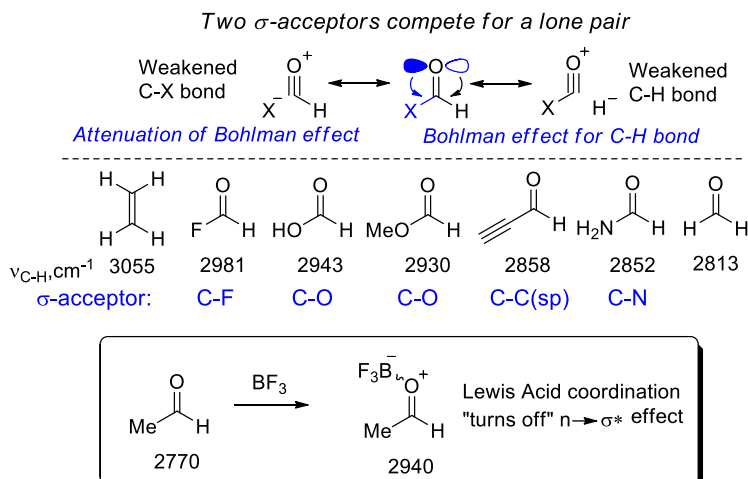


Figure 43. Bohlmann effect observed in C-H IR-stretching frequencies reflect stereoelectronic effects in the carbonyl containing compounds. Bond lengths calculated at B3LYP/6-31G++(d,2p). Values from reference 160. Insert at the bottom: Deactivation of $n_0 \rightarrow \sigma^*_{\text{C-H}}$ interactions by coordination of a Lewis acid at the carbonyl.

$\sigma \rightarrow$ cations

The “umpolung” of the classical negative hyperconjugation pattern of the Bohlman effect is provided by the effects of positive hyperconjugation on the IR-frequencies associated with α -C-H bonds in a cation. Those C-H bonds that are aligned with the empty p-orbital are significantly weakened. For example, the *t*-butyl cation shows a significantly red-shifted C-H stretching frequency in both the gas phase ($\sim 2800 \text{ cm}^{-1}$)⁸⁶ and in the solid state ($\sim 2900 \text{ cm}^{-1}$)⁸⁷ relative to neutral hydrocarbons (methane $\nu_{\text{C-H}} \sim 3000 \text{ cm}^{-1}$). Interestingly, the C-H bonds that are misaligned with the cationic p-orbital have more s-character than the sp^3 bonds of methane and $\text{sp}^{3.3}$ C-H bonds of 2,2-dimethylpropane.⁸⁸ These rehybridization trends should lead to noticeable blue-shifts for the misaligned C-H bonds relative to that for the C-H bonds aligned with the cationic center.⁸⁹

C-H Bonds adjacent to π -bonds

When a vicinal π -system is present, allylic C-H bonds are weakened and elongated by $\sigma_{C-H} \rightarrow \pi^*_{C-X}$ and $\pi_{C-X} \rightarrow \sigma^*_{C-H}$ interactions. As a result, C-H stretching frequencies in allylic, propargylic, and α -C-H bonds relative to carbonyls, cyanides, and isocyanides, are often red-shifted (Figure 44).¹⁶⁰ In allylic and heteroallylic positions, the out-of-plane C-H bonds display lower frequency stretches than the in-plane C-H bonds, whereas all three C-H bonds adjacent to a triple bond are equivalent.

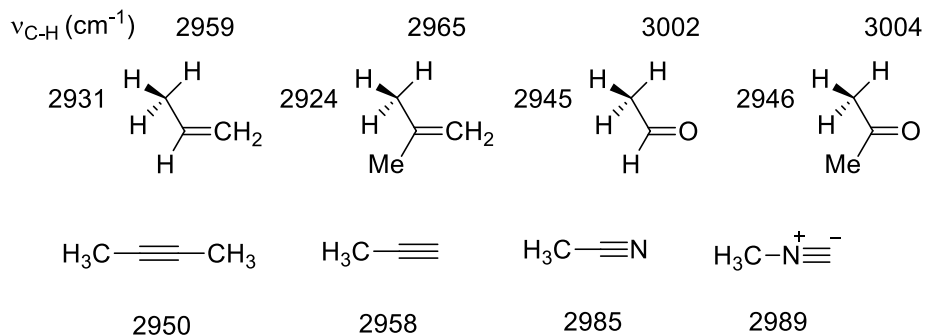


Figure 44. C-H Bonds adjacent to π -bonds displaying red-shifted IR frequencies.

Red-shifting hydrogen bonds - an intermolecular version of the Bohlmann effect.

The intermolecular version of the Bohlmann effect is the well-known spectroscopic signature of H-bonding (the red shift of X-H frequency in the X-H...Y complex). The commonly observed weakening of X-H bonds in X-H...Y complexes, a consequence of $n_Y \rightarrow \sigma^*_{X-H}$ negative hyperconjugation (Figure 45),³ is generally detected via the concomitant red shift in the IR X-H stretching frequencies. This structural and spectroscopic effect can be readily understood as a consequence of increased population of the antibonding σ^*_{X-H} orbital.

Intermolecular Bohlmann Effects:

Hydrogen Bonding

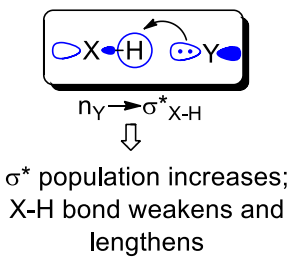


Figure 45. Intermolecular hyperconjugation in H-bonding usually leads to a red-shift in the H-X frequency analogous to that observed in the Bohlmann effect

Factors responsible for H-bonding have been debated for some time, with a consensus that a balance of electrostatics, polarization, charge transfer, and dispersion is responsible for the formation of H-bonds and for the structural consequences of these interactions.⁹⁰

Red-shifted H-bonds

These are the most common and well documented type of H-bonds. The hyperconjugative factor ($n \rightarrow \sigma^*$), responsible for H-bonding, also results in bond weakening and the observed red-shift and broadening in the IR spectrum.⁵⁹ When H-bonds are disfavored, i.e. upon heating or dilution, the “associated” broad O-H stretching bands of an alcohol or an acid disappear, and sharp, high-energy “nonassociated” bands reappear.⁹¹

As early as 1937, it was found that a linear relationship exists between H-bond strength and the shift in the IR H-X stretching frequency, termed the Badger-Bauer rule (Figure 46).⁹² The qualitative correlation between H-bond strengths and stretching frequencies has been observed in many chemical systems.⁹³ Although a single linear relationship does not hold throughout the many diverse types of H-bonding,⁹⁴ satisfactory linear correlations between enthalpy of H-bond formation, the IR stretching frequency shift, and the X-H bond elongation were found for structurally related compounds.⁹⁵

Blue-Shifted H-bonds

The reversal of the trademark behavior of H-bonds is the seemingly paradoxical C-H bond shortening and the blue shift in the respective IR stretching frequency observed in the so-called “improper” or blue-shifting H-bonds.⁹⁶ This behavior reflects rehybridization as the second structural force controlling the evolution of X-H bond length in the process of X-H...Y bond formation (Figure 46).⁵⁸ Blue-shifting is observed when the hyperconjugative component is

relatively weak, allowing rehybridization effects to dominate. Importantly, there is no fundamental difference between the two types of H-bonds, as all structural changes associated with H-bond formation stem from a balance of both effects.

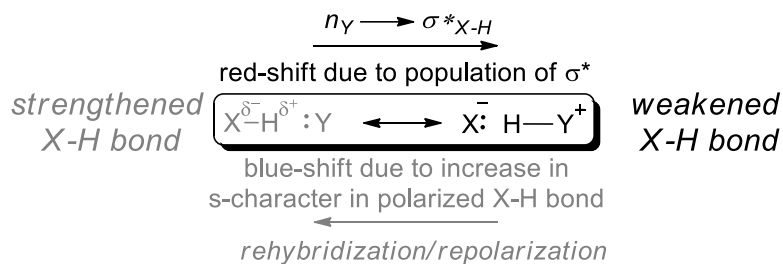


Figure 46. Factors responsible for structural and spectroscopic consequences of H-bond formation. Different dominating effects give “normal” red-shifted H-bonds and “improper” blue-shifted H-bonds.

The most commonly used NMR parameter that is used to study hyperconjugation is the direct one-bond coupling constant

Perlin Effect

In cyclohexane, the direct $^1\text{H}-^{13}\text{C}$ coupling constants are smaller for axial hydrogens.⁹⁷ This phenomenon, commonly referred to as the normal Perlin effect,⁹⁸ reflects the greater length of the axial C-H bonds. Because bond lengthening in the axial position occurs as a result of hyperconjugative $\sigma_{\text{C-H}} \rightarrow \sigma^*_{\text{C-H}}$ interactions of antiperiplanar C-H bonds in the axial position (Figure 47), the normal Perlin effect provides a connection between NMR spectroscopy and stereoelectronic effects.⁹⁹

Perlin effect: smaller one-bond NMR coupling constants for the longer C-H bonds

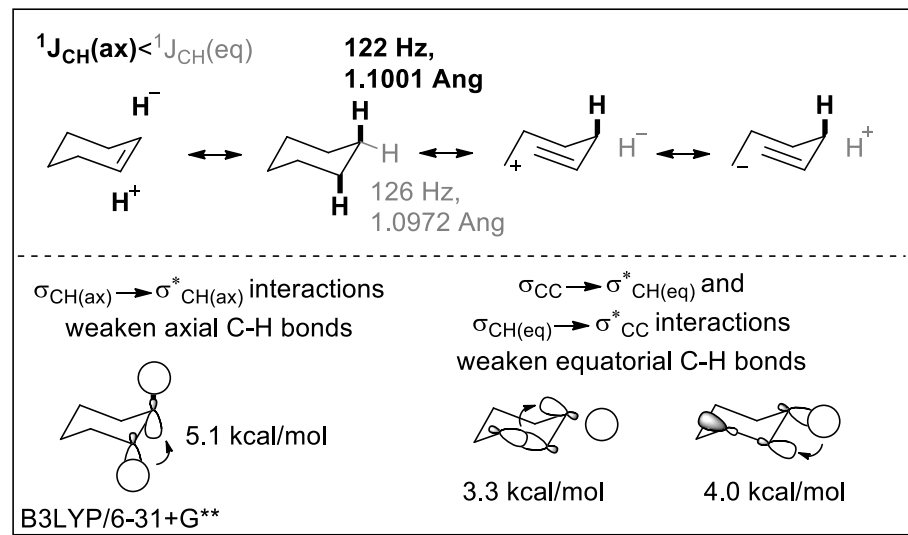


Figure 47. The Perlin effect, where smaller $^1\text{J}_{\text{CH}}$ values are observed experimentally for axial protons in cyclohexane, results from $\sigma_{\text{CH}} \rightarrow \sigma_{\text{CH}}^*$ interactions. The longer and weaker bonds are shown in bold. All data from 63.

Such connections are easier to detect in molecules with stronger stereoelectronic interactions. The sensitivity of the direct H-C coupling constants to the stereoelectronic factors is widely used for stereochemical assignments, especially in carbohydrate chemistry.¹⁰⁰ The differences in the direct coupling constants are manifestations of elongation and weakening of C-H bonds participating in hyperconjugative interactions. All three previously discussed types of negative and neutral hyperconjugation ($n \rightarrow \sigma^*$, $p \rightarrow \sigma^*$, and $\sigma \rightarrow \sigma^*$ interactions) have been implicated in spectroscopic consequences of the Perlin effect.

Anomeric Effects on C-H and C-C coupling

The effects of negative hyperconjugation on the C-H coupling in six-membered saturated heterocycles was systematically investigated by Juaristi and coworkers (Figure 48).^{97a} The axial lone pairs of O and N-atoms increase the magnitude of Perlin effect by selectively weakening the axial C-H bond. The effect is clearly stereoelectronic because, once the lone pair of azacyclohexane is oriented equatorially, the difference between axial and equatorial $^1J_{CH}$ values decreases to its value in cyclohexane. Interestingly, the lone pair of S atom does not impose a similar effect, suggesting either the weakness of sulfur anomeric effect or presence of alternative delocalizing interactions that selectively weaken and elongate the equatorial C-H bond (vide infra).

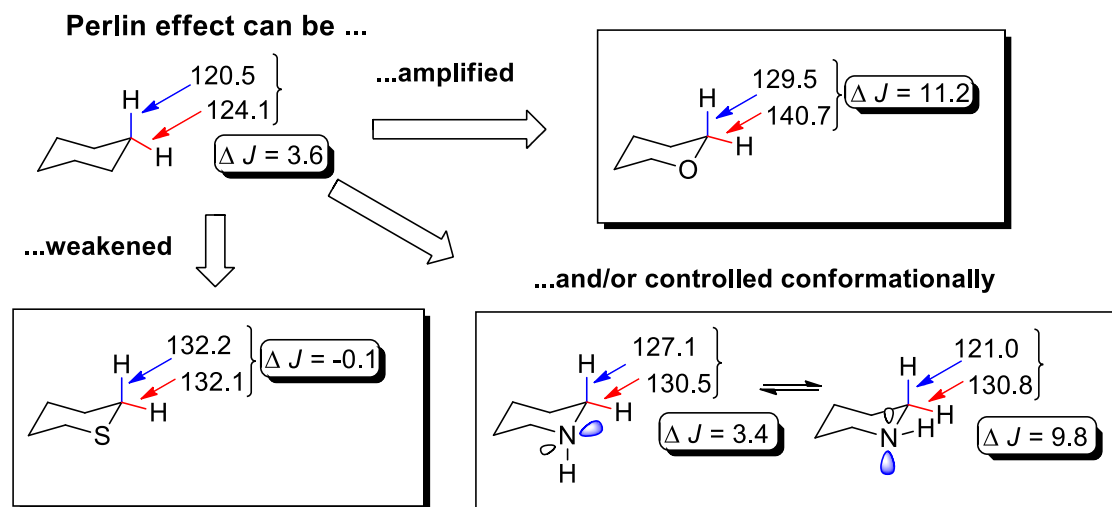


Figure 48. Selected direct C-H coupling constants calculated at B3LYP/6-31G(d,p) level^{Error! Bookmark not defined.}

Analogous effects were reported for N-containing saturated heterocycles (Figure 49) where a similar ~ 10 Hz decrease in the $^1J_{CH}$ value was observed for the axial C-H bond.^{Error! Bookmark not defined.} In rigid tricyclic orthoamides, $^1J_{CH}$ for the C-H bonds antiperiplanar to three nitrogen lone pairs was much smaller (141 Hz) in comparison to C-H bonds syn to the lone pairs (184 Hz), suggesting a ~ 18 Hz per interaction decrease in the $^1J_{CH}$ value (Figure 49).¹⁰¹

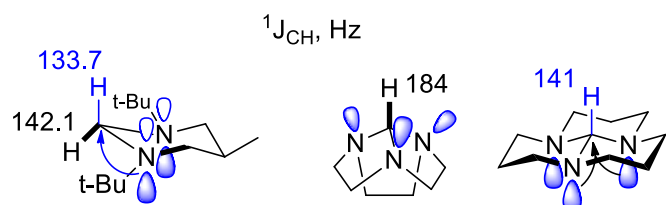


Figure 49. The effect of the adjacent lone pairs on the axial and equatorial $^1J_{CH}$ values in 1,3-di-*tert*-butyl-5-methyl-1,3-diazacyclohexane and on the $^1J_{CH}$ value for the central C-H bond in rigid tricyclic ortho amides.¹⁰¹

The stereoelectronic nature of the observed trends in the $^1J_{CH}$ values is consistent with the conformational dependence of this NMR parameter in formate esters. For seven alkyl formates, the more abundant *s*-cis rotamer had $^1J_{CH} \sim 7$ Hz greater relative to that in the minor *s*-trans conformer. In the *s*-trans geometry, the $n_o \rightarrow \sigma^*_{CH}$ interaction weakens the C-H bond and decreases the magnitude of C-H spin coupling (Figure 50).¹⁰²

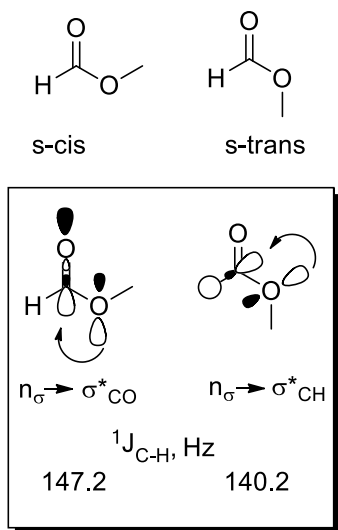


Figure 50. Conformational effects on direct C-H coupling in esters

However, the seemingly perfect unison of hyperconjugation and direct C-H coupling constants is not general. More recently, however, Cuevas, Perrin, Juaristi and coworkers showed the simple picture suggested by the above data needs to be reconsidered. Computational analysis of structures with systematic variations in the HCOC dihedral angle τ in ethers revealed that, although the maximum $n_o \rightarrow \sigma^*_{CH}$ delocalization and minimum $^1J_{CH}$ ought to be at $\tau = 90^\circ$, there is no minimum at this geometry ($^1J_{CH} = \sim 135$ Hz). Instead the $^1J_{CH}$ values monotonously decrease from $\tau = 180$ to 0° (138.6 to 129.3 Hz).⁶³ Similar analysis based on experimental data suggested that direct C-C coupling constant at the anomeric carbons of ethers also cannot be primarily derived from $n_o \rightarrow \sigma^*_{CC}$ delocalization.¹⁰³ Although the contribution of negative hyperconjugation is not negligible, the electronic origin of these intriguing observations seems to be mostly based on polarization effects associated with the local dipole-dipole interactions. Such caveats are important to keep in mind when proceeding to the further discussion of the stereoelectronic features in NMR analysis.

Reverse Perlin Effect

In contrast to cyclohexane, axial protons in at the β -carbons of heterosubstituted cyclohexanes may have coupling constants larger than those of the equatorial protons (i.e., the *reverse* Perlin effect).^{70,104} In 1,3-dioxanes and 1,3-dithianes, equatorial C-H bonds at the 5-position have been shown to display this behavior (Figure 51a).

The term “reverse” can be misleading for these systems, because the normal and the reverse Perlin effects share the same structural origin – the shorter C-H bond has a greater C-H coupling constant. In this sense, the “reverse” Perlin effect is perfectly normal!

Perlin effect: smaller one-bond NMR coupling constants for the longer C-H bonds

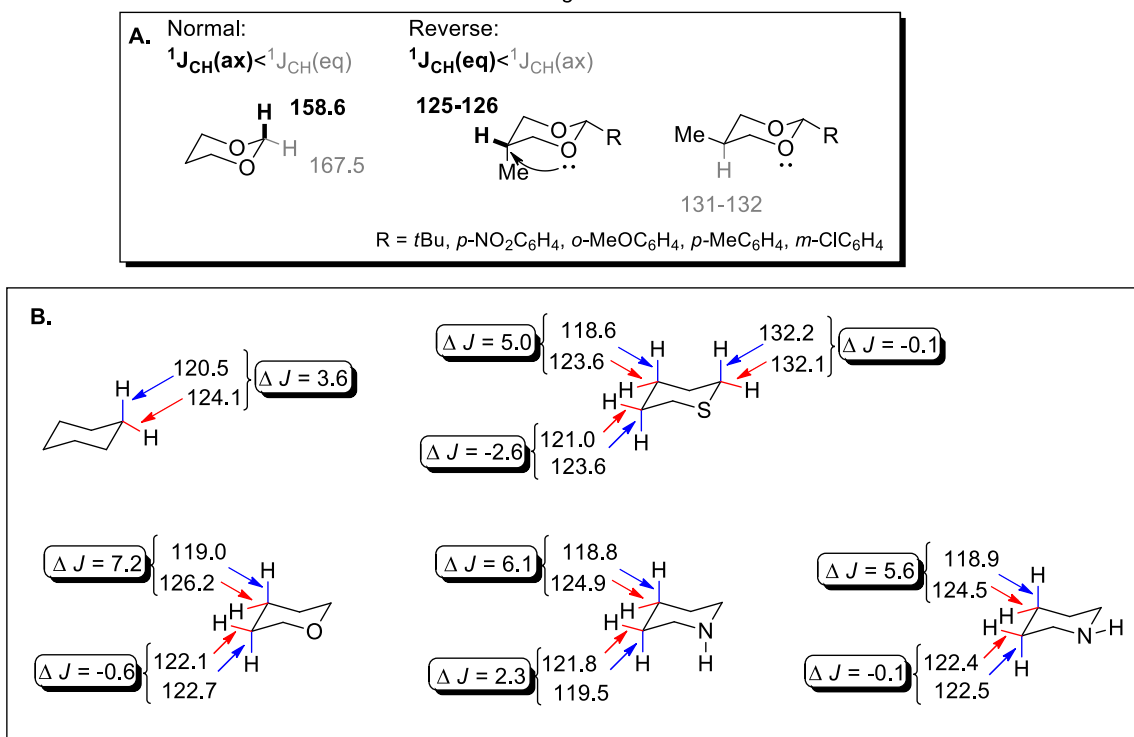


Figure 51. Experimental (A) and theoretical (B, calculated at B3LYP/6-31G(d,p) level) data illustrating the differences between axial and equatorial C-H coupling constants in cyclohexane and its heteroatomic analogues.

The discovery of reverse Perlin effect led to subsequent refinement of the general picture for homoanomeric effects. For example, the C(5)-H equatorial bond in 1,3-dioxane is longer than the C(5)-H axial bond and the respective direct NMR ${}^{13}\text{C}-{}^1\text{H}$ coupling constant is smaller than that for the axial bond (${}^1\text{J}_{\text{CH}_{\text{eq}}} < {}^1\text{J}_{\text{CH}_{\text{ax}}}$).¹⁰⁴ This phenomenon (the reverse Perlin effect) contrasts with the “normal” situation, e.g. in cyclohexane, where the axial C-H bond is longer and the corresponding ${}^1\text{J}_{\text{CH}}$ constant is smaller (the normal Perlin effect). The key hyperconjugative interaction leading to the reverse Perlin effect in 1,3-dioxane is that of the equatorial C(5)-H bond with the pseudoaxial lone electron pair on the β -oxygen (the Plough effect) and that the $\text{n}_{\text{eq}} \rightarrow \sigma^*_{\text{eq}}$ (the W-effect) was unimportant in 1,3-dioxane, 1,3-dithiane and 1,3-oxathiane.⁵¹ The situation changes in azacyclohexanes, where the W-effect is greater than the Plough effect due to more favorable hybridization of nitrogen lone pairs.

Anomeric Effects on C-C coupling

Although the probability of two ${}^{13}\text{C}$ atoms to be directly connected at the natural abundance is exceedingly low (i.e. ~0.01%, or one molecule out of 10 000!), methods based on the observation of ${}^{13}\text{C}$ satellites in the ${}^{13}\text{C}$ NMR spectra with the concomitant “suppression” of the signals of the principal isotopomers (i.e., the INADEQUATE technique) greatly facilitated the measurement of C-C coupling constants in samples with a natural isotopic content.¹⁰⁵ Such constants provide valuable information about the nature of carbon hybridization, overlap, bond strength etc.¹⁰⁶ In this section, we will provide a short selection of examples that describe how

the direct C-C constants respond to changes in the orientation of the substituents at the respective C-C bond.

For example, significant effects are observed in the heteroanalogues of cyclohexane. In such systems, C-C coupling is noticeably decreased for the axial C-C bonds adjacent to heteroatoms. The effect can be cumulative, e.g., at the C2 of 1,3-dioxane where lone pairs of the two oxygen atoms can interact with the axial substituent (Figure 52).¹⁰⁷

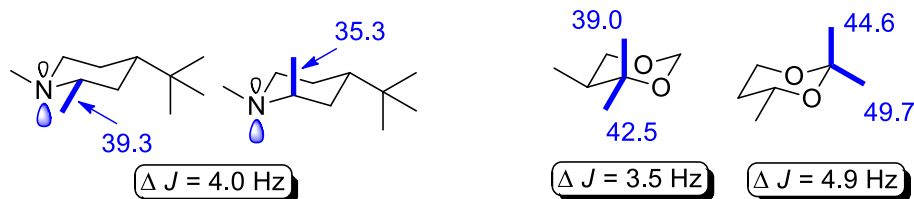


Figure 52. Effects of negative hyperconjugation at the direct C-C coupling at anomeric positions

Even though we have just scratched the surface for the possible applications of spectroscopic techniques in studies of stereoelectronic effects, we hope that we have illustrated the diversity of possible outcomes and the value of such analysis. The correlation between stereoelectronic effects and spectroscopy is sometimes indirect but often reliable. In particular, IR-stretching frequencies and direct coupling constants for X-Y bonds can be useful in detecting stereoelectronic effects that are associated with the X-Y bond weakening with the caveat that the masking effects of hybridization, usually via the connection of the latter with electronegativity, should be taken into account. The tug-of-war between hybridization and delocalization is a common scenario that can mask stereoelectronic trends.

Examples/Stereoelectronic effects

Due to the prevalence of σ -bonds in chemical structures, hyperconjugation displays itself in numerous effects on structure, conformations and reactivity.¹ An important feature of hyperconjugative interactions is their stereoelectronic component – such interactions that depend on overlap of orbitals in space. This feature leads to several preferred overlap modes of intramolecular and intermolecular hyperconjugation patterns, which we will illustrate with several examples given below.

Neutral hyperconjugation in ethane and other hydrocarbons

Rotational barriers

The forces controlling the barrier to rotation around formally single bonds serve as one of the cornerstones of conformational analysis. Not surprisingly, ethane, the parent system for studies of rotational barriers, has been extensively investigated. The origin of the ~ 3 kcal/mol lower energy of the staggered conformation responsible for the rotational barrier in ethane has usually been attributed to steric repulsion between electrons in the C–H bonds in the eclipsed conformation.¹⁰⁸ Alternatively, rotation-induced weakening of the central C–C bond¹⁰⁹ and hyperconjugation^{30,110,111} has been considered to be the reasons for the higher stability of the staggered conformation. Mulliken himself, as early as 1939, conjectured that hyperconjugation plays an important role in the internal rotation potential of ethane-like molecules.⁶

Pophristic and Goodman used NBO analysis to dissect the contributions of the three principal contributors to the ethane's structural preferences and separate steric and hyperconjugative interactions.⁵⁶ They found that removal of vicinal hyperconjugation interactions yields the eclipsed structure as the preferred conformation, whereas Pauli exchange (steric) and electrostatic (coulombic) repulsions, have no influence on the preference for a staggered conformation. The hyperconjugative preference for the staggered conformation is attributed to the antiperiplanar stereoelectronic requirement summarized in Figure 19.

Subsequent studies by Bickelhaupt and Baerends¹² and by Mo et al.¹³ resurrected the steric repulsion explanation as the dominant contribution in the overall barrier. Bickelhaupt's and Baerends's EDA-based study found hyperconjugative stabilization in the staggered conformation to be about 0.4 kcal/mol. BLW-based analysis by Mo and coworkers suggests that hyperconjugation interaction does favor the staggered conformation but provides only 1/3rd of the total barrier. These discrepancies are based on the conceptual differences between the EDA, BLW and NBO models discussed in section "Wavefunction analysis", such as on the non-orthogonality of initial orbitals in the former two procedures and the conceptual differences in the treatment of steric effects.

C-C bond length in ethane and its isoelectronic cousin

The heated discussions presented in the previous section often surround neutral hyperconjugation, where the effects of electrostatics, sterics, and conjugation may be of similar magnitude and where their relative importance depends strongly on the type of theoretical approach utilized for their dissection. In the following section, we show how hyperconjugation, in an interplay with hybridization, is essential for understanding the dramatic differences in the geometry of ethane and its isoelectronic cousin, ammonia borane.

Ethane is a surprising molecule if one thinks deeper about its geometry. This geometry deviates from the ideal tetrahedral arrangement of the textbook sp^3 hybridization. The 107.5° HCH valence angle of ethane is much smaller than the 111° HCC angle. These geometric parameters are fully consistent with the calculated NBO hybridization values. Unlike methane, where every C-H bond is made with sp^3 hybrids, ethane has C-H NBOs made from $sp^{3.25}$ hybrids (Figure 53).

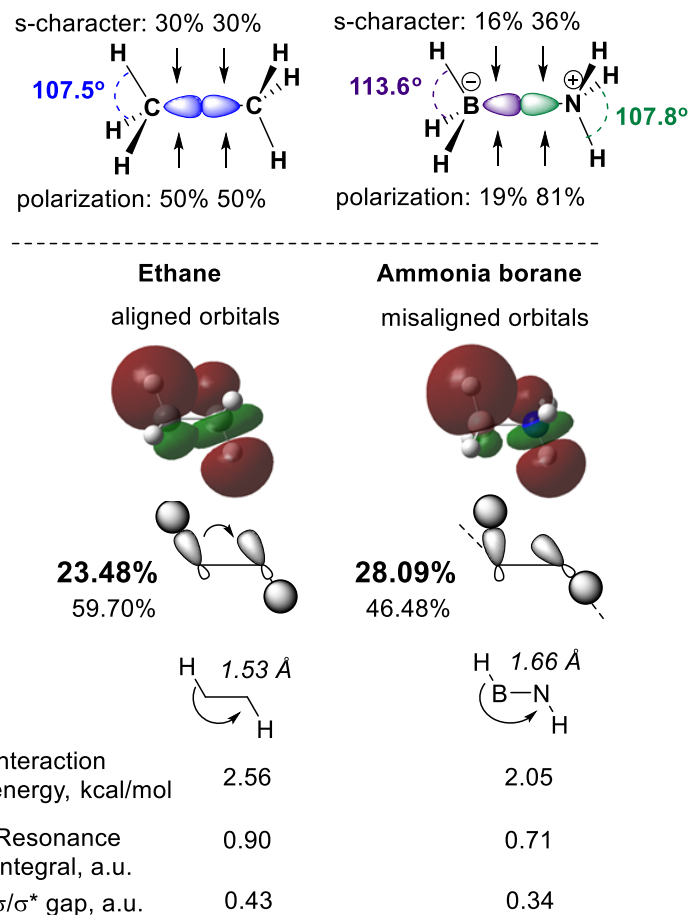


Figure 53. Top: Comparison of hybridization, polarization and HXH bond angles in ethane and ammonia borane (%s in: C-H bonds 23, N-H bonds 21, B-H bonds 28). Calculations are at the B3LYP/6-311++G(d,p) level. Bottom: Comparison of vicinal hyperconjugation in ethane and ammonia borane according to NBO analysis at B3LYP/6-311++G(d,p) level. The $\sigma_{\text{N-H}} \rightarrow \sigma^*_{\text{B-H}}$ interactions are even smaller (< 0.5 kcal/mol). The s-character (larger font, bold) and the polarization (smaller font) of C-H and B-H bonds are indicated.

Not only is the relatively large magnitude of the difference deviation of ethane from the “ideal” hybridization quite intriguing but these observations also indicate that ethane violates Bent’s rule, one of the venerable rules of structural chemistry.⁶⁵ Bent’s rule states that atom directs hybrid orbitals with increased p-character towards a more electronegative element. In the case of ethane, this is not the case: carbon directs more p-character towards hydrogen – a *less* electronegative element. NBO analysis clearly shows that the C-H bonds are polarized towards carbon (62% at carbon, 38% at hydrogen). Why then does not hybridization follow the expected and generally reliable trend?

The reason for this “anti-Bent” behavior in one of the simplest organic molecules is that the tug-of-war between hybridization and hyperconjugation is won by hyperconjugation.⁸⁸ When ethane geometry is recalculated with the hyperconjugative NBO interactions removed, the C-C bond lengthens from 1.530 Å to 1.686 Å and the HCH angle opens from 107.5° to 110.3°. Both changes suggest the need for higher p-character in C-H hybrids for assisting hyperconjugative

effects in reaching their full stabilizing power. In return, hyperconjugation imparts the partial double bond character to ethane and shortens the CC distance.

The 1.69 Å CC bond lengths in the hypothetical “hyperconjugation-free” ethane is very close to the 1.66 Å B-N distance in NH_3BH_3 . Interestingly, although $\text{CH}_3\text{-CH}_3$ and $\text{BH}_3\text{-NH}_3$ are isoelectronic, the importance of vicinal hyperconjugation in ammonia borane is drastically lower (Fig. xx). The decreased importance of vicinal hyperconjugation in ammonia borane explains why its polar B-N bond is noticeable longer (1.66 Å at B3LYP/6-311++G(d,p) level) than the non-polar C-C bond in ethane (1.53 Å).

Hyperconjugation in ethane is responsible for the partial C=C bond character and C-C distance shortening. In ammonia borane, the structure effects of hyperconjugation are weakened by the rehybridization effects on molecular geometry at boron and nitrogen.

Since the B-N bond is strongly polarized towards nitrogen, boron uses hybrids with lower s-character than carbon in C_2H_6 whereas nitrogen uses hybrids with higher s-character than carbon in C_2H_6 . Both trends are fully consistent with the Bent's rule. The drastically different hybridization patterns lead to different valence angles at N and B - the HBH angle opens up whereas the HNH angle contracts. This change renders the perfect parallel alignment of the NH and BH bonds impossible. Rehybridization in ammonia borane imposes changes in orbital alignment, orbital shape and bond length which move the interacting σ/σ^* pair from the favorable π -type overlap. NBO analysis readily illustrates, that because the suboptimal orbital overlap (reflected in the lowered resonance integral) weakens the stabilizing hyperconjugative interaction, ammonia borane finds a compromise where hybridization-imposed molecular distortions are not fully developed.

Axial-equatorial conformers of methyl cyclohexane

Due to their well-defined geometries, cyclic systems lend themselves for studies of hyperconjugative interactions. Hyperconjugation has been proposed to explain why the axial C-H bonds are longer and weaker than the equatorial bonds⁷⁰ as well as the rationale for the lower energy of the equatorial conformer of methyl cyclohexane, its 4-oxa, 4-aza, 4-thia analogues,¹¹² as well as other substituted cyclohexanes¹¹³ and cyclohexenes.¹¹⁴

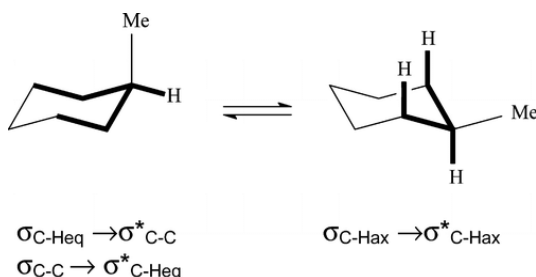


Figure 54. Bonds involved in the main hyperconjugative interactions which influence the conformational equilibrium of methylcyclohexane. (Reprinted with permission from ref. 112).

Hyperconjugation in alkyl fluorides: from gauche and cis effects to counterintuitive BDE trends

CH/CF hyperconjugation is one of most imbalanced examples of hyperconjugation in neutral molecules. It has multiple consequences closely connected to many “anomalies” of fluoroorganics.¹¹⁵ We will illustrate the role of such effects on stability, geometry, and reactivity.

The stabilizing effect of C-H/C-F hyperconjugation is clearly illustrated by the following isodesmic equations (Figure 55).¹¹⁶ Addition of a vicinal methyl group next to a C-F bond leads to ~3-6 kcal/mol stabilization. Although each additional donor has a slightly weaker effect, their contributions are cumulative.

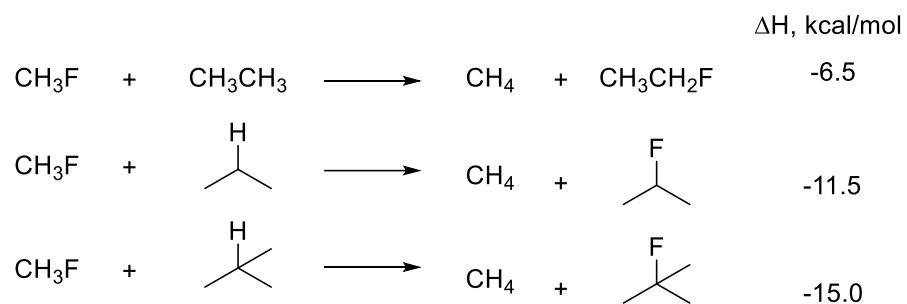


Figure 55. Stabilizing consequences of fluorine introduction to hydrocarbons

The importance of $\sigma_{\text{C-H}} \rightarrow \sigma^*_{\text{C-F}}$ interactions is also reflected in geometric parameters, such as the the C-C bond shortening upon progressive fluorination of one of the ethane carbons (Table 2).¹¹⁷ The increased C=C double bond character is further illustrated by the concomitant increase in the C-C BDE (Bond Dissociation Energy).

Table 2. Carbon–carbon bond lengths and strengths in fluoroethanes

Compound	C-C distance, Å	BDE(C-C), kcal/mol
CH ₃ -CH ₃	1.532	90.4
CH ₃ -CH ₂ F	1.502	91.2
CH ₃ -CHF ₂	1.498	95.6
CH ₃ -CF ₃	1.494	101.2

The conformational consequences of CH/CF hyperconjugation are illustrated by the gauche effect, i.e., the preference for the gauche conformation in X-C-C-Y systems (1,2-disubstituted ethanes) with two acceptor substituents X and Y.¹¹⁸ Although X and Y are usually fluorine or oxygen, the choice of the second substituent Y is quite broad in fluoroethanes of general formula FCH₂CH₂Y, where Y=F, NO₂, OCOH, NHCOH, N₃, NCO.¹¹⁹ A similar preference was observed for 1,2-difluorocyclohexane.¹²⁰ The gauche effect has been studied both experimentally^{121,122} and computationally (Figure 56).^{118,119,123} The importance of the antiperiplanar hyperconjugative $\sigma_{\text{C-H}} \rightarrow \sigma^*_{\text{C-X}}$ and $\sigma_{\text{C-H}} \rightarrow \sigma^*_{\text{C-Y}}$ interactions in the gauche effect in 1,2-difluoroethane has been shown using NBO analysis.¹²³ EDA-based estimates suggest that

both delocalization and electrostatic interactions contribute to stabilizing the gauche conformer.¹²⁴

The magnitude of this preference is very sensitive to solvent effects, due to the large difference in polarity of the two conformers. Electrostatics is an important contributor to the conformational effect because of the differences in dipole moment of the two conformers. Electrostatic contributions are considered to be the dominant cause of the gauche effect in the charged β -ammonium system.^{125,126}

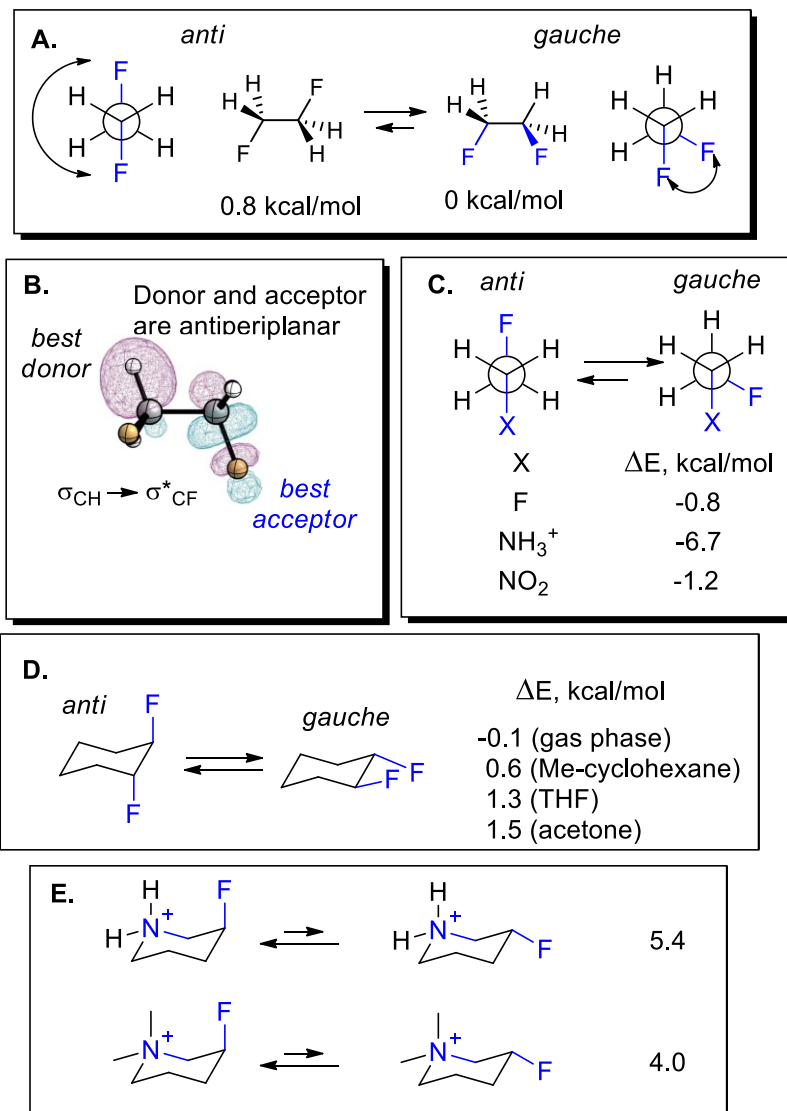


Figure 56. A: The gauche effect for 1,2-difluoroethane. B: The overlap of σ_{C-H} and σ^*_{C-F} bonds in the anti geometry. C: Expanded list of substituents that prefer gauche conformation relative to a σ_{C-F} bond (gas phase energies at B3LYP/ 6-311+G(d,p) level. D: solvent effects on the gauche/anti equilibrium in 1,2-difluorocyclohexane. E: the strong gauche preference in fluoro compounds with positively charged γ -substituents.

Cis-effect

The 1,1-difluoroethene is the most stable of the three difluoroethene isomers (>9 kcal/mol) due to the presence of strong “anomeric” $nF \rightarrow \sigma^*C-F$ interactions (*vide infra*). For 1,2-difluoroethene, the cis isomer is experimentally more stable than the trans isomer (0.9 kcal/mol and 0.43 kcal/mol). A similar trend is observed for the two 1,2-dichloroethenes whereas the two isomers of 1,2-dibromoethene have equal stability, within the experimental error. This conformational phenomenon is called the “cis effect”¹²⁷ and bears similarity to the gauche effect shown in Figure 56.

Yamamoto et al. have estimated the contributions of electron delocalization and steric exchange repulsions using NBO analysis at MP2/6-311++G(3df,3pd) level capable of reproducing the experimental energy differences between the geometric isomers.¹²⁸ Two delocalization mechanisms were found to be the cis stabilizing forces - periplanar hyperconjugations (synperiplanar and antiperiplanar effects) and halogen lone pair delocalizations into the C=C bond antibonding orbitals (LP effect, Figure 57 right).

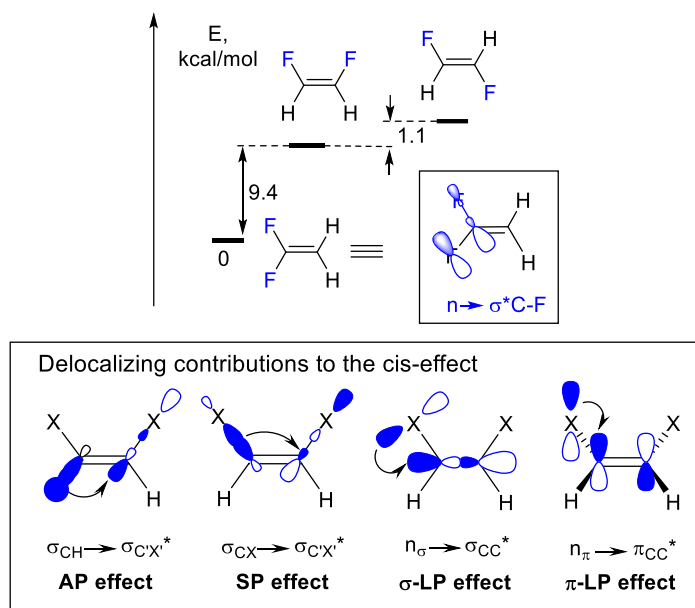


Figure 57. Top: Relative energies of the three difluoroethenes. Bottom: The antiperiplanar hyperconjugation effect (the AP effect), the synperiplanar hyperconjugation effect (the SP effect) and the lone pair delocalization effects (σ - or π -LP effect) coexist in 1,2-dihaloethenes (X = halogen).

Although the common stereoelectronic preference for the anti- arrangement of the best donor and the best acceptor dominated for X=F, the difference in the energies of the antiperiplanar interactions decreased for the two isomers for the heavier halogens where the $\sigma_{C-X} \rightarrow \sigma^*_{C-X}$ interactions increase in relative importance due to the greater donor ability of the σ_{C-Cl} and σ_{C-Br} bonds.

The opposite trends BDE of primary vs. tertiary C-H and C-F bonds

Strong $\sigma_{C-H} \rightarrow \sigma^*_{C-F}$ interactions explain the seemingly anomalous trends in the C-F BDEs of alkyl fluorides (Me-F < Et-F < i-Pr-F < t-Bu-F, Figure 58.). The greater C-F bond strength in *t*-butyl fluoride is in odds with the expectations based on the relative stability of alkyl radicals and the BDE

trends for the analogous C-H bonds.¹²⁹ Because $\sigma_{C-H} \rightarrow \sigma^*_{C-F}$ hyperconjugative stabilization of alkyl fluorides is greater than the analogous interactions of radical the center with the C-H bonds of alkyl substituents, additional substitution stabilizes alkyl fluorides more than alkyl radicals, thus increasing the BDEs. These observations can be expanded to differentiate π -donors from σ -acceptors. For example, alkyl groups decrease BDEs for non-polar C-C bonds whereas they increase BDEs for polar C-O bonds.

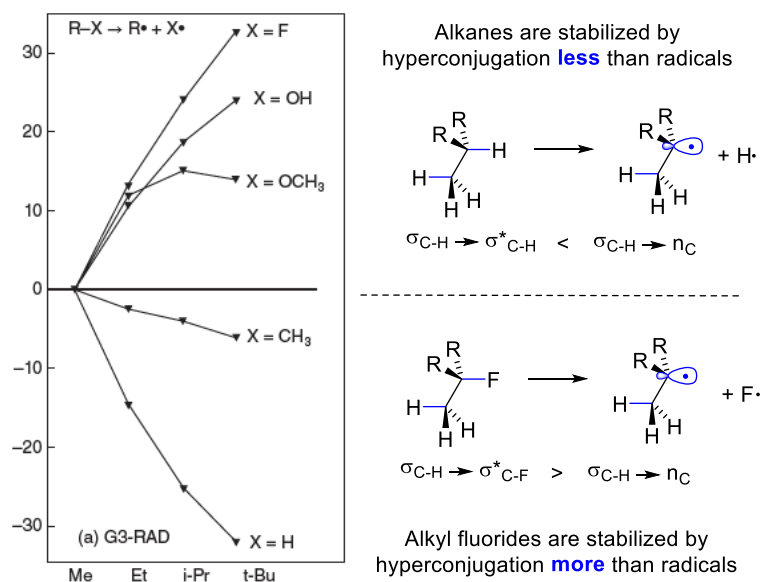


Figure 58. Contrasting effects of alkyl substitution on BDEs for C-H, C-C, C-O and C-F bonds (Reprinted with permission from ref. 129. Copyright 2005 American Chemical Society.). The BDEs (in kJ/mol) increase in the more substituted alkyl fluorides, alcohols and ethers but decrease in respective alkanes. Reprinted with permission from ref. 1

The CH/CF hyperconjugation provides insights into a number of seemingly confusing paradoxes, such as why is CF₃ one of a few anomalous substituents with a negative Radical Stabilization Energy (RSE = -8 kJ/mol);¹³⁰ or why the C-H bond in H-C₆F₅ is stronger than that the C-H bond in benzene whereas the C-F bond in F-C₆F₅ is weaker than that in F-C₆H₅.¹³¹

Neutral hyperconjugation in alkenes and alkynes

Thermochemistry

Not only has neutral hyperconjugation in closed-shell species been controversial, but even the importance of classic π -conjugation came under scrutiny. In a provocative series of papers, Rogers et al.¹³² disclosed that “conjugation stabilization of 1,3-butadiyne is zero” when estimated through the classic approach of Kistiakowsky et al.¹³³ Kistiakowsky suggested that conjugative stabilization in butadiene can be assessed by stepwise hydrogenation first to 1-butene and then to butane (Figure 59). The first step is 3.8 kcal/mol less exothermic than the second step, which according to Kistiakowsky et al. indicates the strength of the π -conjugation in 1,3-butadiene. Although one would expect 1,3-butadiyne, which has two pairs of conjugating double bonds, to have stronger conjugative stabilization than 1,3-butadiene, the two steps in

hydrogenation of 1,3-butadiyne yields are equally exothermic, suggesting that the conjugation in the former compound is zero! Why would conjugation disappear in alkynes?

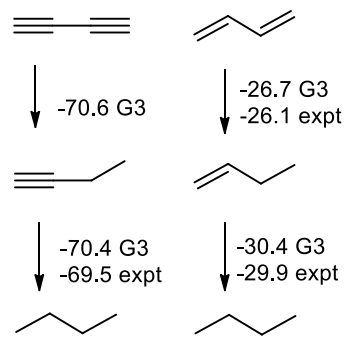


Figure 59. Comparison of the G3(MP2) calculated enthalpies of formation ΔH_f^{298} (italic) and hydrogenation ΔH_{hyd} (expt in kcal/mol) of butenes and butynes. According to these estimates, the conjugation energy of 1,3-butadiene (right) is 3.9 ± 0.1 kcal/mol, but for 1,3-butadiyne (left), it is zero.

Interpretation of the above results clearly underscores the importance of neutral hyperconjugation for the stability of unsaturated compounds. Jarowski et al.¹³⁴ pointed out that the reference compounds for 1,3-butadiyne and 1,3-butadiene are stabilized significantly by hyperconjugation, which is not present in 1,3-butadiyne and 1,3-butadiene. In order to take hyperconjugative interactions into account, the stabilization of ethylene (in kcal/mol) by an ethyl substituent (2.4 G3; 2.2 G3- (MP2); 2.7 experimental) can be estimated from the difference between the heats of hydrogenation of ethylene and 1-butene. Likewise, the hyperconjugative stabilization of acetylene by an ethyl group (4.9 G3; 4.8 G3(MP2); 4.7 expt) is the difference between the heat of hydrogenation of acetylene and 1-butyne. Equivalently, the hyperconjugative stabilization can also be described by isodesmic reactions in Figure 60a that produces data consistent with the above evaluation:

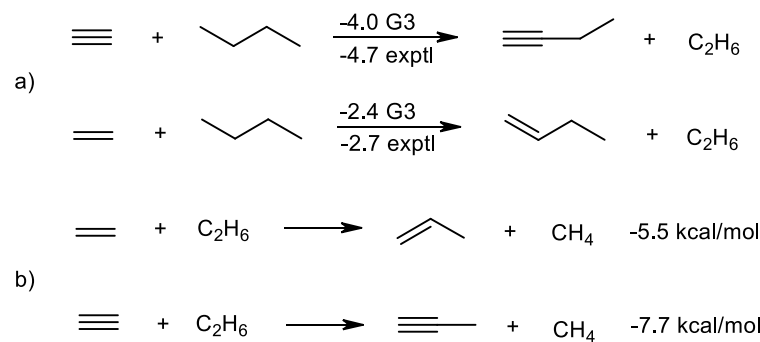


Figure 60. a) Conventional equations for the evaluation of hyperconjugation.¹³⁴ b) Revised bond separation energy (BSE) values for alkene and alkyne hyperconjugation, corrected for protobranching.

Determined by the modified method, the conjugative stabilization of butadiyne and butadiene were found to be both significant.¹³⁵ Pertinent to this discussion is the observation that when evaluated by the conventional method, hyperconjugation in alkynes is twice as large as hyperconjugation in alkenes and that the conjugative stabilization for butadiene and butadiyne

in Kistiakowsky's scheme is partially compensated by the hyperconjugative stabilization of 1-butene and 1-butyne. These hyperconjugative interactions are large enough to fully obscure the conjugative stabilization in 1,3-butadiyne! Later, it has been suggested that hyperconjugative values from Figure 60a are too low since the reference¹³⁶ compound in both these equations, propane, is stabilized by protobranching. Equations in Figure 60b give new estimates for hyperconjugation in alkenes and alkynes (based on the assumption that no protobranching corrections are needed for propyne and propene).

Furthermore, Frenking et al. provided EDA-based evaluation of delocalizing interactions in alkenes and alkynes⁷² and reported that hyperconjugation is roughly half as strong as π -conjugation between two multiple bonds. The calculated values for the hyperconjugation in propene and its trimethyl-substituted derivative $\text{H}_2\text{C}=\text{CHCMe}_3$ ($\Delta E_{\pi} = -9.3\text{--}9.5 \text{ kcal/mol}$) suggests that the hyperconjugative stabilization of C-H and C-C bonds with olefinic double bonds is half as strong as that of alkyne triple bonds. As the result, hyperconjugative stabilization of the degenerate π -systems in alkyl substituted alkynes ($\Delta E_{\pi} = -20.1 \text{ kcal/mol}$) such as 1-propyne and 4,4-dimethyl-1-butyne is as strong as the conjugative stabilization in 1,3-butadiene (-19.5 kcal/mol).⁷²

Stability of alkenes, ketones and aldehydes

Considering the above findings, it is not surprising that hyperconjugation is capable of rationalizing the well-known thermodynamic preferences for the formation of more substituted alkenes (Saytzeff rule). BLW estimates by Hiberty and coworkers suggest that for both C_4H_8 and C_5H_{10} , hyperconjugation effects stabilize the most substituted product by about 6 kcal/mol.¹³⁷ Although BLW usually gives relatively low hyperconjugation energies, this contribution is still larger than the experimental increase in heats of hydrogenation in Figure 61 that also reflects the thermodynamic stabilization of substituted alkenes (~2-3 kcal/mol per substituent). As expected from the greater acceptor ability of the carbonyl π^*_{CO} relative to that of the alkene π^*_{CC} , the differences in the experimental heats of formation for ketones vs. aldehydes vs. formaldehyde are noticeably larger (3-5 kcal/mol)

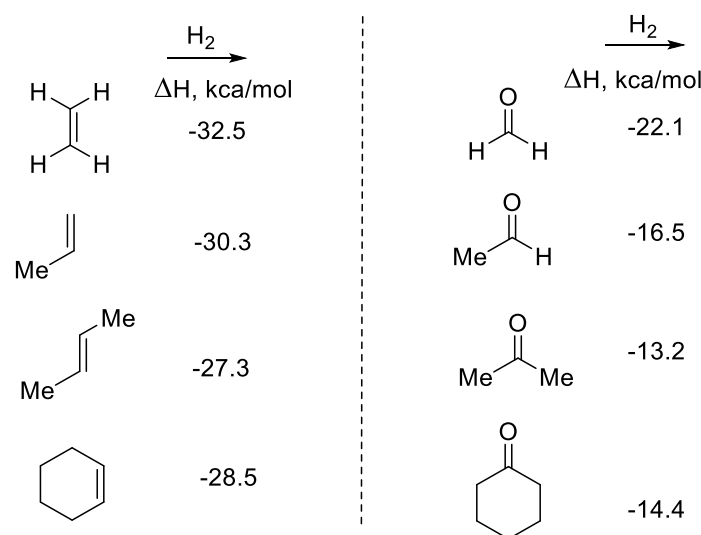


Figure 61. Experimental heats of hydrogenation for selected carbonyl compounds and alkenes.¹³⁸

Conformational equilibria

Another illustration of the importance of neutral hyperconjugation in propene is provided by its conformational profile. The stable propene conformation is called “eclipsed” because one methyl C–H bond eclipses the vicinal $\sigma_{\text{C–C}}$ bond. The “staggered” conformation, in which one methyl C–H bond eclipses the adjacent vinyl C–H bond, is less stable by about 2 kcal/mol.¹³⁹ In a similar fashion, the eclipsed conformation is favored over the bisected in sterically unencumbered aldehydes and ketones.¹⁴⁰ These names are misnomers because the “eclipsed” conformation of propene is stereoelectronically analogous to the staggered conformation of ethane (Figure 62) and vice versa.

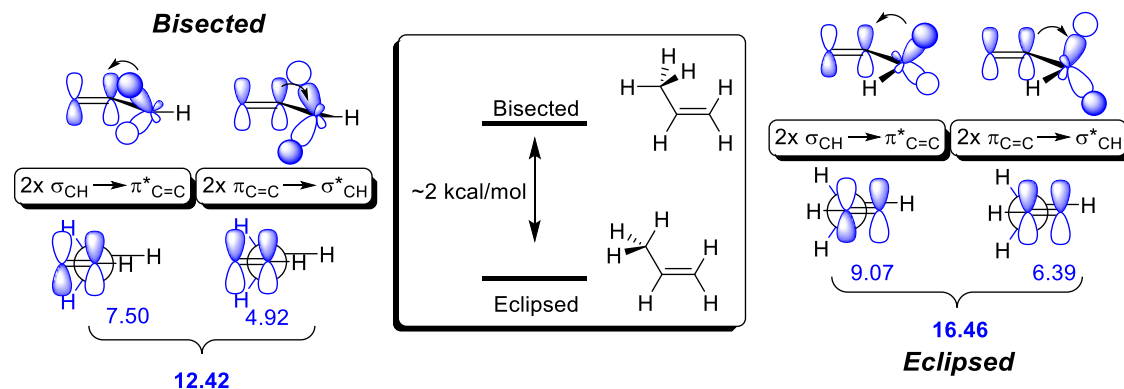


Figure 62. The difference between eclipsed and staggered conformers of propene and NBO energies for the hyperconjugative interactions between the alkene and the CH_2 group. Reprinted with permission from ref. 1.

NBO analyses by Lin et al. confirmed that the hyperconjugation interaction is the main reason for the greater stability of the eclipsed structure of propene.¹⁴¹ The most important hyperconjugation interaction observed between the methyl and vinyl groups is divided into three components: the $\pi_{\text{CH}_3} \rightarrow \pi^*_{\text{C=C}}$ interaction, the $\pi^*_{\text{CH}_3} \rightarrow \pi_{\text{C=C}}$ interaction, and the vicinal interaction between the in-plane $\sigma_{\text{C–H}}$ orbital of the methyl group and the σ^* -orbital of the antiperiplanar vinyl C–H bond. A similar explanation has been offered for the origin of conformational preferences in carbonyl compounds by Basso and coworkers.¹⁴²

The importance of different eclipsed conformations in substituted propenes can be controlled stereoelectronically by variations in the donor and acceptor properties of allylic C–X bonds and the alkene (Figure 63.). For example, the difference between the two conformations of allyl fluoride is small (the ~ 0.2 - 0.8 kcal/mol gas phase preference for the conformation with the C–F eclipsed bond). This is an apparent violation of the main stereoelectronic rule (the best acceptor, $\sigma^*_{\text{C–F}}$, is orthogonal to the best donor $\pi_{\text{C=C}}$ in this conformation). Attractive H...F interaction¹⁴³ is a possible reason for this seeming anomaly. If an electron acceptor (nitro group) is introduced at the alkene, the preference for keeping C–F bond orthogonal to the π -system increases (from 0.7 kcal/mol for Y=H to 2.0 kcal/mol for Y=NO_2). If a donor is introduced (Y=OH), the conformational preference is reversed - the C–F bond in the more stable conformer aligns with the π -system (-1.5 kcal).¹⁴⁴

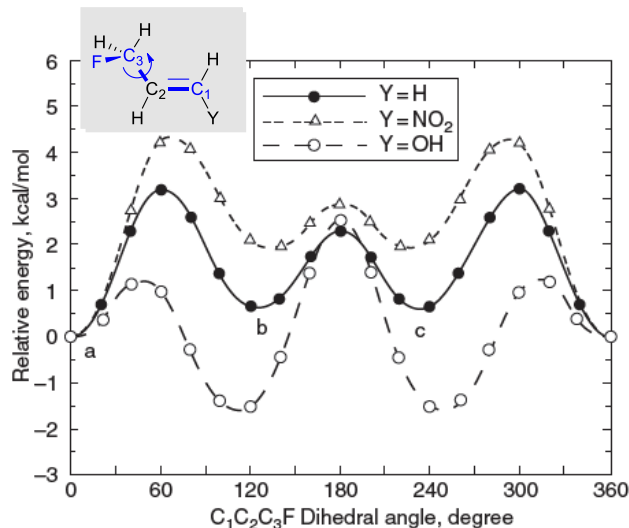


Figure 63. The relative importance of different eclipsed conformations in substituted allyl fluorides at B3P86/6-311G(3d,2p) level. (Reprinted with permission from ref144. Copyright 2010 John Wiley & Sons, Ltd.)

When the complexity of stereoelectronic effects in this system was analyzed by comparing the NBO energies of all vicinal interactions involved in electronic communication between the vinyl moiety and the substituted allyl group, the total hyperconjugative energies were found to follow the overall conformational profiles.

Similar hyperconjugative interactions were suggested to explain the preferred perpendicular orientation of benzylic C-X bonds relative to the plane of the benzene ring (X = S(O)Me, SO₂Me, SH, SMe, Cl) in ArCH₂X compounds.¹⁴⁵ With the exception of X = F, these compounds have a low energy conformation in which the C-X bond is aligned with the benzene π -system (Figure 64). The magnitude of this effect is a function of X: S(O)Me, SO₂Me > Cl > SH, SMe > F. The unusual conformation of X = F stems from an electrostatic attraction between the heteroatom and a syn-periplanar ortho-hydrogen. For X = Cl, $\pi \rightarrow \sigma^*_{C-Cl}$ interaction was suggested to play a dominant role. For X = SH, the interaction between C-X bond and the aromatic π -system is not unidirectional and both $\sigma_{C-S} \rightarrow \pi^*$ and $\pi \rightarrow \sigma^*_{C-S}$ interactions were implicated as the possible sources for the observed conformational preference.

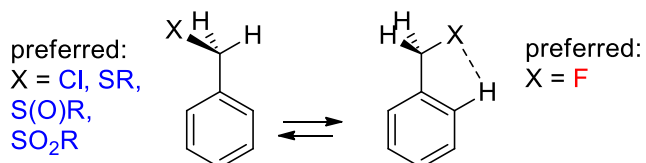


Figure 64. The interplay of hyperconjugative and electrostatic interactions determines orientation of benzylic C-X bonds relative to the adjacent aromatic system.

Hyperconjugation in acyclic and cyclic carbocations. Hyperconjomers.

Positive hyperconjugation from neighboring C-H bonds stabilizes carbocations, as can be seen by the following decreasing order of hydride affinities: methyl > primary > secondary > tertiary carbocations (Figure 65).¹⁴⁶

The role of hyperconjugation increases dramatically in cyclohexyl cations where it has a profound effect on structure and stability. An elegant study of Rauk and coworkers¹⁴⁷ reported the different hyperconjugation stabilization patterns lead to the formation of two chair conformers of 1-Me-1-cyclohexyl cation where the carbocation p-orbital is oriented either “axially” or “equatorially”. These conformers, called “hyperconjomers”, have distinctly different modes of hyperconjugative stabilization. The axial cationic orbital in the first hyperconjomer interacts strongly with the adjacent axial C-H bonds, whereas the equatorial vacant p-orbital in the second cation interacts most strongly with the antiperiplanar C-C bonds (Figure 65).

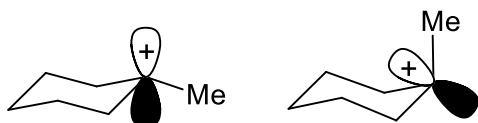


Figure 65. Axial and equatorial “hyperconjomers” of cyclohexyl cations.

A detailed NBO analysis of the electronic structures of these species is summarized in Figure 66. As suggested earlier by Rauk et al. for 1-Me-cyclohexyl cations, the $\sigma_{\text{C-C}} \rightarrow n_{\text{Cl}}$ and $\sigma_{\text{C-Hax}} \rightarrow n_{\text{Cl}}$ interactions play the dominant roles in stabilizing the equatorial and axial “hyperconjomers”. Interestingly, the $\sigma_{\text{C-C}} \rightarrow n_{\text{Cl}}$ interaction is larger than the $\sigma_{\text{C-Hax}} \rightarrow n_{\text{Cl}}$ effect in contrast to the $\sigma_{\text{C-Hax}} \rightarrow \sigma^*_{\text{C-H'ax}} > \sigma_{\text{C-Heq}} \rightarrow \sigma^*_{\text{C-C}}$ order in neutral cyclohexane.⁷⁰ This observation does not indicate inversion of the relative donor ability of C-H/C-C bonds. Instead, its origin is in a non-perfect overlap of the vacant orbital with the “axial” C2-H bond as a result of planarization at C1. On the other hand, planarization also increases the overlap of the positive center with the “equatorial” C2-H bond, thus allowing the cation to benefit from the hyperconjugative interaction with two donors at the same time. Although the energy of combined $\sigma_{\text{C-Hax}} \rightarrow n_{\text{Cl}}$ and $\sigma_{\text{C-Heq}} \rightarrow n_{\text{Cl}}$ interactions in the “axial” conformer is greater than that of $\sigma_{\text{C-C}} \rightarrow n_{\text{Cl}}$ interactions in the “equatorial conformer 31.5 vs. 27.2 kcal mol⁻¹, the balance of hyperconjugative effects is tipped in favor of the “equatorial” conformer by subtle effects involving remote donor moieties: $\gamma_{\text{C-H}} \rightarrow n_{\text{Cl}}$ homohyperconjugation with through space participation of $\gamma_{\text{C-H}}$ bonds and an increase double hyperconjugation manifested in the $\delta_{\text{C-Heq}} \rightarrow \sigma^*_{\text{C-C}}$ interaction.

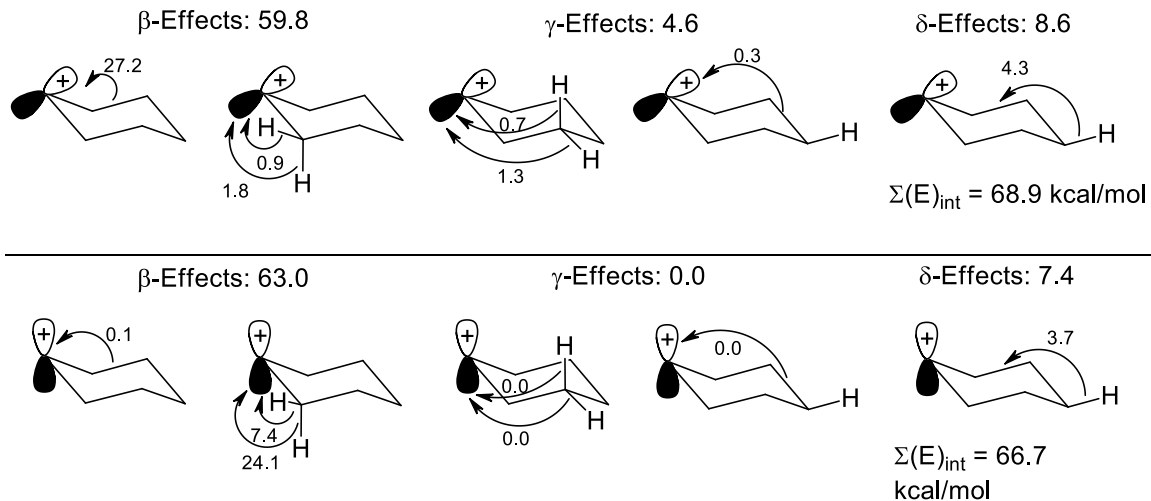


Figure 66. Second order perturbation NBO energies in kcal/mol for important hyperconjugative interactions in axial and equatorial cyclohexyl cations (B3LYP/6-31G**).

These observations underscore the importance of double hyperconjugation in hyperconformers which renders these species useful tools for the analysis of the relative donor ability of σ -bonds (section “Patterns of hyperconjugation”)

Anomeric effects.

The anomeric effect is one of the best documented and the well-studied of hyperconjugative effects.¹⁴⁸ This effect was originally defined as the preference for an electronegative substituent positioned next to an oxygen atom in a tetrahydropyran ring (or at the anomeric carbon of pyranoses) for occupying an axial rather than an equatorial position.^{149,150}

A convenient way to evaluate anomeric stabilization is to compare energy associated with the change from axial to equatorial position in oxacyclohexane and cyclohexane (Figure 67A).¹⁵¹ In order to correct for the fact that C-O bonds are shorter and axial substituents in oxacyclohexane may suffer from greater 1,3-diaxial repulsions with the axial hydrogens, Franck suggested the following equation to correct for this difference: $\Delta\Delta G(\text{AE}) = \Delta G(\text{heterocycle}) - 1.53 * \Delta G^\circ \text{ steric(cyclohexane)} - 0.08$.¹⁵¹

Some of the classic examples where the anomeric effect was first recognized are, in fact, quite complicated. The true importance of anomeric effect can be masked when other steric or stereoelectronic interactions exert their own influence. In such cases, it is the balance of multiple effects that defines the overall conformational preferences. In particular, the gauche effect (preference for conformations with fewer anti CX/CY interactions between vicinal bonds with acceptor elements X and Y) may be either enforce or oppose the anomeric effect (Figure 67B).

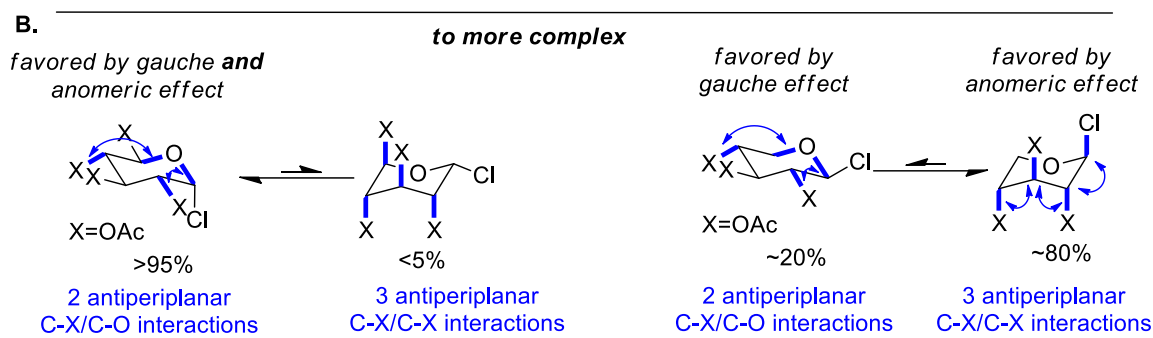
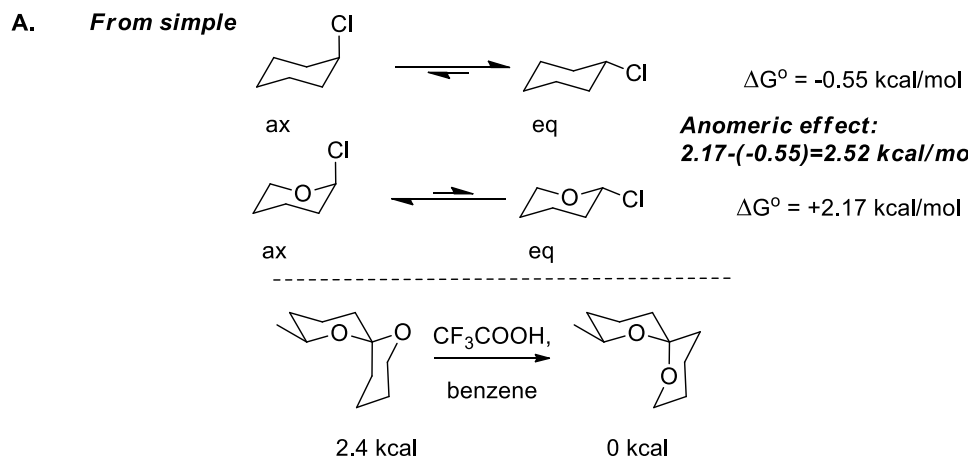


Figure 67. A: Axial preference for acceptor groups at the anomeric positions.¹⁵² B: Combinations of gauche and anomeric effects in control of sugar conformations. [Error! Bookmark not defined.c](#)

It was subsequently recognized that this preference is a consequence of a more general effect which requires that a lone pair n_X at heteroatom X and C-Y bond in a YCH_2X moiety are aligned in an antiperiplanar geometry^{118,153,154} that maximizes the hyperconjugative $n_X \rightarrow \sigma^*_{C-Y}$ interaction (Figure 69). Similar stereoelectronic requirements for the relative positions of donor and acceptor orbitals are also manifested in conformational equilibria of substituted cyclohexanes.¹⁵⁵

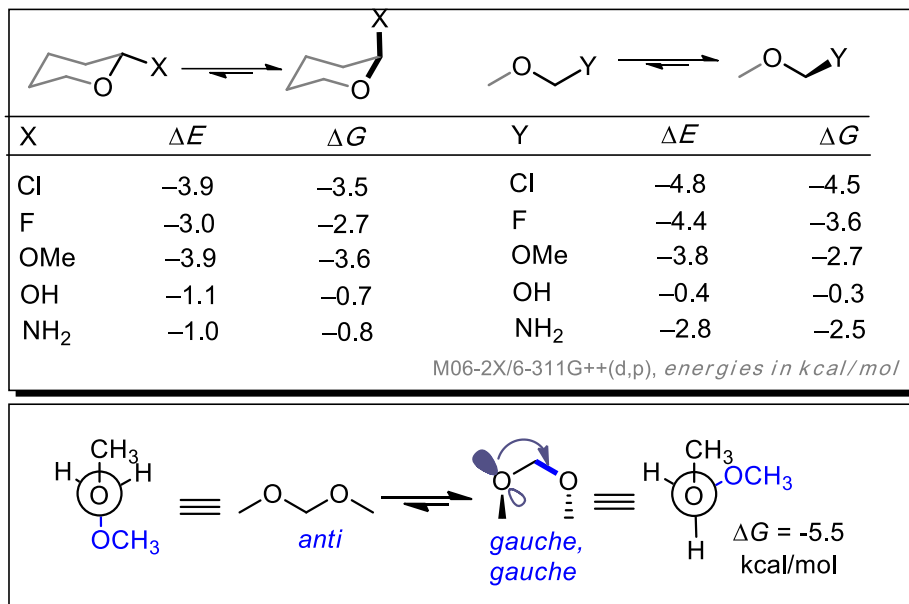


Figure 68. Top: Conformational preferences illustrate the generalized anomeric effect in cyclic and acyclic systems in the gas phase (M06-2X/6-311G++(d,p) data in kcal/mol)¹¹ Bottom: hyperconjugational contribution to the generalized anomeric effect.

Although there are several components of the anomeric effect, such as an electrostatic component, (e.g. electrostatic interactions and steric effects), the above hyperconjugative interaction of the antiperiplanar orbitals plays a particularly important role. This is reflected in structural changes (C-Y bond elongation and C-X bond shortening), in the distribution of electron density (increased negative charge on Y) and in reactivity (C-Y bond weakening). An analogous interaction with the lone pair of an exocyclic heteroatom Y and σ^*_{c-x} of the ring provides a stereoelectronic basis for the so-called exo-anomeric effect – preference for the synclinal (gauche) arrangement of the Y-C and C-X bonds. The same preference is observed for the acyclic X-C-Y-C systems where X and Y are heteroatoms with at least one lone pair, commonly oxygen, nitrogen and fluorine.¹⁵⁶ The latter is important for determining the conformational energy profiles of acetals and esters.

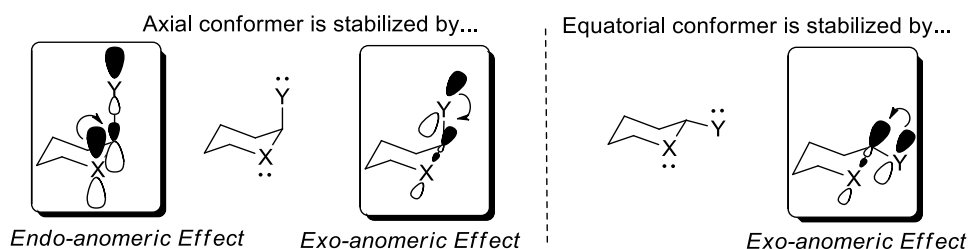


Figure 69. Antiperiplanar negative hyperconjugative interaction in the endo- and exo-anomeric effects.

In addition to the hyperconjugative model, alternative explanations have been proposed to rationalize the anomeric effect. In particular, the electrostatic model¹⁴⁹ is based on favorable local dipole-dipole interactions and a smaller net dipole in the axial conformation relative to the

equatorial conformation. BLW, NBO and EDA analyses give slightly different weights to the importance of electrostatic and conjugative effects. For example, a computational study by Y. Mo based on the block-localized wavefunction (BLW) method suggested the hyperconjugative delocalization plays a much smaller factor in the anomeric effect than sterics (electrostatic interactions + Pauli repulsion).¹⁵⁷ A more recent NBO study by Freitas suggested that there are examples where each model plays the major role.¹⁵⁸ Yet another recent study utilizing EDA suggests that the anomeric effect is dominated by exchange energies and electrostatics have minor contribution.¹⁵⁹

An advantage of the hyperconjugative model is that it readily explains the structural changes associated with the anomeric effect. In particular, preference for axial position is accompanied by a characteristic combination of structural changes that can be attributed to the increased contribution of $n_O \rightarrow \sigma_{C-X}^*$ interactions.¹ Shortening the O-C2 distance in the axial conformer is consistent with the increased O-C2 double bond character whereas C-X bond elongation reflects the transfer of additional electron density to the antibonding σ_{C-X}^* orbital.¹

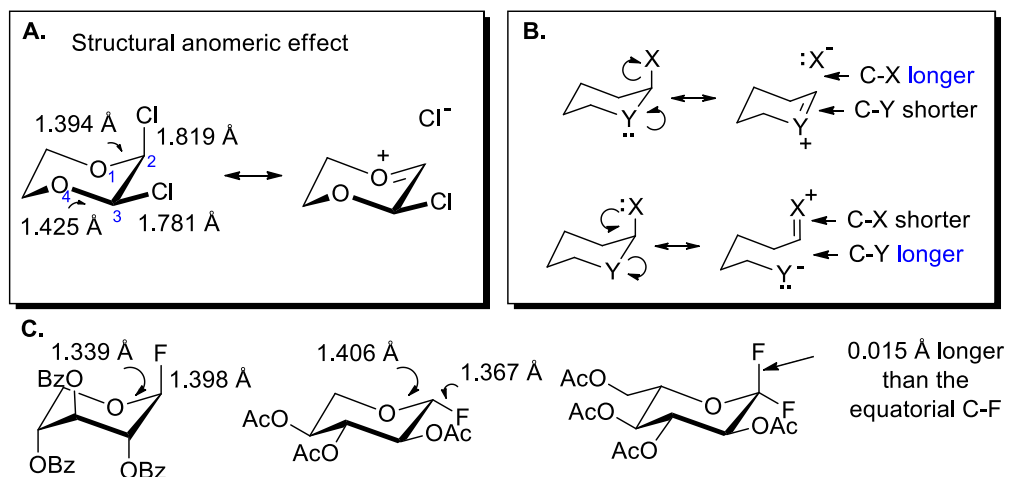


Figure 70. Structural consequences of anomeric effect. A: Selected bond lengths in *cis*-2,3-dichloro-2,4-dioxane. B: The opposing effects of endo- and exo-anomeric effects on geometries. C: Selected structural consequences of anomeric effect in OCF moiety. (Reprinted with permission from ref. 1)

Electron density changes at the exocyclic atoms is also consistent the hyperconjugative model: both hydrogen and fluorine gain additional electron density when they move from an equatorial to an axial position. The observation that both H and F gain similar amount of electron density when moving from the equatorial to the axial position may seem surprising in view of the different acceptor abilities of the C-H and C-F antibonding orbitals.¹⁶⁰ However this is not unexpected once the interplay of different electronic effects is analyzed in more detail. For example, NBO analysis shows that the mechanisms by which the electron density is increased at the axial H and F are different. Most of gained electron density at the axial F is due to the σ_{CF}^* population increase as a consequence of $n_F \rightarrow \sigma_{CF}^*$ interaction. In contrast, the density increase at the axial H comes from two sources: increase in the σ_{CH}^* population and increase in the σ_{CH} population (back to ~ 2.0 electrons). The latter change is not surprising because the axial C-H bond has no vicinal hyperconjugative acceptors (only the three lone pairs at the three

heteroatoms), so all vicinal $\sigma_{\text{CH}_{\text{eq}}}$ \rightarrow σ^* interactions, depleting electrons CH bond from its electron density, are deactivated by the conformational change.

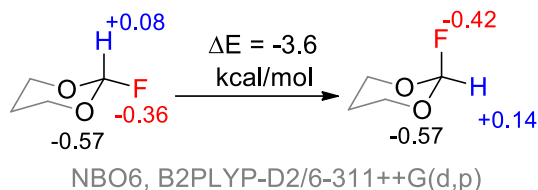


Figure 71. Changes in the charge distribution in the axial and equatorial conformers of 2-fluoro-1,3-dioxane.

The generalized anomeric effect is manifested broadly. For example, the anomeric effect contributes to the inertness of CF_2 moieties incorporated in many pharmaceuticals. It also plays important role in stabilization of fluorinated ethers, sulfides, and amines. It also operates in many common systems such as hydrogen peroxide, phosphates, boronates, freons, and hydrazines. However, the anisotropic properties of $n_{\text{O}} \rightarrow \sigma^*_{\text{X-Y}}$ interactions greatly diminish the importance of anomeric effect in alkyl peroxides. As we discussed earlier, the $n_{\text{O}} \rightarrow \sigma^*_{\text{O-C}}$ interactions are weak, and the situation is made worse in bis-alkyl peroxide by hybridization effects that make the OOC angle smaller and add an additional antibonding interaction (Figure 72).

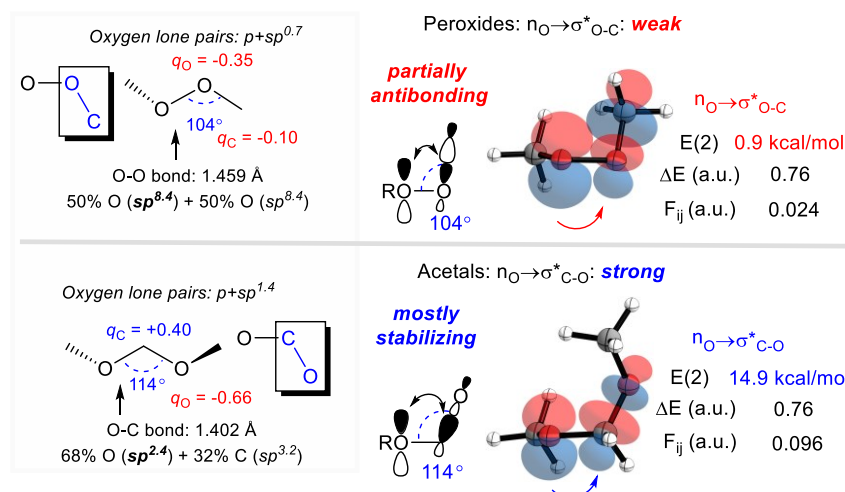


Figure 72. Electronic and structural differences that account for the extreme weakness of anomeric effect in peroxides

A “comeback” of the anomeric effect in peroxides was identified as the source of unusual stability of bis- and tris-peroxides.¹¹ The anomalous stability of these molecules contradicts the conventional wisdom - such bis-peroxides can even melt without decomposition at temperatures exceeding 100°C. This surprising behavior is associated with the stereoelectronic stabilizing effect that two peroxide groups can exert on each other. This stabilization originates from strong anomeric $n_{\text{O}} \rightarrow \sigma^*_{\text{CO}}$ interactions that are absent in mono-peroxides but appear when the additional peroxide moiety is introduced and separated by a one-atom bridge. From the stereoelectronic perspective, such bis-peroxides are analogous to bis-acetals.

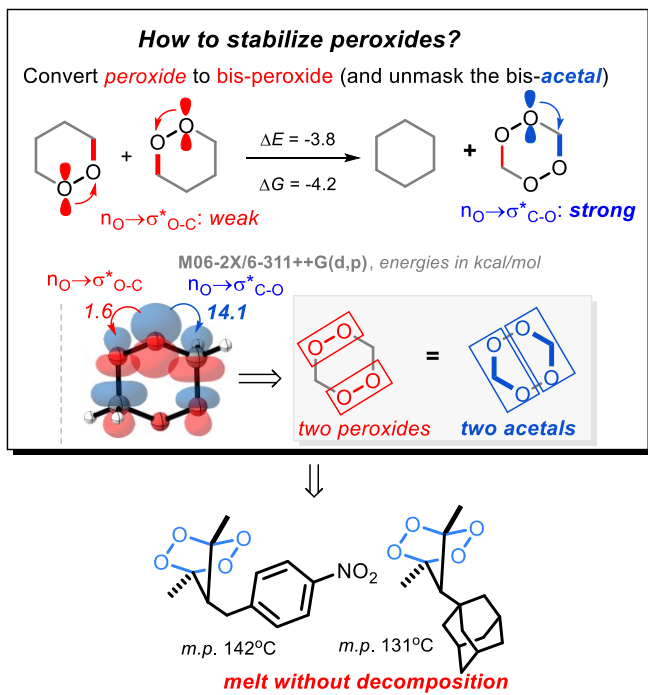


Figure 73. Activation of anomeric effect explains why bis-peroxides can be more thermodynamically stable than mono-peroxides

Understanding of anomeric effects in peroxides led to the recent discovery of ozone-free synthesis of ozonides¹⁶¹ and to stereoelectronic interruption of the Baeyer-Villiger reaction that allowed the isolation of stable Criegee intermediates (vide infra).¹⁶²

Extended hyperconjugation

Homoanomeric effects

The patterns of homoanomeric effects were presented in Figure 22. The relative role of the W- and the Plough homoanomeric effects in aza-, oxa-, thio- and selenaheterocycles was investigated with NMR experiments and NBO analysis (

Table 1.^{62,163} These effects play an important role in the relative trends in one-bond $^1\text{J}_{\text{CH}}$ coupling constants, needed for the understanding of conformational properties of carbohydrates, azacarbohydrates and other substrates of biological interest.^{100b,c,d}

Although the homoanomeric effects are considerably weaker than the classic vicinal anomeric $n_{\text{ax}} \rightarrow \alpha-\sigma^* \text{C-Y}_{\text{ax}}$ interactions, their importance increases significantly when the acceptor ability of σ^* -orbitals increases as a result of bond stretching and/or polarization. For example, solvolysis of piperidines and pyrrolidines with a leaving group at the β -carbon proceeds through the formation of cyclic aziridinium cations, due to anchimeric assistance from the nitrogen lone pair.¹⁶⁴ The presence of such intermediates leads to retention of configuration and efficient transfer of chirality in their respective ring contraction or expansion reactions.¹⁶⁵ Topologically similar transformations are the key mechanistic steps of Payne and aza-Payne rearrangements.¹⁶⁶

In addition to the anchimeric assistance in the formation of bridged cationic intermediates, there is clear structural and spectroscopic evidence for homoanomeric interactions in neutral ground state molecules at their energy minimum conformations.⁵¹

Homohyperconjugation

The importance of homohyperconjugation can be glimpsed from significant stabilization of meta-X-substituted aryl anions (X = F, Cl, Br) relative to phenyl anion. The larger effect of Cl and Br in comparison to F suggests that this stabilization does not result from the inductive effect but rather represents an orbital phenomenon (Figure 74). The reasons of increased acceptor ability of bonds to heavier halogens²⁰ will be explained in the following section.

Experimental gas phase stabilization relative to phenyl anion, kcal/mol

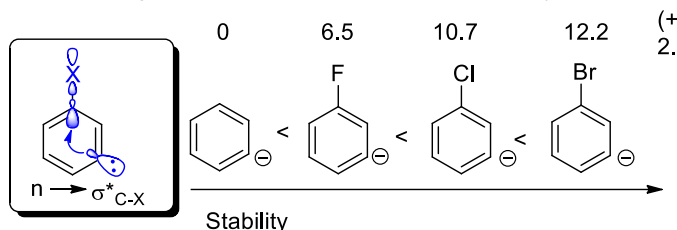


Figure 74. Effect of negative homohyperconjugation on the stability of aryl anions

Double hyperconjugation

The stabilizing effect of negative double hyperconjugation is illustrated by increased stability of para halosubstituted aryl cations. The greater stabilization by the heavier halogens, F<Cl<Br (2.1<7.3<8.9 kcal/mol), suggests that inductive and field effects are of secondary importance relative to the donor acceptor interaction between carbanion and σ^*_{C-X} orbital mediated by the C-C bridge. An example of negative double hyperconjugation in a neutral system is provided by the large effect of C4 fluorine substitution on the basicity of piperidines.¹⁶⁷ Although the fluorine effect has inductive and electrostatic components, the importance of stereoelectronic hyperconjugative contribution is supported by the much smaller pKa change for the axial fluorine introduction (Figure 75B).

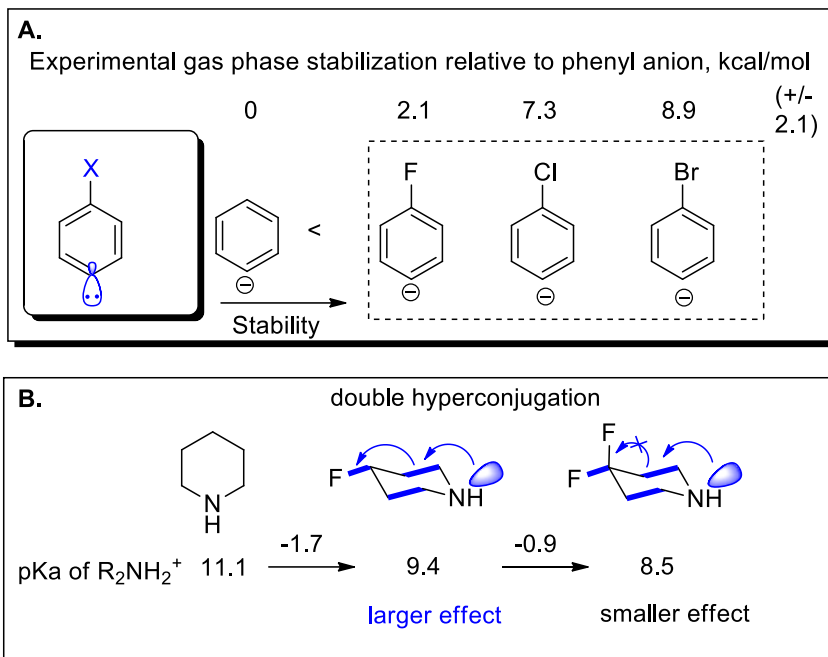


Figure 75. Effect of negative double hyperconjugation on the stability of aryl anions (A) and on basicity of 4-substituted piperidines (B).

Double hyperconjugation plays important role in chemistry of 1,4-diradicals where it is usually referred to as Through-Bond (TB) coupling between the two radical centers. This interaction renders the Bergman cyclization a symmetry allowed process¹⁶⁸ and provides an additional 3-5 kcal/mol of stabilization energy to the *p*-benzyne-type diradical which is not available in related monoradicals.^{169,170} Because this stabilizing effect is lost in the first H-abstraction by *p*-benzyne, it renders this species less reactive and more selective in H-abstraction reactions in comparison to the phenyl radical. The energetic consequence of this interaction is evaluated by the Biradical Stabilization Energy (Figure 76).

Through-Bond coupling plays an even larger role in similar systems with increased polarization. For example, it is responsible for stabilization provided by the Au-moiety provides in the product of Au-catalyzed Bergman cyclization to the cationic center. This stabilization leads to delocalization of positive charge in the Au-Bergman product in comparison to the parent phenyl cation. Remarkably, the latter stabilizing effect is much larger (20 kcal/mol) than the mutual stabilization due to the coupling of two radical centers of p-benzene.¹⁷¹ Interestingly, coupling between the non-bonding orbitals is dramatically enhanced upon one-electron reduction.¹⁷²

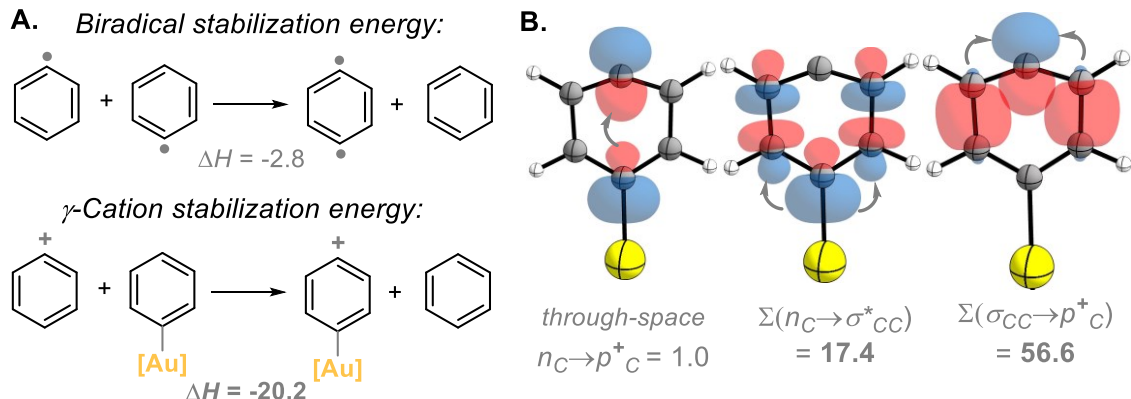


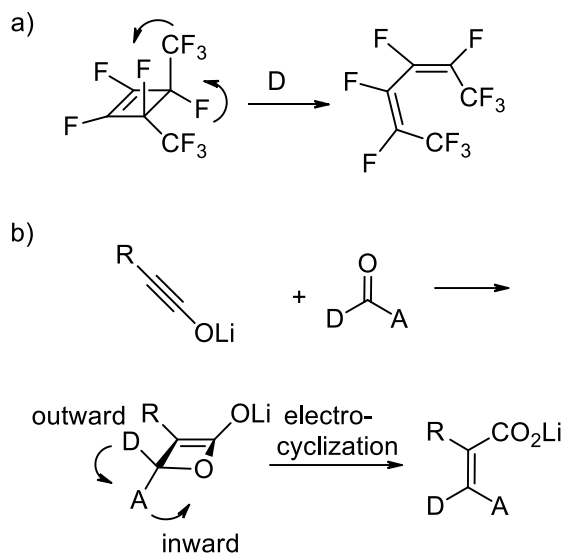
Figure 76 A. top: stabilization in p-benzyne stems from the through-bond coupling between the two radical centers; bottom: stabilization in the product of Au-catalyzed Bergman cyclization is dramatically increased. Energies in kcal/mol. B. Selected NBO interactions (in kcal/mol) stabilizing the positive charge in the product. PR₃ group omitted for clarity.

Stretched and breaking bonds as partners in hyperconjugative interactions: new patterns of selective TS stabilization

Below we will provide a few examples that illustrate the diversity of hyperconjugative patterns that are involved in transition state stabilization. At the top of each section, we will list the dominant hyperconjugative interaction that involves a breaking σ - or π -bond.

Torquoselectivity: Lone pair \rightarrow breaking σ^ -orbital or breaking σ -orbital \rightarrow π^* -orbital.*

An example of dramatic hyperconjugative effects on reactivity is provided by torquoselectivity (the preference for ‘inward’ or ‘outward’ rotation of substituents in electrocyclic ring opening reactions) in thermal cyclobutene ring opening.¹⁷³ Although the opening can proceed through two symmetry-allowed conrotatory pathways, Dolbier, Burton, Koroniak, and co-workers observed a dramatic kinetic preference for the inward vs. outward rotation for different substituents (Figure 77a).¹⁷⁴ Another illustrative example in Figure 77b is provided by elegant work of Shindo and coworkers who efficiently used hyperconjugation to obtain stereodefined products from oxacyclobutenes.¹⁷⁵ Similarly, Murakami et al. reported that boryl and silyl groups behave as σ -acceptors and prefer to rotate inward in the cyclobutene ring-opening reaction despite the steric congestion.¹⁷⁶ In all examples, electron donors rotate outward whereas the acceptors prefer an inward rotation.



D: electron donating (R'O- etc.)

A: electron accepting (R'3Si-, R'2OCH2-, R'2NCH2- etc.)

Figure 77. Examples of of torqueoselectivity in stereoselective cyclobutene and oxacyclobutene ring-openings.

Houk and coworkers provided convincing theoretical rationale for these striking selectivities. The key stereodefining effect is interaction of the σ and σ^* associated with the breaking C-C bonds with donor and acceptor orbitals of the substituents. As the C-C bond is stretched, the energy of the σ -orbital is raised and the σ^* -orbital is lowered and, in the TS, they become the HOMO and the LUMO respectively.

Antiperiplanar orbital arrangement in the outward rotation maximizes interaction between the donor orbital of the substituent and σ^* -orbital of the stretched cyclobutene bond (the LUMO of the transition state). On the other hand, acceptor substituents with a low-lying vacant orbital prefer an inward conrotation, where this orbital overlaps directly with the σ^* -orbital of the stretched bond (the HOMO of the transition state). Both of these effects correspond to a two-electron interaction and stabilize the transition state.

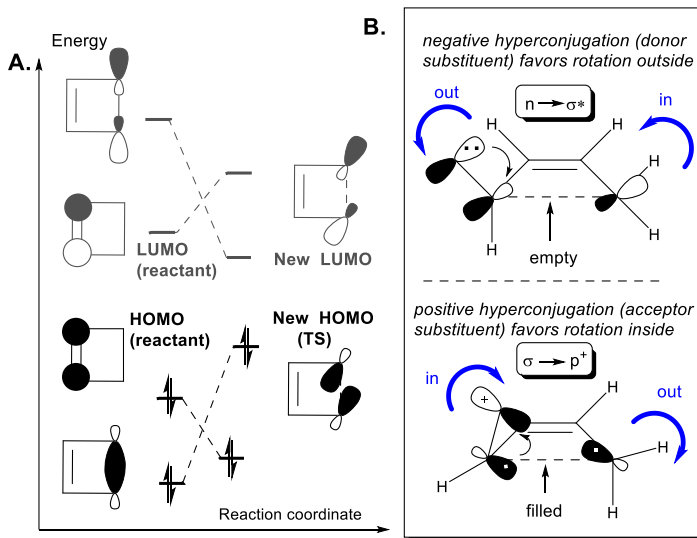


Figure 78. A: Changes in HOMO and LUMO upon stretching and twisting of the central σ -bond. B: Dominant hyperconjugative interactions which control outward rotation of a donor substituent and inward rotation of an acceptor substituent. In the first case, the key interaction is negative hyperconjugation between the transition state HOMO (a stretched and twisted σ -orbital) with a substituent empty p-orbital (same topology is important for an acceptor σ^* - or a π^* -orbital). In the second case, the key interaction is positive hyperconjugation between the transition state LUMO (a stretched and twisted σ^* -orbital) with a substituent filled p-orbital (same topology is important for a donor σ - or a π -orbital).

Oxyanionic assistance: Lone pair \rightarrow breaking σ^ -orbital*

Torquoselectivity is not the only example of hyperconjugative effects in pericyclic reactivity. For example, the oxy-Cope rearrangement is dramatically ($10^{17}!$) accelerated by deprotonation of the OH group at the central C-C bond (Figure 79).¹⁷⁷ Even when significant electron assistance is available in the neutral state (e.g., an OR group is present at the other carbon of the breaking C-C bond), the effect weakens but does not disappear – the deprotonation still leads to 10^{12} -fold acceleration. The electronic origin of this effect is in the dramatic increase of the donor ability of the lone pairs of oxygen upon its deprotonation.

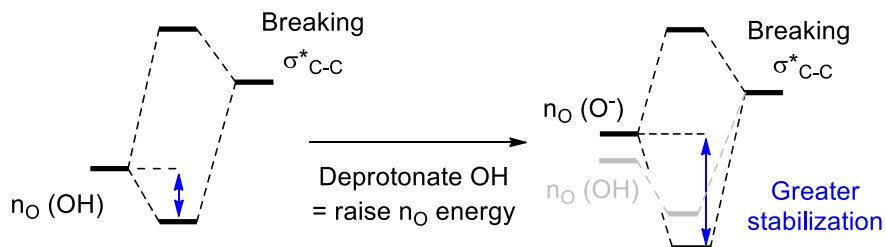
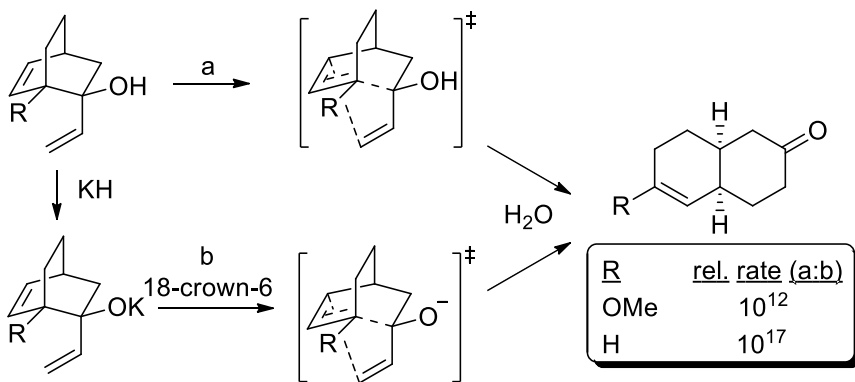


Figure 79. Large rate enhancements of the oxy-Cope rearrangement provided by anionic TS stabilization.

The bis-anionic oxy-Cope¹⁷⁸ rearrangement of bis-alkynes produced by the reaction of acetyliides with benzil occurs below room temperature (Figure 80).¹⁷⁹ Computational studies the cumulative effect of the four radical stabilizing groups (Ph and O⁻) on the central C-C bond weakening. Interestingly, the two deprotonations decrease the activation energy even more (15-16 kcal/mol) than the two Ph groups (~12 kcal/mol). As a result, the calculated Cope rearrangement barrier falls from >30 to ~5 kcal/mol. The central C-C bond weakened so much that the anionic Cope rearrangement can be diverted into a dissociative process¹⁸⁰ in the presence of bulky TIPS substituents at the alkyne termini.

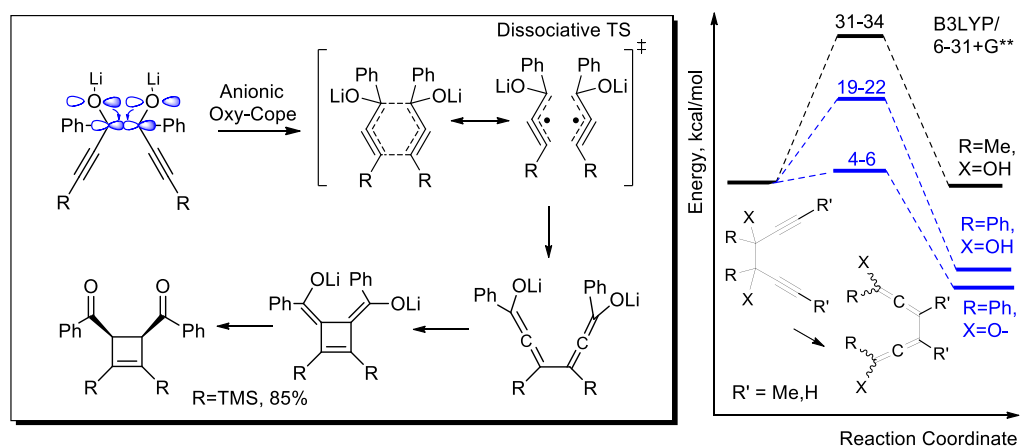


Figure 80. Lone pair/radical stabilization dramatically accelerates the anionic oxy-Cope rearrangement.

Anchimeric assistance by alkene: π -Orbital \rightarrow breaking σ^* -orbital

Both lone pairs (as illustrated by the textbook formation of bromonium and sulfonium ions) and π -bonds participate can assist in heterolytic σ -bond scission. Although such effects are usually described in the context of carbocation stabilization, the effects are kinetic in nature and thus has to apply to systems where the C-X bond is only partially broken, hence straddling the line between hyperconjugation and conjugation (Figure 2).

The measured kinetic consequences of such through space delocalization are enormous. For example, a properly positioned alkene provides dramatic acceleration (10^{11}) of ionization of anti C-X bonds with perfect stereospecificity of substitution.¹⁸¹

An interesting feature of this effect is that it is provided “on demand” and utilized fully only when additional stabilization of the cationic center is needed. The accelerating effect is not activated in the presence of a directly attached cation-stabilizing group. For example, the *p*-anisyl group at C7 (Figure 81) can stabilize the developing carbonium ion center to the extent where the difference in reactivity between the two classes of compounds almost disappears (a factor of 3) along with the stereospecificity of substitution.¹⁸²

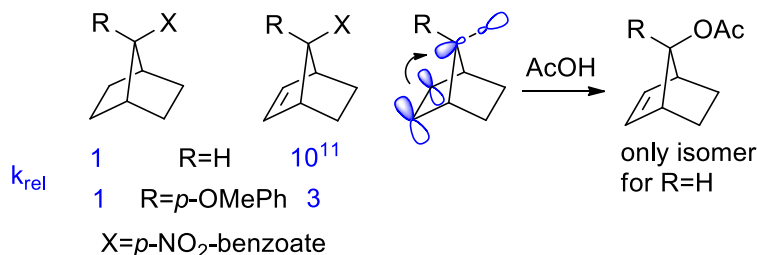


Figure 81. Solvolysis assisted by homoconjugation

Anchimeric assistance by cyclopropane: Strained σ -orbital \rightarrow breaking σ^* -orbital

The ability of the cyclopropyl ring to assist in the C-X bond ionization via homohyperconjugation is even higher, leading to the impressive 10^{14} acceleration relative to the respective 7-X-substituted norbornane and 10^3 acceleration relative to the already highly activated 7-X-substituted norbornene (Figure 82).¹⁸³

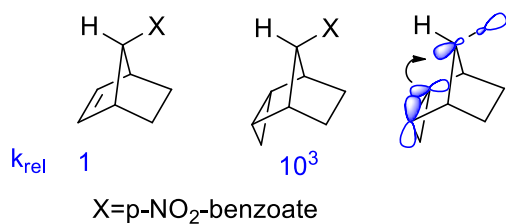


Figure 82. Comparison of homoconjugative and homohyperconjugative effects

Alkyne-azide cycloaddition reactions: π -Orbital \rightarrow breaking σ^* -orbital

Interaction of substituents with distorted π -bonds can provide TS stabilization similar to what we have discussed above for the stretched σ -bonds. Such effects can include both intra- and intermolecular contributions. The intramolecular contributions can compensate for distortion

and bond breaking whereas intermolecular contributions can facilitate bond formation. Below we will show how intra- and intermolecular effects work in synergy in non-catalyzed alkyne-azide cycloadditions. In this case, both effects originate from the presence of the same σ -acceptor at the propargylic carbon.

The >50-fold acceleration of the azide-alkyne cycloaddition by the propargylic fluorine substituent in α,α -difluorocyclooctyne (DIFO) was reported by Bertozzi and coworkers.¹⁸⁴ Subsequently, it was shown that the effect has a stereoelectronic component - it is maximized once the optimal orbital overlap between the σ_{C-F} bond and the in-plane alkyne π -system is achieved.¹⁴³

NBO analysis found that the accelerating effect originates from two sources. The first of them, is assistance to alkyne distortion by propargylic C-F bonds and other sigma acceptors. It originates from the higher donor ability of distorted π -bonds discussed previously (section “Decreasing the energy gap: Stretched bonds as donors and acceptors in hyperconjugative interactions.”).

The stabilizing effect increases even further in the full TS, where azide is brought to the close proximity to the bent alkyne. This increase indicates that the propargylic acceptor facilitates bond formation in the transition state (Figure 83) as the alkyne LUMO (the in-plane π^* orbital) gains electron density as the azide approaches.

An intermolecular hyperconjugative TS stabilizing effect

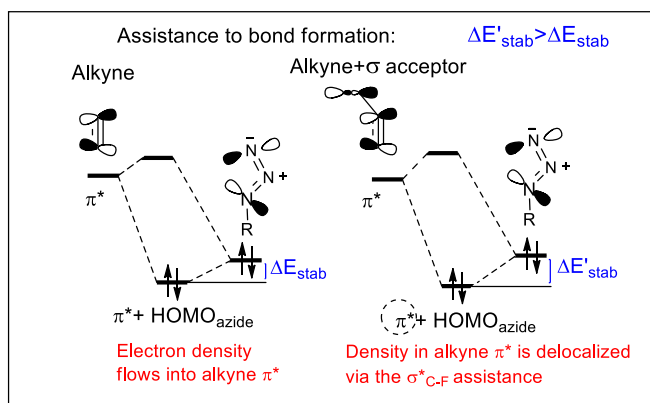


Figure 83. Hyperconjugative assistance to bond formation provided by σ -acceptors in azide-alkyne cycloadditions. This example illustrates how intermolecular transfer of electron density can benefit from hyperconjugation. Reprinted with permission from ref. 1.

While exocyclic fluorine substituents in DIFO cannot achieve the antiperiplanar orbital arrangement, cyclooctynes bearing endocyclic acceptors allow for much stronger interactions and enhanced reactivity.^{185,186} In addition to assisting in bending linear alkynes to the TS geometry, when acceptors are contained within a cycle, they alleviate strain in bent alkynes. Although the premature activation of this interaction is a, potentially decelerating, reactant-stabilizing effect, the calculated TS energies suggest that alkynes with endocyclic acceptors are still more reactive than the parent cyclooctyne (Figure 84). Such increase in reactivity is possible because the stabilizing interactions grow even stronger in the TS. This increase illustrates the power of hyperconjugative TS stabilization as an element of reaction control.

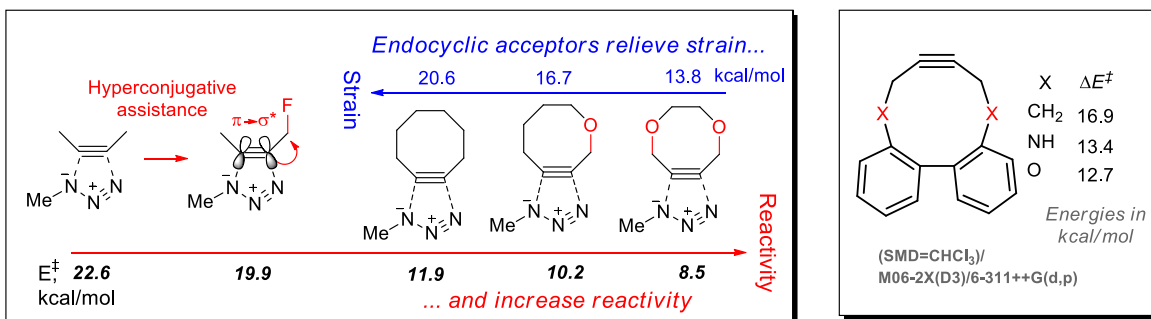


Figure 84. Simultaneous hyperconjugative alleviation of strain and enhancement of reactivity in cyclooctynes and twisted cyclodecynes for metal-free click chemistry.

Stabilization of bent alkynes is not limited to cycloadditions – it can be applied to other alkyne-forming and “alkyne-consuming” reactions, such as formation and reactivity of *o*-benzyne.¹⁸⁷

Stretched bonds as efficient partners in Through-Bond interactions: Lone pair+radical → breaking σ-orbital*

More complex patterns of hyperconjugation interactions can emerge in multifunctional transformations where multiple bonds are formed and broken at the same time.

A new stereoelectronic interaction was found in fragmentations that complete radical cascades which convert aromatic enyes into α -Sn-substituted naphthalenes (Figure 85a). After a sequence of reactions that provide the formal 6-endo-trig product, the penultimate species of this cascade, the final step involves a C-C bond scission. The efficiency of fragmentation can be enhanced by stabilizing the rational design of radical leaving groups.¹⁸⁸

Comparison of fragmentations leading to the α -oxy radical (CH_2OMe) vs. the propyl radical, suggested the presence of a selective reactant stabilization for the O-containing fragmentation precursor via through-bond (TB) interaction between benzylic radical and the lone pair at the δ -position. Such TB coupling involves two non-bonding orbitals populated with three electrons (the lone pair of X and the radical center). Although such reactant stabilization is a potentially deactivating effect, the odd-electron TB communication between the radical and the lone pair through the σ -bridge increases even further at the transition state.

The increase in TB interaction through stretched bonds is documented by NBO orbital interaction energies. In the fragmentation process, the energy of the σ^* -antibonding bridge orbital is lowered, decreasing the ΔE_{ij} term for the stabilizing interaction that couples the non-bonding orbitals (i.e., the radical and lone pair). In addition, as the fragmentation progresses, the $\sim\text{sp}^3$ σ -bond is transformed into two p-orbitals (one π -bonded in naphthalene and the other in a 2c-3e “half-bond”), increasing overlap between interacting orbitals in (Figure 85b). Together these interactions are responsible for selective TS stabilization for the fragmentation process.

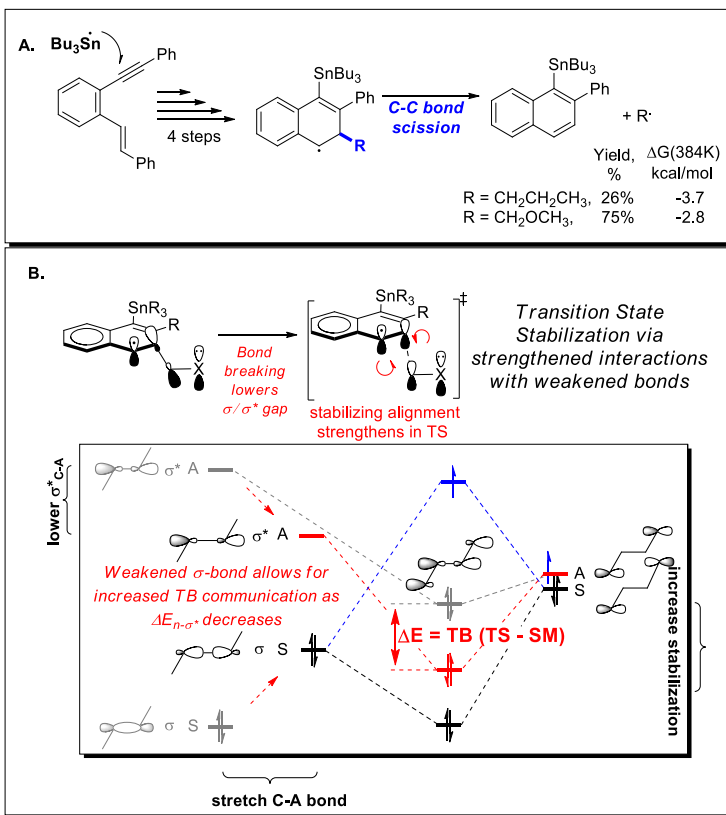


Figure 85. A: Increase in efficiency of fragmentation by substituent modification at the alkene terminus. B. Electronic coupling between non-bonding orbitals in 1,4-diradicals and β -heteroatom substituted radicals strengthens in the TS, facilitating C-C bond fragmentation. Additional stabilization due to TB coupling through abreaking bridging bond is shown as ΔE (red). σ and σ^* energies in the starting radical are shown in grey.

Deactivation of hyperconjugation as an approach to stabilizing reactive intermediates by raising transition state energies

Deeper understanding of hyperconjugative effect in transition states can be also used for raising transition state energies. Recently, selective deactivation of stereoelectronic effects was used to build a stereoelectronic trap for the Criegee intermediate of the Baeyer-Villiger rearrangement, a valuable synthetic route for converting ketones into esters.¹⁶²

It is now accepted that the mechanism of Baeyer-Villiger rearrangement involves a tetrahedral intermediate formed by the addition of a peroxyacid to the carbonyl group of an ester. This high-energy oxygen-rich intermediate rearranges via an 1,2-alkyl shift that is assisted by two stereoelectronic effects that involve the *p*-type lone pair of O₁, the breaking C₂-R_m bond and the O₃-O₄ acceptor (Figure 86).¹⁸⁹ The “primary stereoelectronic effect” requires antiperiplanarity of the breaking O-O bond and the migrating C-R_m bond. The “secondary effect” is switched on when the lone pair of the O₁H group aligns with the breaking C-R_m bond. The perfect synergy between the two effects assures an uninterrupted electron flow from the donor to acceptor: donation from the lone pair assists in breaking the C-R_m bond and stabilizing the incipient cationic center as the R_m group moves to O₃ and the O₃O₄ bond breaks.

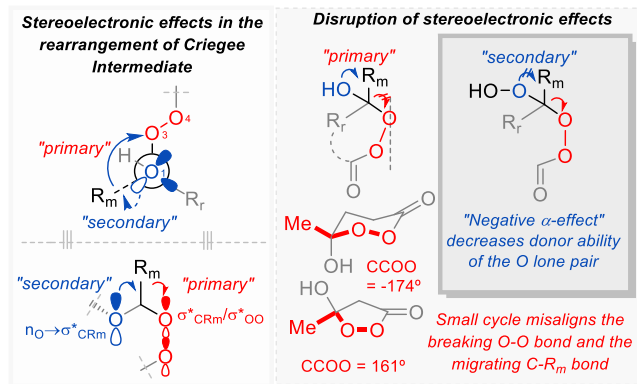


Figure 86. Left: Alternative representations of the two stereoelectronic effects for the 1,2-shift in the Criegee intermediate of the Baeyer-Villiger rearrangement. Right: strategies for weakening the primary and secondary stereoelectronic effects in the 1,2-alkyl shift. Reprinted with permission from ref. 162.

Considering the connection between the two effects, one can weaken the two effects and, by destabilizing the 1,2-shift transition state, kinetically trap the Criegee intermediate. In particular, assistance provided by the "primary" effect is partially deactivated in the cyclic five-membered peroxy lactones where the RCOO dihedral is distorted from antiperiplanarity (161 degrees). Diverting the "migrating" bond from the stereoelectronically favorable alignment with the O-O moiety imposes ~ 8 kcal/mol penalty on non-catalyzed BV rearrangement with the migration of a methyl (~ 700 thousand-fold decrease in the reaction rate). Furthermore, the change from the OH to OOH group imposes an additional protecting effect on the Cl by adding an extra 4.4 kcal/mol penalty to the 1,2-shift free energy barrier.

The Criegee intermediate is stabilized by a strong *exo*-anomeric interaction (Figure 87). In the 1,2-shift TS, departure of the migrating group develops a positive charge, which induces the *p*-type lone pair of the external HO-group to change its orientation and align with the breaking C-C bond (as the latter becomes the best acceptor). This selective TS-stabilization can be significantly weakened by introduction of an α -heteroatom, as another example of the *negative α -effect*.⁶⁷ By swapping the external HO-group by an HOO-moiety, the activation energy for the 1,2-shift is raised by >4 kcal/mol.

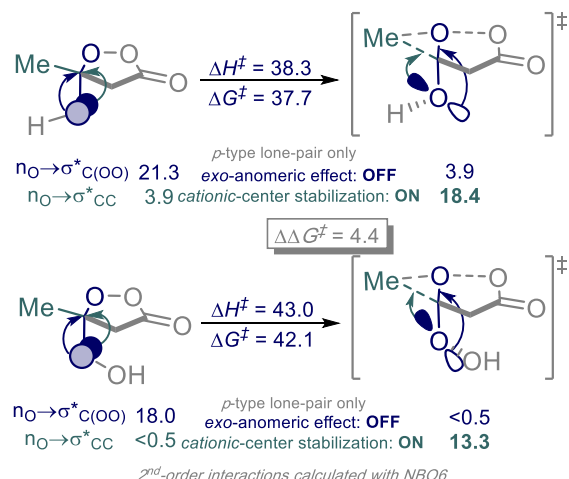


Figure 87. Weakening of the 2nd stereoelectronic effect of 1,2-Me shift of OOH versions of the trapped Cls. Energies in kcal/mol. Reprinted with permission from ref. 162.

The new strategies for stereoelectronic trapping of the elusive Criegee intermediate should allow interruption and restarting of the Bayer-Villiger cascade. This finding should facilitate future mechanistic analysis of the key migration step that determines the regio- and stereoselectivity of the overall process.

Hydrogen bonding

In the absence of intramolecular constraints, the donor acceptor orbital interaction returns to the preferred sigma symmetry of overlaps. This is well-illustrated by directionality of H-bonding.¹ Although hydrogen bonding is a complex phenomenon and many factors are involved in the formation of X-H...Y hydrogen bonded complexes,^{96a,190,,191,192} $n_Y \rightarrow \sigma^*_{X-H}$ negative hyperconjugation (which is often called “covalent component”, or “charge transfer (CT) component”, Figure 88) is one of the two largest H-bond stabilizing effects, along with the electrostatic interaction between inherent and induced dipoles.

The importance of hyperconjugative interactions from a lone pair of the H-bond acceptor to the σ^*_{X-H} orbital of the H-bond donor is well-documented by NBO energetic analysis.³ Because such interactions lead to an increase in the population of an antibonding X-H orbital, they elongate the X-H bond and explain the classic spectroscopic signature of H-bonding, the red-shift in the IR X-H stretching frequency. Only when the hyperconjugative component of H-bonding is weak, the above bond-lengthening effect can be compensated by bond repolarization and rehybridization, can the formation of the so-called blue-shifting H-bonds occur.¹⁷²

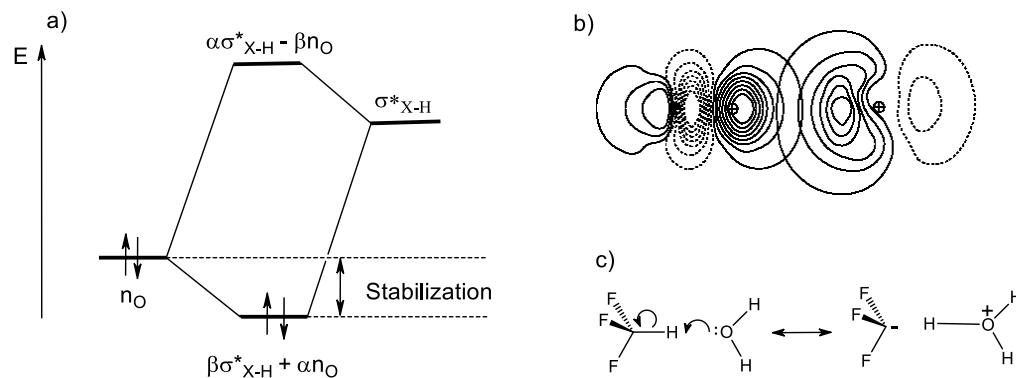


Figure 88. a) Energy lowering due to hyperconjugative interaction between n_Y and σ^*_{X-H} orbitals in X-H...Y complex. b) NBO plots illustrating the overlap of the σ^*_{C-H} of fluoroform and the n_O orbital of the oxygen atom in water in the fluoroform/ water complex and c) description of the hyperconjugative $n_O \rightarrow \sigma^*_{C-H}$ interaction in this complex in terms of resonance theory illustrating effective charge transfer from H-bond acceptor (water) to H-bond donor (fluoroform).

Conclusion

Hyperconjugation is a manifestation of the quantum nature of molecules. It illustrates that delocalization does not become inactive after the formation of two-center two-electron bonds that constitute molecular skeletons. Although the rich and complex role of hyperconjugation in

chemical structure and reactivity is impossible to describe within a short review, we hope that this summary will contribute to further research in this important area. The ubiquitous nature of hyperconjugation in chemistry is illustrated by the key role it plays in numerous stereoelectronic effects on structure and reactivity. With the arrival of powerful computational techniques which can assist future experimental studies in disentangling the relative importance of hyperconjugation in comparison to other electronic and steric effects, the true role of hyperconjugation will continue to reveal itself in many chemical phenomena.

Acknowledgements

We are grateful to the National Science Foundation (CHE- 1465142) for partial support of our research.

Further Reading

Reed AE, Curtiss LA, Weinhold F. Intermolecular Interactions from a Natural Bond Orbital, Donor-Acceptor Viewpoint. *Chem. Rev.* 1988, 88:899-926.

Juaristi E, Guevas G. *The Anomeric Effect*, CRC Press: Boca Raton, FL, 1994.

Schreiner PR. Teaching the Right Reasons: Lessons from the Mistaken Origin of the Rotational Barrier in Ethane. *Angew. Chem. Int. Ed.* 2002, 41:3579-3581.

Kirby AJ. *Stereoelectronic Effects*. Oxford University Press, Inc, New York. 2000, 25-27.

Weinhold F, Landis CR. *Valency and Bonding*. Cambridge University Press, Cambridge, UK, 2005.

Dolbier, Jr. WR, Koroniak H, Houk KN, Sheu CC. Electronic Control of Stereoselectivities of Electrocyclic Reactions of Cyclobutenes: A Triumph of Theory in the Prediction of Organic Reactions. *Acc. Chem. Res.* 1996, 29:471-477.

Alabugin, I. V. *Stereoelectronic Effects: A Bridge between Structure and Reactivity*. John Wiley & Sons Ltd, Chichester, UK, 2016.

Cross-References

CMS-015 Qualitative valence bond theory

CMS-032 Rotational Barriers in Alkanes

CMS-036 Conjugation

Reference

1. Alabugin IV. *Stereoelectronic Effects: A bridge between structure and reactivity*. Chichester: John Wiley & Sons Ltd; 2016.
2. Dewar MJS. *Hyperconjugation*. New York: Ronald Press Co.; 1962.

3. Reed AE, Curtiss LA, Weinhold F. Intermolecular interactions from a natural bond orbital, donor-acceptor viewpoint. *Chem Rev* 1988, 88:899-926.
4. Alabugin IV, Manoharan M, Buck M, Clark RJ. Substituted Anilines: The Tug-Of-War between pyramidalization and resonance inside and outside of crystal cavities. *J Mol Struct (Theochem)* 2007, 813:21-27.
5. Mulliken RS, Rieke CA, Brown WG. Hyperconjugation. *J Am Chem Soc* 1941, 63:41-56.
6. Mulliken RS. Intensities of electronic transitions in molecular spectra. IV. Cyclic dienes and hyperconjugation. *J Chem Phys* 1939, 7:339-352.
7. Karpichev B, Reisler H, Krylov AI, Diri K. Effect of hyperconjugation on ionization energies of hydroxyalkyl radicals. *J Phys Chem A* 2008, 112:9965-9969.
8. Hernández-Soto H, Weinhold F, Francisco JS. Radical hydrogen bonding: origin of stability of radical-molecule complexes. *J Chem Phys* 2007, 127:164102.
9. Wheeler SE, Houk KN, Schleyer PVR, Allen WD. A hierarchy of homodesmotic reactions for thermochemistry. *J Am Chem Soc* 2009, 131:2547-2560.
10. Wodrich MD, Wannere CS, Mo Y, Jarowski PD, Houk KN, Schleyer PvR. The concept of protobranching and its many paradigm shifting implications for energy evaluations. *Chem Eur J* 2007, 13:7731-7744.
11. dos Passos Gomes G, Vil' V, Terent'ev A, Alabugin IV. Stereoelectronic source of the anomalous stability of bis-peroxides. *Chem Sci* 2015, 6:6783-6791.
12. Bickelhaupt FM, Baerends EJ. The case for steric repulsion causing the staggered conformation of ethane. *Angew Chem Int Ed* 2003, 42:4183-4188. See also: (a) Cappel D, Tullmann S, Krapp A, Frenking G. Direct estimate of the conjugative and hyperconjugative stabilization in diynes, dienes, and related compounds. *Angew Chem Int Ed* 2005, 44:3617-3620; (b) Fernandez I, Frenking G. Direct estimate of conjugation and aromaticity in cyclic compounds with the EDA method. *Faraday Discuss* 2007, 135:403-421; (c) Fernandez I, Frenking G. Direct estimate of the strength of conjugation and hyperconjugation by the energy decomposition analysis method. *Chem Eur J* 2006, 12:3617-3629.
13. Mo Y, Wu W, Song L, Lin M, Zhang Q, Gao J. The magnitude of hyperconjugation in ethane: A perspective from ab initio valence bond theory. *Angew Chem Int Ed* 2004, 43:1986-1990.
14. Weinhold F, Carpenter JE. Some remarks on non-orthogonal orbitals in quantum chemistry. *J Mol Struct (Theochem)* 1988, 165:189-202.
15. Corcoran CT, Weinhold F. Antisymmetrization effects in bond-orbital models of internal rotation barriers. *J Chem Phys* 1980, 72:2866-2868.

16. (a) Weinhold F. Chemistry: A new twist on molecular shape. *Nature* 2001, 411:539-540. (b) Weinhold F. Rebuttal to the Bickelhaupt-Baerends case for steric repulsion causing the staggered conformation of ethane. *Angew Chem Int Ed* 2003, 42:4188-4194.

17. Gross KC, Seybold PG. Substituent effects on the physical properties and pKa of phenol. *Int J Quantum Chem* 2001, 85:569-579.

18. Weinhold F, Schleyer PvR, eds. *Encyclopedia of Computational Chemistry* (Vol. 3). New York: John Wiley and Sons; 1998,

19. Reed AE, Weinhold F. Natural localized molecular-orbitals. *J Chem Phys* 1985, 83:1736-1740.

20. Alabugin IV, Zeidan TA. Stereoelectronic effects and general trends in hyperconjugative acceptor ability of σ bonds. *J Am Chem Soc* 2002, 124:3175-3185.

21 Goodman L, Sauers RR. Diffuse functions in natural bond orbital analysis. *J Comput Chem* 2007 28:269-275.

22. Badenhoop JK, Weinhold F. Natural bond orbital analysis of steric interactions. *J Chem Phys* 1997, 107:5406-5422; Badenhoop JK, Weinhold F. Natural steric analysis of internal rotation barriers. *Int J Quantum Chem* 1999, 72:269-280.

23. Weisskopf VF. Of atoms, mountains, and stars: a study in qualitative physics. *Science* 1975, 187:605-612.

24. EDA: (a) Bickelhaupt FM, Baerends EJ, Evert J. Kohn-Sham density functional theory: predicting and understanding chemistry. *Rev Comput Chem* 2000, 15:1-86; (b) te Velde G, Bickelhaupt FM, Baerends EJ, Fonseca Guerra C, van Gisbergen Snijders JG, Ziegler T. Chemistry with ADF. *J Comput Chem* 2001, 22:931-967; See also: (c) Ziegler T, Rauk A. On the calculation of bonding energies by the Hartree-Fock Slater method. I. The transition state method. *Theor Chim Acta* 1977, 46:1-10; (d) Morokuma K. Molecular orbital studies of hydrogen bonds III. C=O...H-O hydrogen bond in H₂CO...H₂O and H₂CO...2H₂O. *J Chem Phys* 1971, 55:1236-1244.

25. Mo Y. Intramolecular electron transfer: computational study based on the orbital deletion procedure (ODP). *Current Organic Chemistry* 2006, 10:779-790.

26. Mo Y, Gao J. Theoretical analysis of the rotational barrier of ethane. *Acc Chem Res* 2007, 40:113-119.

27. (a) Mo Y, Peyerimhoff SD. Theoretical analysis of electronic delocalization. *J Chem Phys* 1998, 109:1687-1697. (b) Mo Y, Zhang Y, Gao J. A simple electrostatic model for trisilylamine: theoretical examinations of the $n \rightarrow \sigma^*$ negative hyperconjugation, $p\pi \rightarrow d\pi$ bonding, and stereoelectronic interaction. *J Am Chem Soc* 1999, 121:5737-5742. (c) Mo Y, Gao J, Peyerimhoff SD. Energy decomposition analysis of intermolecular interactions using a block-localized wave function approach. *J Chem Phys* 2000, 112:5530-5538. (d) Mo Y, Subramanian G, Ferguson DM, Gao J. Cation- π interactions: an energy decomposition analysis and its implication in δ -opioid receptor-ligand binding. *J Am Chem Soc* 2002, 124:4832-4837. (e) Mo Y, Song L, Wu W, Zhang Q. Charge transfer in the electron donor-acceptor complex BH₃NH₃. *J Am Chem Soc* 2004,

126:3974-3982. (f) Mo Y, Gao J. An ab initio molecular orbital-valence bond (MOVB) method for simulating chemical reactions in solution. *J Phys Chem* 2000, 104:3012-3020. (g) Mo Y, Gao J. Ab initio QM/MM simulations with a molecular orbital-valence bond (MOVB) method: application to an S_N2 reaction in water. *J Comput Chem* 2000, 21:1458-1469. (h) Mo Y. Resonance effect in the allyl cation and anion: A revisit. *J Org Chem* 2004, 69:5563-5567.

28. dos Passos Gomes G, Alabugin IV. Stereoelectronic effects: Analysis by computational and theoretical methods. In Tantillo D, eds., *Applied theoretical organic chemistry* pp. 451-502 London: World Scientific Publishing

29. Blanksby SJ, Ellison GB. Bond dissociation energies of organic molecules. *Acc Chem Res* 2003, 36:255-263.

30. Muller N, Mulliken RS. Strong or isovalent hyperconjugation in some alkyl radicals and their positive ions. *J Am Chem Soc* 1958, 80:3489-3497.

31. Selected examples: Exner O, Boehm S. Negative hyperconjugation of some fluorine containing groups. *New J Chem* 2008, 32:1449-1453. Frenking G, Koch W, Schwarz H. Theoretical investigations on fluorine-substituted ethylene dications $C_2H_nF_{4-n}^{2+}$ (n = 0-4). *J Comput Chem* 1986, 7:406-416. Saunders Jr, WH. Negative ion hyperconjugation in fluorocarbanions and the nature of the borderline between E1cB and E2 mechanisms: An ab initio study. *J Org Chem* 1999, 64:861-865. Wiberg KB, Rablen PR. Origin of the stability of carbon tetrafluoride: negative hyperconjugation reexamined. *J Am Chem Soc* 1993, 115:614-625.

32. Bohlmann F. Configuration determination of quinolizidine derivatives. *Angew Chem* 1957, 69:641-642.

33. Alabugin IV. Probing stereoelectronic effects with spectroscopic methods. In: Alabugin IV. *Stereoelectronic effects: A bridge between structure and reactivity* pp. 322-367. Chichester: John Wiley & Sons Ltd; 2016.

34. Grabowski SJ. Tetrel bond- σ -hole bond as a preliminary stage of the S_N2 reaction. *Phys Chem Chem Phys* 2014, 16:1824-1834.

35. Mo Y, Jiao H, Schleyer PvR. Hyperconjugation effect in substituted methyl boranes: An orbital deletion procedure analysis. *J Org Chem* 2004, 69:3493-3499.

36. Prakash S, Schleyer PvR, eds. *Stable Carbocation Chemistry*. New York: John Wiley & Sons; 1996. Olah GA. 100 years of carbocations and their significance in chemistry. *J Org Chem* 2001, 66:5943-5957.

37. Wieting RD, Staley RH, Beauchamp JL. Relative stabilities of carbonium ions in the gas phase and solution. Comparison of cyclic and acyclic alkylcarbonium ions, acyl cations, and cyclic halonium ions. *J Am Chem Soc* 1974, 96:7552-7554.

38. Anslyn EV, Dougherty DA. *Modern Physical Organic Chemistry*. Mill Valley, CA: University Science Books; 2006, 88.

39. Wierschke SG, Chandrasekhar J, Jorgensen WL. Magnitude and origin of the β -silicon effect on carbenium ions. *J Am Chem Soc* 1985, 107:1496-1500. Lambert JB, Wang G, Finzel RB, Teramura DH. Stabilization of positive charge by β -silicon. *J Am Chem Soc* 1987, 109:7838-7845. Lambert JB. The interaction of silicon with positively charged carbon. *Tetrahedron* 1990, 46:2677-2689.

40. Lambert JB, Wang G, Teramura DH. Interaction of the carbon-germanium or carbon-tin bond with positive charge on a β carbon. *J Org Chem* 1988, 53:5422-5428. Lambert JB, Emblidge RW. Nucleophilic catalysis in deoxymercurcation: the beta effect of mercury. *J Phys Org Chem* 1993, 6:555-560.

41. Mayr H, Patz M. Nucleophilic and electrophilic scales as the principles for classification of polar organic and organometallic reactions. *Angew Chem Int Ed* 1994, 33:938-955.

42. Laube T, Ha TK. Detection of hyperconjugative effects in experimentally determined structures of neutral molecules. *J Am Chem Soc* 1988, 110:5511-5517.

43. Lambert JB, Singer RA. Neutral hyperconjugation. *J Am Chem Soc* 1992, 114:10246-10248.

44. Wu JJC, Wang C, McKee WC, Schleyer PvR, Wu W, Mo Y. On the large σ -hyperconjugation in alkanes and alkenes. *J Mol Model* 2014, 20:2228.

45. About 15% of total delocalization was estimated to originate from geminal interactions: Kemnitz CR, Mackey JL, Loewen MJ, Hargrove JL, Lewis JL, Hawkins WE, Nielsen AF. Origin of stability in branched alkanes. *Chem Eur J* 2010, 16:6942-6949.

46 McKee MC, Schleyer PvR. Correlation effects on the relative stabilities of alkanes, *J Am Chem Soc* 2013, 135:13008-13014.

47. Kemnitz CR. Electron delocalization explains much of the branching and protobranching stability. *Chem Eur J* 2013, 19:11093-11095. For a dissenting view, see: Gronert S. Electron delocalization is not a satisfactory explanation for the preference for branching in the alkanes, *Chem Eur J* 2013, 19:11090-11092.

48. Schepers T, Michl J. Optimized ladder C and ladder H models for sigma conjugation: chain segmentation in polysilanes. *J Phys Org Chem* 2002, 15:490-498.

49. Lambert JB, Ciro SB. The interaction of π orbitals with a carbocation over three σ bonds. *J Org Chem* 1996, 61:1940-1945.

50. (a) Shiner, Jr. V, Ensinger MW, Rutkowske RD. γ -Silicon stabilization of carbonium ions in solvolysis. 2. Solvolysis of 4-(trimethylsilyl)-2-butyl p-bromobenzenesulfonates. *J Am Chem Soc* 1987, 109:804-809. (b) Grob CA, Gruendel M, Sawlewicz P. Polar effects. Part 15. Twin γ -substituent effects in the formation of 1-adamantyl cations. *Helv. Chim. Acta* 1988, 71:1502-1507. (c) Bentley TW, Kirmse W, Llewellyn G, Soellenboehmer F. Geometrical dependence of γ -trimethylsilyl groups on norbornyl solvolyses *J Org Chem* 1990, 55:1536-1540. (d) Davis DD, Black RH. Deoxymetalation reactions. Concerted nature of 1,3-deoxystannylation. *J Organomet Chem* 1974, 82:C30-C34.

51. Alabugin IV, Manoharan M, Zeidan TA. Homoanomeric effects in saturated heterocycles. *J Am Chem Soc* 2003, 125:14014-14031.

52. (a) Lambert JB, Salvador LA, So JH. The γ and δ effects of tin. *Organometallics* 1993, 12:697-703. (b) Adcock W, Coope J, Shiner Jr. VJ, Trout NA. Evidence for 2-fold hyperconjugation in the solvolysis of 5-(trimethylsilyl) and 5-(trimethylstannyl)-2-adamantyl sulfonates. *J Org Chem* 1990, 55:1411-1412. (c) Adcock W, Krstic AR, Duggan PJ, Shiner Jr. VJ, Coope J, Ensinger MW. Through-bond transmission of substituent effects in the bicyclo[2.2.2]octane ring system: solvolysis of 4-deutero- and 4-metallocidal ($M(CH_3)_3$, M = silicon, germanium and tin)-substituted bicyclo[2.2.2]oct-1-yl p-nitrobenzenesulfonates and methanesulfonates. *J Am Chem Soc* 1990, 112:3140-3145.

53. Alabugin IV, Manoharan M. Effect of double hyperconjugation on the apparent donor ability of σ -bonds: Insights from the relative stability of δ -substituted cyclohexyl cations. *J Org Chem* 2004, 69:9011-9024.

54. Gilmore K, Mohamed RK, Alabugin IV. The Baldwin rules: Revised and extended. *WIREs: Comput Mol Sci* 2016, 6:487–514. Alabugin IV, Gilmore K. Finding the right path: Baldwin “Rules for Ring Closure” and stereoelectronic control of cyclizations. *Chem Commun* 2013, 49:11246-11250.

55. Kirby AJ. *Stereoelectronic effects*. New York: Oxford University Press, Inc.; 2000, 25-27.

56. Pophristic V, Goodman L. Hyperconjugation not steric repulsion leads to the staggered structure of ethane. *Nature* 2001, 411:565-568.

57. Schreiner PR. Teaching the right reasons: Lessons from the mistaken origin of the rotational barrier in ethane. *Angew Chem Int Ed* 2002, 41:3579-3581.

58. Alabugin IV, Manoharan M, Peabody S, Weinhold F. The electronic basis of improper hydrogen bonding: A subtle balance of hyperconjugation and rehybridization. *J Am Chem Soc* 2003, 125:5973-5987.

59. Allerhand A, Schleyer PvR. A survey of C-H groups as proton donors in hydrogen bonding. *J Am Chem Soc* 1963, 85:1715-1723.

60. Alabugin IV, Manoharan M, Weinhold F. Blue-shifted and red-shifted hydrogen bonds in hypervalent rare-gas FRg-HY sandwiches. *J Phys Chem A* 2004, 10:4720-4730.

61. Fukuto JM, Jensen FR. Mechanisms of S_E2 Reactions: Emphasis on Organotin Compounds. *Acc. Chem. Res.* 1983, 16:177-184.

62. Anderson JE, Cai J, Davies AG. NMR study of stereoelectronic anomeric and homoanomeric effects on the axial and equatorial CH bonds in 1,3-diazacyclohexanes and 1,5-diazabicyclo[3.2.1]octanes. *J Chem Soc, Perkin Trans 2* 1997, 12:2633-2637.

63. For a recent effect of another stereoelectronic effect not associated with hyperconjugative stabilization see: Cuevas G, Martínez-Mayorga, K, Fernández-Alonso MdC, Jiménez-Barbero J,

Perrin CL, Juaristi E, López-Mora N. The origin of one-bond C–H coupling constants in OCH fragments: Not primarily $n_O \rightarrow \sigma_{CH}^*$ delocalization. *Angew Chem Int Ed* 2005, 44:2360-2364.

64. For an earlier study, see: Apeilog Y, Schleyer PvR, Pople JA. Molecular orbital theory of the electronic structure of molecules. 35. β -Substituent effects on the stabilities of ethyl and vinyl cations. Comparison with isoelectronic methyl boranes. The relative importance of hyperconjugative and inductive effects. *J Am Chem Soc* 1977, 99:5901-5909.

65. Bent HA. An appraisal of valence-bond structures and hybridization in compounds of the first-row elements. *Chem Rev* 1961, 61:275-311. Alabugin IV, Bresch S, Manoharan M. Hybridization trends for main group elements and expanding the bent's rule beyond carbon: More than electronegativity. *J Phys Chem A* 2014, 118:3663-3677.

66. Allen FH, Bird CM, Rowland RS, Raithby PR. Resonance-induced hydrogen bonding at sulfur acceptors in $R_1R_2C=S$ and R_1CS_2 systems. *Acta Cryst* 1997, 53:680–695.

67. Juaristi E, Alabugin IV, Terent'ev AO, dos Passos Gomes G, Notario R. Stereoelectronic interactions as a probe for the existence of the α -effect. *J Amer Chem Soc* 2017, 139:10799–10813.

68. (a) Green AJ, Giordano J, White JM. Gauging the donor ability of the C-Si bond. Results from low-temperature structural studies of gauche and antiperiplanar β -trimethylsilylcyclohexyl esters and ethers by use of the variable oxygen probe. *Aust J Chem* 2000, 53:285-292. For a review of interactions of C-MR₃ bonds with acceptor orbitals, with remote electron-deficient orbitals, π systems etc., see: White JM, Clark CI. Stereoelectronic effects of Group IVA metal substituents in organic chemistry. *Top Stereochem* 1999, 22:137-200. (b) Lambert JB, Zhao Y, Emblidge RW, Salvador LA, Liu X, So JH, Chelius EC. The β effect of silicon and related manifestations of σ conjugation. *Acc Chem Res* 1999, 32:183-190. Lambert JB, Wang GT, Teramura DH. Interaction of the carbon-germanium or carbon-tin bond with positive charge on a β carbon. *J Org Chem* 1988, 53:5422-5428. Lambert JB, Wang GT, Finzel RB, Teramura DH. Stabilization of positive charge by β -silicon. *J Am Chem Soc* 1987, 109:7838-7845. (c) Cook MA, Eaborn C, Walton DRM. Substituent effects of mono-, bis-, and tris(trimethylsilyl)-methyl groups; determination of σ^- and σ^+ -constants. *J Organomet Chem* 1970, 24:293-299.

69. For the most recent experimental study and an excellent historic survey of this problem, see: Spiniello M, White JM. Low-temperature X-ray structural studies of the ester and ether derivatives of cis- and trans-4-tert-butyl cyclohexanol and 2-adamantanol: application of the variable oxygen probe to determine the relative σ -donor ability of C-H and C-C bonds. *Org Biomol Chem* 2003, 1:3094-3101.

70. Alabugin IV. Stereoelectronic interactions in cyclohexane, 1,3-dioxane, 1,3-oxathiane, and 1,3-dithiane: W-effect, $\sigma_{C-X} \leftrightarrow \sigma_{C-H}$ interactions, anomeric effect-What is really important? *J Org Chem* 2000, 65:3910-3919 and references therein.

71. Rablen PR, Hoffmann RW, Hrovat DA, Borden WT. Is hyperconjugation responsible for the "gauche effect" in 1-fluoropropane and other 2-substituted-1-fluoroethanes? *J Chem Soc, Perkin Trans 2* 1999, 8:1719-1726.

72. Cappel D, Ilmann ST, Krapp A, Frenking G. Direct estimate of the conjugative and hyperconjugative stabilization in diynes, dienes, and related compounds *Angew Chem Int Ed* 2005, 44:3617–3620.

73. Baker JW, Nathan WS. Mechanism of aromatic side-chain reactions with special reference to the polar effects of substituents. V. The polar effects of alkyl groups. *J Chem Soc* 1935, 1844–1847.

74. Cooney BT, Happer DAR. The Baker-Nathan order: hyperconjugation or a solvent effect? *Aus J Chem* 1987, 40:1537–1544.

75. Taylor R, Smith GG, Wetzel, WH. Substituent effects in pyrolysis. V. A $p - \sigma^+$ correlation in the pyrolysis of 1-arylethyl acetates. *J Am Chem Soc* 1962, 84:4817–4824.

76. For a discussion of the role of polarizability in donor ability, see: (a) Taft RW, Topsom RD. The nature and analysis of substituent electronic effects. *Prog Phys Org Chem* 1987, 16:1–83 (b) Exner O, Böhm S. Baker-Nathan effect, hyperconjugation and polarizability effects in isolated molecules. *J Chem Soc* 1997, 6:1235–1240.

77. (a) Borden WT. Pyramidalized alkenes. *Chem Rev* 1989, 89:1095–1109. (b) Volland WV, Davidson ER, Borden WT. Effect of carbon atom pyramidalization on the bonding in ethylene. *J Am Chem Soc* 1979, 101:533–537. (c) Houk KN. Theoretical studies of alkene pyramidalizations and addition stereoselectivities. In Watson WH, Bartlett PD. *Stereochemistry and reactivity of systems containing π -electrons*. Deerfield Beach: Verlag Chemie International, 1983. (d) Hrovat DA, Borden WT. Ab initio calculations of the olefin strain energies of some pyramidalized alkenes. *J Am Chem Soc* 1988, 110:4710–4178.

78. Whiffen DH. The CH_2 hyperfine coupling in cyclohexadienyl. *Mol Phys* 1963, 6:223–224.

79. Davies AG. The Whiffen effect of symmetry-enhanced and symmetry-forbidden hyperconjugation in spin-paired molecules. *J Chem Soc, Perkin Trans 2* 1999, 11:2461–2467.

80. Winstein S. Homoaromatic structures. *J Am Chem Soc* 1959, 81:6524–6525. For recent discussions of homoaromaticity, see: Holder A. Further comments on the lack of homoaromaticity in triquinacene. *J Comput Chem*, 1993, 14:251. Williams RV. Homoaromaticity. *Chem Rev* 2001, 101:1185–1204. Stahl F, Schleyer PvR, Jiao H, Schaefer HF, Chen KH, Allinger NL. Resurrection of Neutral Tris-homoaromaticity. *J Org Chem* 2002, 67:6599–6611. Homoaromaticity in transition states: Jiao H, Nagelkerke R, Kurtz HA, Williams RV, Borden WT, Schleyer PvR. Annelated Semibullvalenes: A theoretical study of how they "cope" with strain. *J Am Chem Soc* 1997, 119:5921–5929. Homoaromaticity in carbenes and cationic intermediates: Freeman PK, Dacres JE. A study into the possible homoaromatic nature of some related carbene and cationic intermediates with the potential for transannular interaction. *J Org Chem* 2003, 68:1386–1393. Bishomoaromatic Semibullvalenes: Goren AC, Hrovat DA, Seefelder M, Quast H, Borden WT. The search for bishomoaromatic vembranvalenes and barbaralanes: Computational evidence of their identification by UV/Vis and IR spectroscopy and prediction of the existence of a blue bishomoaromatic semibullvalene. *J Am Chem Soc* 2002, 124:3469–3472.

81. (a) Hoffmann R, Imamura A, Hehre WJ. Benzyne, dehydroconjugated molecules, and the interaction of orbitals separated by a number of intervening sigma bonds. *J Am Chem Soc* 1968, 90:1499-1509. Hoffmann R. Interaction of orbitals through space and through bonds. *Acc Chem Res* 1971, 4:1-9. (b) Paddon-Row MN. Some aspects of orbital interactions through bonds: physical and chemical consequences. *Acc Chem Res* 1982, 15:245-251. (c) Gleiter R, Paddon-Row MN. Effects of through-bond interaction. *Angew Chem Int Ed Engl* 2003, 42:696-701. (d) Brodskaya EI, Ratovskii GV, Voronkov MG. Orbital interactions through-space and through-sigma bonds. *Usp Khim* 1993, 62:975-990. See also: Paddon-Row MN, Shephard MJ. Through-bond orbital coupling, the parity rule, and the design of "superbridges" which exhibit greatly enhanced electronic coupling: A natural bond orbital analysis. *J Am Chem Soc* 1997, 119:5355-5365. Verhoeven JW. Sigma-assistance; the modulation of intramolecular reactivity by through-bond interaction. *Recl Trav Chim Pays-Bas* 1980, 99:369-379.

82. (a) McKean DC. Individual C-H bond strengths in simple organic compounds: effects of conformation and substitution. *Chem Soc Rev* 1978, 7:399-422. (b) McKean DC, Duncan JL, Batt L. C-H stretching frequencies, bond lengths and dissociation energies. *Spectrochim. Acta A* 1973, 29:1037-1049.

83. (a) Bohlmann F. Zur konfigurationsbestimmung von chinolizin-derivaten. *Angew Chem* 1957, 69:641-642. (b) Bohlmann F. Zur konfigurationsbestimmung von chinolizidin-derivaten. *Ber Dtsch Chem Ges* 1958, 91:2157-2167. (c) Wolfe S, Kim CK. A theoretical study of conformational deuterium isotope effects and bond dissociation energies of diastereotopic hydrogens. *Can J Chem* 1991, 69:1408-1412.

84. Bellamy LJ, Mayo DW. Infrared frequency effects of lone pair interactions with antibonding orbitals on adjacent atoms. *J Phys Chem* 1976, 80:1217-1220.

85 Andrade LAF, Silla JM, Cormanich RA, Freitas MP. Infrared fingerprints of $n_N \rightarrow \sigma^*_{NH}$ hyperconjugation in hydrazides. *J Org Chem* 2017, 82:12181-12187.

86. (a) Doublerly GE, Ricks AM, Ticknor BW, Schleyer PvR, Duncan MA. Infrared spectroscopy of the *tert*-butyl cation in the gas phase. *J Am Chem Soc* 2007, 129:13782-13783. (b) Olah GA, Tolgyesi WS, Kuhn SJ, Moffatt ME, Bastien IJ, Baker EB. Stable carbonium ions. IV. Secondary and tertiary alkyl and aralkyl oxocarbonium hexafluoroantimonates. Formation and identification of the trimethylcarbonium ion by decarbonylation of the *tert*-butyl oxocarbonium ion. *J Am Chem Soc* 1963, 85:1328-1334. (c) Olah GA, Baker EB, Evans JC, Tolgyesi WS, McIntyre JS, Bastien IJ. Stable carbonium ions. V. Alkylcarbonium hexafluoroantimonates. *J Am Chem Soc* 1964, 86:1360-1373. (d) Prakash GKS, Schleyer PvR, Eds. *Stable Carbocation Chemistry*. New York: John Wiley and Sons; 1997. (e) Olah GA, Prakash GKS, Eds. *Carbocation Chemistry*. Hoboken: John Wiley and Sons; 2004.

87. (a) Olah GA, Svodoba JJ, Ku AT. Preparative carbocation chemistry; VII. Isolation of alkyl(cycloalkyl)carbenium ion salts: Trimethylcarbenium (*t*-butyl), tricyclopropylcarbenium, and 1-adamantyl fluoroantimonates. *Synthesis* 1973, 492-493. (b) Hollenstein S, Laube T. Crystal structure of the *tert*-butyl cation. *J Am Chem Soc* 1993, 115:7240-7245. (c) Kato T, Reed CA. Putting *tert*-butyl cation in a bottle. *Angew Chem Int Ed* 2004, 43:2908-2911. (d) Schormann M, Garratt S, Hughes DL, Green JC, Bockmann M. Isolation and structure of $[\text{HC}\{\text{CH}(\text{SiMe}_3)(\text{SnMe}_3)\}_2]^+$: A remarkably stable *sec*-alkyl cation. *J Am Chem Soc* 2002, 124:11266-11267. (e) Muller T, Juhasz M, Reed CA. The X-ray structure of a vinyl cation. *Angew*

Chem Int Ed 2004, 43:1543-1546. (f) Stoyanov ES, Stoyanova IV, Tham FS, Reed CA. Evidence for C-H hydrogen bonding in salts of *tert*-butyl cation. *Angew Chem Int Ed* 2012, 51:9149-9151.

88. Alabugin IV, Bresch S, dos Passos Gomes G. Orbital hybridization: a key electronic factor in control of structure and reactivity. *J Phys Org Chem* 2015, 28:147-162.

89. Stoyanov ES, Gomes G dos P. *tert*-Butyl carbocation in condensed phases: Stabilization via hyperconjugation, polarization, and hydrogen bonding. *J Phys Chem A* 2015, 119:8619-8629.

90. (a) Pimentel GC, McClellan AL. *The hydrogen bond*. San Francisco: W. H. Freeman and Co.; 1960. (b) Scheiner S. *Hydrogen Bonding: A Theoretical Perspective*. Cary: Oxford University Press; 1997. (c) Steiner T. The hydrogen bond in the solid state. *Angew Chem Int Ed* 2002, 41:48-76. Pimentel GC, McClellan AL. *The hydrogen bond*. New York: Reinhold Publishing Corporation; 1960.

91. (a) Freymann R. On the question of the intra and intermolecular "hydrogen bond" and the absorption spectra in the near infrared. *J Chem Phys* 1938, 6:497-498. (b) Hilbert GE, Wulf OR, Hendricks SB, Liddel U. Hydrogen bond formation between hydroxyl groups and nitrogen atoms in some organic compounds *J Am Chem Soc* 1936, 58:1991-1996.

92. (a) Badger RM, Bauer SH. Spectroscopic studies of the hydrogen bond. II. The shift of the O-H vibrational frequency in the formation on the hydrogen bond. *J Chem Phys* 1937, 5:839-851. (b) Rao CNR, Dwivedi PC, Ratajczak H, Orville-Thomas WJ. Relation between O-H stretching frequency and hydrogen-bond energy: Re-examination of Badger-Bauer rule. *J Chem Soc, Faraday Trans* 1975, 71:955-966.

93. (a) Lin YW, Nie CM, Liao LF. Probing the weak interactions between amino acids and carbon monoxide. *Chin Chem Lett* 2008, 19:119-122. (b) Pinakoulaki E, Yoshimura H, Daskalakis V, Yoshioka S, Aono S, Varotsis C. Two ligand-binding sites in the O₂-sensing signal transducer HemAT: Implications for ligand recognition/discrimination and signaling. *Proc Natl Acad Sci U.S.A.* 2006, 103:14796-14801. (c) Nutt DR, Meuwly M. Ligand dynamics in myoglobin: calculation of infrared spectra for photodissociated NO. *Chem Phys Phys Chem* 2004, 5:1710-1718. (d) Devereux M, Meuwly M. Structural assignment of spectra by characterization of conformational substates in bound MbCO. *Biophys J* 2009, 96:4363-4375. (e) Daskalakis V, Varotsis C. Binding and docking interactions of NO, CO, and O₂ in heme proteins as probed by density functional theory. *Int J Mol Sci* 2009, 10:4137-4156. (f) Makshakova O, Chachkov D, Ermakova E. Geometry and vibrational frequencies of the helical polypeptide complexes with ligand molecules. *Int J Quantum Chem* 2011, 111:2525-2539. (g) Dabo I. Resilience of gas-phase anharmonicity in the vibrational response of adsorbed carbon monoxide and breakdown under electrical conditions. *Phys Rev B* 2012, 86:035139(1)-035139(10). (h) Thijss R, Zeegers-Huyskens TH. Infrared and raman studies of hydrogen-bonded complexes involving acetone, acetophenone, and benzophenone. 1. Thermodynamic constants and frequency-shifts of the ν_{OH} and ν_{C=O} stretching vibrations. *Spectrochim Acta A* 1984, 40:307-313.

94. (a) Arnett EM, Joris L, Mitchell E, Murty TSSR, Gorrie TM, Schleyer PvR. Studies of hydrogen-bonded complex formation. III. Thermodynamics of complexing by infrared spectroscopy and calorimetry. *J Am Chem Soc* 1970, 92:2365-2377. (b) West R, Powell DL, Whatley LS, Lee MKT, Schleyer PvR. The relative strengths of alkyl halides as proton acceptor groups in hydrogen bonding. *J Am Chem Soc* 1962, 84:3221-3222.

95. Bhatta RS, Iyer PP, Dhinojwala A, Tsige M. A brief review of Badger–Bauer rule and its validation from a first-principles approach. *Mod Phys Lett B* 2014, 28:1430014.

96. (a) Hobza P, Havlas Z. Blue-shifting hydrogen bonds. *Chem Rev* 2000, 100:4253-4264. (b) Budesinsky M, Fiedler P, Arnold Z. Triformylmethane: An efficient preparation, some derivatives, and spectra. *Synthesis* 1989, 858-860. (c) Boldeskul IE, Tsymbal IF, Ryltsev EV, Latajka Z, Barnes AJ. Reversal of the usual $\nu_{(C-H/D)}$ spectral shift of haloforms in some hydrogen-bonded complexes. *J Mol Struct* 1997, 436:167-171. (d) Hobza P, Spirko V, Selzle HL, Schlag EW. Anti-hydrogen bond in the benzene dimer and other carbon proton donor complexes. *J Phys Chem A* 1998, 102:2501-2504.

97. (a) Juaristi E, Cuevas G. Manifestations of stereoelectronic interactions in $^1J_{C-H}$ one-bond coupling constants. *Acc Chem Res* 2007, 40:961-970. (b) Cuevas G, Juaristi E, Vela A. Rationalization of the anomalous 1H NMR chemical shifts in 1,3-diheterocyclohexanes. *J Mol Struct: (Theochem)* 1997, 418:231-241.

98. Perlin AS, Casu B. Carbon-13 and proton magnetic resonance spectra of D-glucose- ^{13}C . *Tetrahedron Lett* 1969, 10:2921-2924.

99. Juaristi E, Cuevas G, Vela A. Stereoelectronic interpretation for the anomalous 1H NMR chemical shifts and one-bond C-H coupling constants (Perlin effects) in 1,3-dioxanes, 1,3-oxathianes, and 1,3-dithianes. Spectroscopic and theoretical observations. *J Am Chem Soc* 1994, 116:5796-5804.

100. Representative examples: (a) Serianni AS, Wu J, Carmichael I. One-bond $^{13}C-^1H$ spin-coupling constants in aldonofuranosyl rings: effect of conformation on coupling magnitude. *J Am Chem Soc* 1995, 117:8645-8650. (b) Church TJ, Carmichael I, Serianni AS. $^{13}C-^1H$ and $^{13}C-^{13}C$ spin-coupling constants in methyl β -D-ribofuranoside and methyl 2-deoxy- β -D-erythro-pentofuranoside: Correlations with molecular structure and conformation. *J Am Chem Soc* 1997, 119:8946-8964. (c) Tvaroska I, Taravel FR. Carbon-proton coupling constants in the conformational analysis of sugar molecules. *Adv Carbohydr Chem Biochem* 1995, 51:15-61. (d) Peruchena NM, Contreras RH. Theoretical analysis of interactions affecting $^1J(CH)$ NMR couplings in an sp^3 hybridized carbon atom. Part 1. The exo-anomeric effect in 3-methoxy-1,2,4,5-tetroxane. *J Mol Struct: (Theochem)* 1995, 338:25-30. (e) Andersson P, Nordstrand K, Sunnerhagen M, Liepinsh E, Turovskis I, Otting G. Heteronuclear correlation experiments for the determination of one-bond coupling constants. *J Biomol NMR* 1998, 11:445-450.

101. Weisman GR, Johnson, V., Fiala, R. E. (1980). Tricyclic ortho amides: effects of lone-pair orientation upon NMR spectra. *Tetrahedron Letters* 21(38), 3635–8.

102. de Kowalewski DG, Kowalewski VJ, Contreras RH, Diez E, Esteban AL. Conformational effects on ^{13}C NMR parameters in alkyl formates. *Magn Reson Chem* 1998, 336–342.

103. Perrin CL, Erdelyi M. One-bond C-C coupling constants in ethers are not primarily determined by $n-\sigma^*$ delocalization. *J Am Chem Soc* 2005, 127:6168-6169.

104. a) Anderson JE, Bloodworth AJ, Cai JQ, Davies AG, Tallant NA. One-bond C-H NMR coupling constants in 1,2,4-trioxanes: A reversed Perlin effect. *J Chem Soc, Chem Comm* 1992, 1689-1691. b) Anderson JE, Bloodworth AJ, Cai JQ, Davies AG, Schiesser CH. An NMR and *ab initio* MO study of the effect of β -oxygen in 1,3-dioxanes. *J Chem Soc, Perkin Trans 2* 1993, 601-602. c) Cai JQ,

Davies AG, Schiesser CH. NMR parameters for 1,3-dioxanes: evidence for a homoanomeric interaction. *J Chem Soc, Perkin Trans 2* 1994, 6:1151-1156.

105. Bax A, Freeman R, Kempsell SP. Natural abundance carbon-13-carbon-13 coupling observed via double-quantum coherence. *J Am Chem Soc* 1980, 102:4849-4851.

106. Krivdin LB, Kalabin GA. Directly bonded ^{13}C - ^{13}C spin-spin coupling constants in structural studies. *Russ Chem Rev* 1988, 57:1-16.

107. Krivdin LB, Shcherbakov VV, Kalabin GA. Constants of C-13-C-13 spin-spin interaction in structure interactions. 1. New method for determination of oximes and their derivative configurations. *Zhur Org Khim* 1986, 22:342-348.

108. Sovers OJ, Kern CW, Pitzer RM, Karplus M. Bond-function analysis of rotational barriers: ethane. *J Chem Phys* 1968, 49:2592-2599. Christiansen PA., Palke WE. A study of the ethane internal rotation barrier. *Chem Phys Lett* 1975, 31:462-466.

109. Bader RFW, Cheeseman JR, Laidig KE, Wiberg KB, Breneman C. Origin of rotation and inversion barriers. *J Am Chem Soc* 1990, 112:6530-6536.

110. Lowe JP. Simple molecular orbital explanation for the barrier to internal rotation in ethane and other molecules. *J Am Chem Soc* 1970, 92:3799-3800. Brunck TK, Weinhold F. Quantum mechanical studies on the origin of barriers to internal rotation about single bonds. *J Am Chem Soc* 1979, 101:1700-1709.

111. Goodman L, Pophristic, V, Weinhold F. Origin of methyl internal rotation barriers. *Acc Chem Res* 1999, 32:983-993.

112. Ribeiro DS, Rittner R. The role of hyperconjugation in the conformational analysis of methylcyclohexane and methylheterocyclohexanes. *J Org Chem* 2003, 68:6780-6787.

113. (a) Kleinpeter E, Taddai F, Wacher P. Electronic and steric substituent influences on the conformational equilibria of cyclohexyl esters: the anomeric effect is not anomalous! *Chemistry* 2003, 9:1360-1368. (b) Kleinpeter E, Rolla N, Koch A, Taddai F. Hyperconjugation and the increasing bulk of OCOCX_3 substituents in trans-1,4-disubstituted cyclohexanes destabilize the diequatorial conformer. *J Org Chem* 2006, 71:4393-4399.

114. Shishkina SV, Shishkin OV, Desenko SM, Leszczynski J. Conjugation and hyperconjugation in conformational analysis of cyclohexene derivatives containing an exocyclic double bond. *J Phys Chem A* 2008, 112:7080-7089. Anizelli PR, Vilcachagua JD, Cunha NA, Tormena CF. Stereoelectronic interaction and their effects on conformational preference for 2-substituted methylenecyclohexane: An experimental and theoretical investigation. *J Phys Chem A* 2008, 112:8785-8789.

115 Borden WT. Effects of electron donation into C-F σ^* orbitals: explanations, predictions and experimental tests. *J Chem Soc, Chem Comm* 1998, 18:1919-1925.

116. Lam Y, Stanway SJ, Gouverneur V. Recent progress in the use of fluoroorganic compounds in pericyclic reactions. *Tetrahedron* 2009, 65:9905-9933.

117. Chambers RD. Polyfluoroalkanes, polyfluoroalkenes, polyfluoroalkynes and derivatives, In: Chambers RD. *Fluorine in Organic Chemistry* pp. 162–235, Oxford: Blackwell Publishing Ltd.; 2004.

118. Wolfe S. Gauche effect. Stereochemical consequences of adjacent electron pairs and polar bonds. *Acc Chem Res* 1972, 5:102-111.

119. Buissonneaud DY, van Mourik T, O'Hagan D. A DFT study on the origin of the fluorine gauche effect in substituted fluoroethanes. *Tetrahedron* 2010, 66:2196–2202.

120. Wiberg KB, Hinz W, Jarret RM, Aubrecht KB. Conformational preferences for 1,2- and 1,4-difluorocyclohexane. *J Org Chem* 2005, 70:8381–8384. Richardson AD, Hedberg K, Utzat K, Bohn RK, Duan JX, Dolbier WR. Molecular structures and compositions of trans-1,2-dichlorocyclohexane and trans-1,2-difluorocyclohexane in the gas phase: An electron-diffraction investigation. *J Phys Chem A* 2006, 110:2053-2059.

121. (a) Durig JR, Liu J, Little TS, Kalasinsky VF. Conformational analysis, barriers to internal rotation, vibrational assignment, and ab initio calculations of 1,2-difluoroethane. *J Phys Chem* 1992, 96:8224–8233. (b) Craig NC, Chen A, Suh KH, Klee S, Mellau GC, Winnewisser BP, Winnewisser M. Complete structure of the anti rotamer of 1,2-difluoroethane from high-resolution infrared spectroscopy. *J Phys Chem A* 1997, 101:9302–9308. (c) Wiberg KB, Keith TA, Frisch MJ, Murcko M. Solvent effects on 1,2-dihaloethane gauche/trans ratios. *J Phys Chem* 1995, 99:9072–9079.

122. Search of Cambridge crystal database reveals that such preference is very strong in the gas phase. See: Rzepa H. (2013) The gauche effect: seeking evidence by a survey of crystal structures. *The Winnower* 5:e142795.55871 2015, DOI: [10.15200/winn.142795.55871](https://doi.org/10.15200/winn.142795.55871). <https://thewinnower.com/papers/443-the-gauche-effect-seeking-evidence-by-a-survey-of-crystal-structures>

123. (a) Goodman L, Gu H, Pophristic V. Gauche effect in 1,2-difluoroethane. Hyperconjugation, bent bonds, steric repulsion. *J Phys Chem A* 2005, 109:1223–1229. (b) Souza FR, Freitas MP, Rittner R. On the stereoelectronic effects governing the rotational isomerism of 1,2-dihaloethanes. *J Mol Struct (Theochem)* 2008, 863:137–140.

124. Baranac-Stojanović M. Gauche preference in 1,2-difluoroethane originates from both orbital and electrostatic stabilization interactions. *RSC Advances* 2014, 4:43834–43838.

125. Sun A, Lankin DC, Hardcastle K, Snyder JP. 3-Fluoropiperidines and N-methyl-3-fluoropiperidinium salts: The persistence of axial fluorine. *Chem Eur J* 2005, 11:1579–1591.

126. Gooseman NEJ, O'Hagan D, Peach MJG, Slawin AMZ, Tozer DJ, Young RJ. An electrostatic *gauche* effect in β -fluoro- and β -hydroxy-N-ethylpyridinium cations. *Angew Chem Int Ed* 2007, 46:5904–5908.

127. Pitzer KS, Hollenberg JL. *cis*- and *trans*-dichloroethylenes. The infrared spectra from 130 to 400 cm^{-1} and the thermodynamic properties. *J Am Chem Soc* 1954, 76:1493-1496. Craig NC, Piper LG, Wheeler VL. Thermodynamics of *cis-trans* isomerizations. II. 1-Chloro-2-

fluoroethylenes, 1,2-difluorocyclopropanes, and related molecules. *J Phys Chem* 1971, 75:1453-1460. Wiberg WB. Bent bonds in organic compounds. *Acc Chem Res* 1996, 29:229-234. Engkvist O, Karlstrom G, Widmark PO. On the origin of the gauche effect. A quantum chemical study of 1,2-difluoroethane. *Chem Phys Lett* 1997, 265:19-23. Yamamoto T, Tomoda S. On the origin of cis-effect in 1,2-difluoroethene. *Chem Lett* 1997, 10:1069-1070. Novak I. Chlorofluoroethenes. Thermochemical stability and cis-effect. *J Org Chem* 2000, 65:5057-5058. Kanakaraju K, Senthilkumar K, Kolandaivel P. Origin of the cis effect-nonbonded intramolecular interactions: quantum chemical studies on 1,2-dihaloethylene molecules. *J Mol Struct (Theochem)* 2002, 589-590:95-102. Yamamoto T, Kaneno D, Tomoda S. The importance of lone pair electron delocalization in the cis-trans isomers of 1,2-dibromoethenes. *Chem Lett* 2005, 34:1190-1191. Binkley JS, Pople JA. Relative stability of 1,2-difluoroethylenes. *Chem Phys Lett* 1977, 45:197-200. Cremer D. The role of correlation in calculations on 1,2-difluoroethylenes. The cis-trans energy difference. *Chem Phys Lett* 1981, 81:481-485. Gandhi SR, Benzel MA, Dykstra CE, Fukunaga T. Role of electron correlation and polarization functions in the energy difference between cis- and trans-1,2-difluoroethylene. *J Phys Chem* 1982, 86:3121-3126. Dixon DA, Fukunaga T, Smart BE. Geometries and energies of the fluoroethylenes. *J Am Chem Soc* 1986, 108:1585-1588. Saebø S, Sellers H. Effect of electron correlation on the structures and relative stability of cis- and trans-1,2-difluoroethylene. *J Phys Chem* 1988, 92:4266-4269. Epotis ND, Yates RL. Overlap repulsion as an important contributor to aromaticity. *J Am Chem Soc* 1976, 98:461-469. Bernardi F, Bottini A, Epotis ND, Guerra M. Quantitative nonempirical estimates of the effects of orbital interactions. Applications to difluoroethylenes. *J Am Chem Soc* 1978, 100:6018-6022.

128. Yamamoto T, Kaneno D, Tomoda S. The origin of cis effect in 1,2-dihaloethenes: the quantitative comparison of electron delocalizations and steric exchange repulsions. *Bull Chem Soc Japan* 2008, 81:1415-1422.

129. Izgorodina EI, Coote ML, Radom L. Trends in R-X bond dissociation energies (R = Me, Et, i-Pr, t-Bu; X = H, CH₃, OCH₃, OH, F): A surprising shortcoming of density functional theory. *J Phys Chem A* 2005, 109:7558-7566.

130. Menon AS, Henry DJ, Bally T, Radom L. Effect of substituents on the stabilities of multiply-substituted carbon-centered radicals. *Org Biomol Chem* 2011, 9:3636-3657.

131. Eisenstein O, Milani J, Perutz RN. Selectivity of C-H activation and competition between C-H and C-F bond activation at fluorocarbons. *Chem Rev* 2017, 117:8710-8753.

132. (a) Rogers DW, Matsunaga N, Zavitsas AA, McLafferty FJ, Liebman JF. The conjugation stabilization of 1,3-butadiyne is zero. *Org Lett* 2003, 5:2373-2375. (b) Rogers DW, Matsunaga N, McLafferty FJ, Zavitsas AA, Liebman JF. On the lack of conjugation stabilization in polyynes (polyacetylenes). *J Org Chem* 2004, 69:7143-7147.

133. Kistiakowsky GG, Ruhoff JR, Smith HA, Vaughan WE. Heats of organic reactions. IV. Hydrogenation of some dienes and of benzene. *J Am Chem Soc* 1936, 58:146-153.

134. Jarowski PD, Wodrich MD, Wannere CS, Schleyer PvR, Houk KN. How large is the conjugative stabilization of diynes? *J Am Chem Soc* 2004, 126:15036-15037.

135. After correction for unequal hyperconjugative stabilization, the conjugation energies were estimated as 9.3 kcal/mol for diynes and 8.2 kcal/mol for dienes.

136. See reference 10. For a critique of protobranching, see: Gronert S. The folly of protobranching: Turning repulsive interactions into attractive ones and rewriting the strain/stabilization energies of organic chemistry. *Chem Eur J* 2009, 15:5372-5382.

137. Benoit B, Vinca P, Hiberty PC. The physical origin of Saytzeff's rule. *Angew Chem Int Ed* 2009, 48:5724-5728.

138. Wiberg KB. Accuracy of calculations of heats of reduction/hydrogenation: Application to some small ring systems. *J Org Chem* 2012, 77:10393-10398.

139. Lide Jr. DR, Mann DE. Microwave spectra of molecules exhibiting internal rotation. I. Propylene. *J Chem Phys* 1957, 27:868-873.

140. (a) Guirgis GA, Drew BR, Gounev TK, Durig JR. Conformational stability and vibrational assignment of propanal. *Spectrochim Acta A Mol Biomol Spectrosc* 1998, 54:123-143. (b) Karabatsos GJ, Hsi N. Structural studies by nuclear magnetic resonance. X. Conformations of aliphatic aldehydes. *J Am Chem Soc* 1965, 87:2864-2870.

141. Lin BL, Xie Z, Liu R, Liu L, Guo QX. Importance of σ -type hyperconjugation to the eclipsed structure of propylene. *J Mol Struct (Theochem)* 2003, 633:15-19.

142. Jalbouta AF, Basso EA, Pontesc RM, Dasa D. Hyperconjugative interactions in vinylic systems: the problem of the barrier to methyl rotation in acetone. *J Mol Struct (Theochem)* 2004, 677:167-171.

143. Gold B, Shevchenko NE, Bonus N, Dudley GB, Alabugin IV. Selective transition state stabilization via hyperconjugative and conjugative assistance: stereoelectronic concept for copper-free click chemistry. *J Org Chem* 2012, 77:75-89.

144. Qiu Y, Han D. Substituent effects on the conformational stability of allyl fluorides. *J Phys Org Chem* 2011, 24:431.

145. Penner GH, Schaefer T, Sebastian R, Wolfe S. The benzylic anomeric effect. Internal rotational potentials of ArCH_2X compounds (X = F, Cl, SH, SCH_3 , S(O)CH_3 , SO_2CH_3). *Can J Chem* 1987, 65:1845-1852.

146. Aue DH. Gas-phase chemistry. in: Rappoport Z, Stang PJ, Eds. *Dicoordinated Carbocations* pp. 105-156. Chichester: John Wiley & Sons Inc.; 1997.

147. (a) Rauk A, Sorensen TS, Maerker C, de M. Carneiro JW, Sieber S, Schleyer PvR. Axial and equatorial 1-methyl-1-cyclohexyl cation isomers both have chair conformations but differ in C-C and C-H hyperconjugation modes. *J Am Chem Soc* 1996, 118:3761-3762. (b) Rauk A, Sorensen TS, Schleyer PvR. Tertiary cyclohexyl cations. Definitive evidence for the existence of isomeric structures (hyperconformers). *J Chem Soc, Perkin Trans 2* 2001, 6:869-874.

148. (a) Juaristi E. *Conformational behavior of six-membered rings*. New York: VCH Publishers; 1995. (b) Juaristi E, Cuevas G. *The Anomeric Effect*. Boca Raton: CRC Press; 1994.

149. Edward JT. Stability of glycosides to acid hydrolysis. *Chemistry & Industry* 1955, 1102-1104.

150. For a reverse of this conformational preference in the case of positively charged-electronegative substituents, see: Perrin CL. The reverse anomeric effect: Fact or fiction? *Tetrahedron* 1995, 51:11901-11935.

151. Franck RW. A revision of the value for the anomeric effect. *Tetrahedron* 1983, 39:3251-3252.

152. Deslongchamps P. Intramolecular strategies and stereoelectronic effects. Glycosides hydrolysis revisited. *Pure Appl Chem* 2009, 65:1161-1178.

153. David S, Eisenstein O, Hehre WJ, Salem L, Hoffmann R. Superjacent orbital control. Interpretation of the anomeric effect. *J Am Chem Soc* 1973, 95:3806-3807.

154. Reed AE, Schleyer PvR. The anomeric effect with central atoms other than carbon. 2. Strong interactions between nonbonded substituents in mono- and polyfluorinated first- and second-row amines, $F_nAH_mNH_2$. *Inorg Chem* 1988, 27:3969-3987.

155. (a) Taddei F, Kleinpeter E. The anomeric effect in substituted cyclohexanes. I. The role of hyperconjugative interactions and steric effect in monosubstituted cyclohexanes. *J Mol Struct: (Theochem)* 2004, 683:29-41. (b) Taddei F, Kleinpeter E. The anomeric effect in substituted cyclohexanes. II. The role of hyperconjugative interactions and steric effect in 1,4-disubstituted cyclohexanes. *J Mol Struct (Theochem)* 2005, 718:141-151.

156. Tvaroska I, Carver JP. *Ab initio* molecular orbital calculation of carbohydrate model compounds. 5. Anomeric, *exo*-anomeric, and reverse anomeric effects in C-, N-, and S-glycosyl compounds. *J Phys Chem* 1996, 100:11305-11313.

157. Mo Y. Computational evidence that hyperconjugative interactions are not responsible for the anomeric effect. *Nat Chem* 2010, 2:666-671.

158. Freitas MP. The anomeric effect on the basis of natural bond orbital analysis. *Org Biomol Chem* 2013, 11:2885-2890.

159. Bauerfeldt GF, Cardozo TM, Pereira MS, da Silva CO. The anomeric effect: the dominance of exchange effects in closed-shell systems. *Org Biomol Chem* 2013, 11:299-308.

160. Wiberg KB, Bailey WF, Lambert KM, Stempel ZD. The anomeric effect: it's complicated. *J Org Chem* 2018.

161. Yaremenko I, dos Passos Gomes G, Radulov P, Belyakova Y, Vilikotskiy A, Vil' V, Korlyukov A, Nikishin G, Alabugin IV, Terent'ev AO. Ozone-free synthesis of ozonides: Assembling bicyclic structures from 1,5-diketones and hydrogen peroxide. *J Org Chem* 2018, 83:4402-4426. dos Passos Gomes G, Yaremenko IA, Radulov PS, Novikov RA, Chernyshev VV, Korlyukov AA, Nikishin

Gl, Alabugin IV, Terent'ev AO. Stereoelectronic control in the ozone-free synthesis of ozonides. *Angew Chem Int Ed* 2017, 56:4955–4959.

162. Vil' VA, dos Passos Gomes G, Bityukov OV, Lyssenko KA, Nikishin GI, Alabugin IV, Terent'ev AO. Interrupted Baeyer-Villiger rearrangement: Building a stereoelectronic trap for the Criegee intermediate. *Angew Chem Int Ed* 2018, 57:3372-3376.

163. For other interesting structural studies on related systems, see: Reany O, Goldberg I, Abramson S, Golender L, Ganguly B, Fuchs B. The 1,3,5,7-tetraazadecalins: structure, conformation, and stereoelectronics. Theory vs. experiment. *J Org Chem* 1998, 63:8850-8859. Ritter J, Gleiter R, Irngartinger H, Oeser T. Conformations of azacyclodeca-3,8-diyne and 1,6-diazacyclodeca-3,8-diyne and the generalized anomeric effect: A test for current conformational models for azaheterocycles. *J Am Chem Soc* 1997, 119:10599-10607.

164. Fuson RC, Zirkle CL. Ring enlargement by rearrangement of the 1,2-aminochloroalkyl group; rearrangement of 1-ethyl-2-(chloromethyl)pyrrolidine to 1-ethyl-3-chloropiperidine. *J Am Chem Soc* 1948, 70:2760-2762. Reitsema RH. Novel rearrangement of a piperidine ring. *J Am Chem Soc* 1949, 71:2041-2043. Hammer CF, Heller SR, Craig JH. Reactions of β -substituted amines. II. Nucleophilic displacement reactions on 3-chloro-1-ethylpiperidine. *Tetrahedron* 1972, 35:239-253 and references therein.

165. Sakagami H, Ogasawara K. Diastereocontrolled synthesis of enantiopure 5-allylprolinols. *Synlett* 2001, 1:45-48.

166. Payne GB. Epoxide migrations with α,β -epoxy alcohols. *J Org Chem* 1962, 27:3819-3822. Hanson RM. Epoxide migration (Payne rearrangement) and related reactions. *Org React* 2002, 60:1-156. Ibuka T. The aza-Payne rearrangement: a synthetically valuable equilibration. *Chem Soc Rev* 1998, 27:145-154.

167. For a recent review that includes analysis of the earlier work, see: Morgenthaler M, Schweizer E, Hoffmann-Röder A, Benini F, Martin RE, Jaeschke G, Wagner B, Fischer H, Bendels S, Zimmerli D, Schneider J, Diederich F, Kansy M, Müller K. Predicting and tuning physicochemical properties in lead optimization: Amine basicities. *ChemMedChem* 2007, 2:1100–1115.

168. Alabugin IV, Manoharan M. Reactant destabilization in the bergman cyclization and rational design of light and pH-activated enediynes. *J Phys Chem A* 2003, 107:3363-3371.

169. Logan CF, Chen P. *Ab initio* calculation of hydrogen abstraction reactions of phenyl radical and p-benzyne. *J Am Chem Soc* 1996, 118:2113-2114. Schottelius MJ, Chen P. 9,10-dehydroanthracene: p-benzyne-type biradicals abstract hydrogen unusually slowly. *J Am Chem Soc* 1996, 118:4896-4903.

170. Kraka E, Cremer D. Computer design of anticancer drugs. a new enediyne warhead. *J Am Chem Soc* 2000, 122:8245-8264. Pickard IV. FC, Shepherd RL, Gillis AE, Dunn ME, Feldgus S, Kirschner KN, Shields GC, Manoharan M, Alabugin IV. Ortho effect in the Bergman cyclization:

electronic and steric effects in hydrogen abstraction by 1-substituted naphthalene 5,8-diradicals., *J Phys Chem A* 2006, 110:2517-2526.

171. dos Passos Gomes G, Alabugin IV. Drawing catalytic power from charge separation: stereoelectronic and zwitterionic assistance in the Au(I)-catalyzed bergman cyclization. *J Am Chem Soc* 2017, 139:3406–3416.

172. This observation is similar to the increased through-space interaction upon addition of electrons to 1,4-diradicals: Alabugin IV, Manoharan M. Radical-anionic C1-C5 and C1-C6 cyclizations of enediynes: Remarkable substituent effects in cyclorearomatization reactions. *J Am Chem Soc* 2003, 125:4495-4509.

173. (a) Dolbier, Jr. WR, Koroniak H, Houk KN, Sheu CC. Electronic control of stereoselectivities of electrocyclic reactions of cyclobutenes: A triumph of theory in the prediction of organic reactions. *Acc Chem Res* 1996, 29:471-477. (b) Kirmse W, Rondan NG, Houk KN. Stereoselective substituent effects on conrotatory electrocyclic reactions of cyclobutenes. *J Am Chem Soc* 1984, 106:7989-1991.

174. (a) Dolbier Jr. WR, Koroniak H, Burton DJ, Bailey AR, Shaw GS, Hansen SW. Remarkable, contrasteric, electrocyclic ring opening of a cyclobutene. *J Am Chem Soc* 1984, 106:1871-1872. (b) Dolbier Jr. WR, Koroniak H, Burton DJ, Heinze PL, Bailey AR, Shaw GS, Hansen SW. Kinetic and thermodynamic studies of the thermal electrocyclic interconversions of perfluorinated dienes and cyclobutenes. *J Am Chem Soc* 1987, 109:219-225.

175. Yoshikawa T, Mori S, Shindo M. The effect of alkynyl groups on torqueoselectivity. Highly stereoselective olefination of alkynyl ketones with ynolates. *J Am Chem Soc* 2009, 131:2092–2093.

176. (a) Murakami M, Miyamoto Y, Hasegawa M, Usui I, Matsuda T. Torque control by metal-orbital interactions. *Pure Appl Chem* 2006, 78:415-423. (b) Masahiro M. Stabilizing effect of silicon by negative hyperconjugation. *Organometallic News*. 2003, 2:46-49.

177. Evans DA, Golob AM. [3,3]Sigmatropic rearrangements of 1,5-diene alkoxides. Powerful accelerating effects of the alkoxide substituent. *J Am Chem Soc* 1975, 97:4765-4766.

178. (a) Carpenter BK. A simple model for predicting the effect of substituents on the rates of thermal pericyclic reactions. *Tetrahedron* 1978, 34:1877-1884. (b) Evans DA, Baillargeon DJ, Nelson JV. A general approach to the synthesis of 1,6-dicarbonyl substrates. New applications of base-accelerated oxy-Cope rearrangements. *J Am Chem Soc* 1978, 100:2242-2244.

179. Pal R, Clark RJ, Manoharan M, Alabugin IV. Fast oxy-Cope rearrangements of bis-alkynes: competition with central C–C bond fragmentation and incorporation in tunable cascades diverging from a common bis-allenic intermediate. *J Org Chem* 2010, 75:8689–8692.

180. Black KA, Wilsey S, Houk KN. Alkynes, allenes, and alkenes in [3,3]-sigmatropy: Functional diversity and kinetic monotony. A theoretical analysis. *J Am Chem Soc* 1998, 120:5622-5627. (b) Yoo HY, Houk KN, Lee JK, Scialdone MA, Meyers Al. New paradigm for anionic heteroatom Cope rearrangements. *J Am Chem Soc* 1998, 120:205–206. (c) Black KA, Wilsey S, Houk KN.

Dissociative and associative mechanisms of cope rearrangements of fluorinated 1,5-hexadienes and 2,2'-bis-methylenecyclopentanes. *J Am Chem Soc* 2003, 125:6715–6724.

181. Winstein S, Shatavsky M, Norton C, Woodward RB. 7-Norbornenyl and 7-norbornyl cations. *J Am Chem Soc* 1955, 77:4183–4184.
182. Gassman PG, Zeller J, Lumb JT. The levelling effect of the p-anisyl group on solvolysis reactions. *ChemComm (London)* 1968, 0:69-71.
183. Haywood-Farmer JS, Pincock RE. Synthesis and solvolytic reactivity of 8-tricyclo[3.2.1.0]octane derivatives. *J Am Chem Soc* 1969, 91:3020-3028.
184. Sletten EM, Bertozzi CR. From mechanism to mouse: A tale of two bioorthogonal reactions. *Acc Chem Res* 2011, 44:666-676.
185. Gold B, Dudley GB, Alabugin IV. Moderating strain without sacrificing reactivity: Design of fast and tunable noncatalyzed alkyne–azide cycloadditions via stereoelectronically controlled transition state stabilization. *J Am Chem Soc* 2013, 135:1558-1569.
186. Hagendorn T, Bräse S. A new route to dithia- and thiaoxacyclooctynes via Nicholas reaction. *RSC Adv* 2014, 4:15493-15495. Gold B, Batsomboon P, Dudley GB, Alabugin IV. Alkynyl crown ethers as a scaffold for hyperconjugative assistance in non-catalyzed azide-alkyne click reactions: Ion sensing through enhanced transition state stabilization. *J Org Chem* 2014, 79:6221–6232. Ni R, Mitsuda N, Kashiwagi T, Igawa K, Tomooka K. Heteroatom-embedded medium-sized cycloalkynes: concise synthesis, structural analysis, and reactions. *Angew Chem Int Ed* 2015, 54:1190-1194. Harris T, dos Passos Gomes G, Ayad S, Clark RJ, Lobodin VV, Tuscan MA, Hanson K, Alabugin IV. Twisted chiral cycloalkynes and remote activation of click reactivity. *Chem* 2017, 3:629–640. Burke EG, Gold B, Hoang TT, Raines RT, Schomaker JM. Fine-tuning strain and electronic activation of strain-promoted 1,3-dipolar cycloadditions with endocyclic sulfamates in SNO-OCTs. *J Am Chem Soc* 2017, 139:8029-8037.
187. (a) Huisgen R, Mack W, Herbig K, Ott N, Anneser E. Nucleophile aromatische Substitutionen, XIV. Partielle Geschwindigkeitskonstanten der Arin-Bildung aus Bromaromaten mittels Lithiumpiperidids. *Ber Dtsch Chem Ges* 1960, 93:412-424. (b) Riggs JC, Ramirez A, Cremeens ME, Bashore CG, Candler J, Wirtz MC, Coe JW, Collum DB. Structural and rate studies of the formation of substituted benzynes. *J Am Chem Soc* 2008, 130:3406-3412. (c) Truong T, Daugulis O. Transition-metal-free alkynylation of aryl chlorides. *Org Lett* 2011, 13:4172-4175. (d) Hoye TR, Baire B, Niu D, Willoughby PH, Woods BP. The hexadehydro-Diels-Alder reaction. *Nature* 2012, 490:208-212. (e) Umedu S, dos Passos Gomes G, Sakae M, Yoshinaga T, Matsumoto K, Iwata T, Alabugin IV, Shindo M. Regioselective one-pot synthesis of triptycenes via triple-cycloadditions of arynes to ynolates. *Angew Chem Int Ed* 2017, 56:1298-1302. (f) Leroux F, Schlosser M. The “aryne” route to biaryls featuring uncommon substituent patterns. *Angew Chem Int Ed* 2002, 41:4272-4274. (g) Tadross PM, Stoltz BM. A comprehensive history of arynes in natural product total synthesis. *Chem Rev* 2012, 112:3550-3577.
188. (a) Mondal S, Gold B, Mohamed RK, Alabugin IV. Design of leaving groups in radical C-C fragmentations: Through-bond 2c–3e interactions in self-terminating radical cascades. *Chem Eur J* 2017, 23:1023-1032.

J 2014, 20:8664–8669. (b) Mohamed RK, Mondal S, Gold B, Evoniuk CJ, Banerjee T, Hanson K, Alabugin IV. Alkenes as alkyne equivalents in radical cascades terminated by fragmentations: Overcoming stereoelectronic restrictions on ring expansions for the preparation of expanded polyaromatics. *J Am Chem Soc* 2015, 137:6335–6349.

189. Crudden CM, Chen AC, Calhoun LA. A demonstration of the primary stereoelectronic effect in the Baeyer–Villiger oxidation of α -fluorocyclohexanones. *Angew Chem Int Ed* 2000, 39:2851–2855. Chandrasekhar S, Roy CD. Conformationally restricted Criegee intermediates: Evidence for formation and stereoelectronically controlled fragmentation. *J Chem Soc, Perkin Trans 2* 1994, 2141–2143.

190. Scheiner S. *Hydrogen Bonding*. New York: Oxford University Press; 1997. Jeffrey GA. *An Introduction to Hydrogen Bond*. New York: Oxford University Press; 1997. Desiraju GR, Steiner T. *The Weak Hydrogen Bond*; Oxford: Oxford University Press; 1999.

191. For characterization of hydrogen bonds based on sharing of electrons in molecules. see: Fulton RL, Perhacs P. Sharing of electrons in molecules: Characterization of hydrogen bonds. *J Phys Chem A* 1998, 102:9001–9020.

192 . H-bonding in DNA base pairs has a substantial charge-transfer character caused by hyperconjugative orbital interactions (between O or N lone pairs and N-H σ^* -acceptor orbitals) according to bond-energy decomposition analysis. Guerra CF, Bickelhaupt FM, Snijders JG, Baerends EJ. The nature of the hydrogen bond in DNA base pairs: The role of charge transfer and resonance assistance. *Chem Eur J* 1999, 5:3581–3594. Guerra CF, van der Wijst T, Bickelhaupt FM. Supramolecular switches based on the guanine-cytosine (GC) Watson-Crick Pair: Effect of neutral and ionic substituents. *Chem Eur J* 2006, 12:3032–3042. Guerra CF, Baerends EJ, Bickelhaupt FM. Orbital interactions and charge redistribution in weak hydrogen bonds: Watson-Crick GC mimic involving C-H proton donors and F proton acceptor groups. *Int J Quantum Chem* 2006, 106:2428–2443.